Steam allocation optimization and control for SAGD process

by

Yashas Mohankumar

A thesis submitted in partial fulfillment of the requirements for the degree of

Master of Science

in

Process Control

Department of Chemical and Materials Engineering
University of Alberta

Abstract

Steam allocation is an important decision to be made for bitumen thermo-recovery using the Steam Assisted Gravity Drainage (SAGD) technique. This is due to the significant amount of steam requirement and often limited steam generation capacity. Steam-to-oil ratio (SOR) is an important parameter affecting the production performance. It is necessary to address uncertainty in SOR to prevent constraint violation in SAGD reservoir states such as subcool, and also to maximize the overall steam utilization efficiency. This SAGD steam allocation problem is addressed first, by formulating a NMPC such that uncertainty in SOR is taken into consideration. The allocation is further optimized by managing the development of well pads and controlling the steam injection to different well pairs in a given developed well pad.

The first part of this thesis studies the problem of steam allocation and oil production optimization in the SAGD process considering SOR uncertainty. A first principle model for the SAGD process is developed and further incorporated into the Nonlinear Model Predictive Control (NMPC) problem, which enforces the system to be within various constraints while optimizing an economic objective. The uncertainty is dealt with using three methods in this work: (i) open-loop worst-case optimization, (ii) scenario tree based closed-loop optimization and (iii) affine policy based closed-loop optimization. Performances of the above methods are compared through Monte-Carlo simulations. Results demonstrate the superiority of affine policy based optimization method, which has around 50% improvement of economic performance over static robust and scenario based method in handling SOR uncertainty.

Subsequently, we study the problem of integrated well pad development scheduling with nonlinear model predictive control based steam injection in steam-assisted gravity drainage (SAGD). The scheduling problem has been modeled as a mixed integer program to find optimal development sequence and timing of multiple well pads. Model predictive control problems are solved to find optimal steam injection plan such that the reservoir is under control. The integrated problem is solved using open-loop and closed-loop methods: 1) Scheduling problem is only solved at the beginning of project operation, 2) Scheduling problem is solved every year with shrinking horizon implementation, and 3) Shrinking horizon implementation of scheduling with reservoir model update based on feedback from control level. Simulation results demonstrate the benefits of closed-loop integrated scheduling and control: the NPV increase is 18.93%.

Acknowledgements

I would like to start by expressing my utmost gratitude to my supervisors, Dr. Biao Huang and Dr. Zukui Li. I am grateful for the opportunity given to me to explore my research interests and for the patience extended towards me every time I ran into an impasse. Dr. Li, I would like to especially thank you for guiding me through the intricacies possessed by optimization and encouraging me to learn more. I am especially thankful to Dr. Huang for his support in keeping me on track with deadlines and submissions. I would like to thank my parents, brother and extended family in India for their unconditional support throughout my Master's program. I would like to thank NSERC, Canada for the funding received to support my research for the duration of my graduate studies.

I would like to acknowledge my research group members - Rahul, Ranjith, Alireza, Dave, Hareem, Agustin, Nabil, Arun, Faraz, Sanjula, Said, Farough and Aris, it has been a pleasure to work alongside you, and I thank you for your help at various stages of my studies. A special thanks to Rahul, Sanjula, Ranjith and Said for taking time off their busy schedule and helping me through all the issues with research.

I would like to thank my girlfriend Sneha for all her support all the way from New Delhi. Hope to spend a lot more time with you now. Special thanks to my buddies, Kapil and Pranav, for being there from the first day of my Masters program. I would like to thank my office family at DICE, Pai, Ananthan, Nilesh, AMD, Anuar and many more. Working at DICE would not be the same without you. A special thanks to my buddy Dave for his constant presence (not so much). Conversations with you have helped me learn how to manage work-life and partying better.

Contents

List of Tables

List of Figures

Nomenclature

Parameters

α	Thermal diffusivity of reservoir(m^2/s)
α_t^o	Revenue from oil production in year t, CAD/m^3
α_t^{st}	Cost of steam production in year t, CAD/m^3
ΔS_o	initial oil saturation minus residual oil saturation, dimensionless
ΔT	Temperature rise above initial condition, $\circ C$
λ^s	Latent heat of evaporation of steam (kJ/kg)
ν_s	Kinematic viscosity of oil at the temperature of the steam, m^2/s
ω_s	Probability of scenario occurring
ϕ	Porosity, dimensionless
ρ_n^f	Density of formation of well n (kg/m^3)
ρ_n^o	Density of oil in well n (kg/m^3)
ρ_n^w	Density of water in well n (kg/m^3)
σ_c	Cost of steam (CAD/m^3)
σ_p	Price of oil (CAD/m^3)
A^p	Top area of the liquid pool per unit length of chamber(m^2)
b	Exponent in Cardwell and Parson's (1948) equation for relative permeability, dimensionless

C_n^{pf} Heat capacity of formation of well n (J/kg·°C)

C_n^{po} Heat capacity of oil well n (J/kg·°C)

C_n^{pw} Heat capacity of water well n(J/kg·°C)

C^{vo} Overburden volumetric heat capacity ($MJ/m^3 \cdot K$)

C^{vr} Initial reservoir volumetric heat capacity($MJ/m^3 \cdot K$)

e Constant between lateral and vertical growth of steam chamber at first stage

g Gravity acceleration, m^2/s

H Enthalpy, MJ/m^3

k Permeability, m^2

k_t Overburden thermal conductivity, $MJ/m \cdot K \cdot s$

l_n Height of the liquid pool(m)

M^w Molar mass of water

P Pressure in steam chamber (kPa)

$q_{w,t}^{smax}$ Maximum steam available to inject into well pads w in year t ($m^3/year$)

S_{oi} Initial oil saturation, dimensionless

S_{or} Residual oil saturation, dimensionless

t Time since first steam injection, years

T_n^r Temperature at the reservoir n (°C)

T_n^s Temperature of steam at the end of steam injector n (°C)

Sets

$\tau \in T^w$ Set of lifetimes of different well pads

$i \in \mathcal{I}$ Set of elements

$j \in \mathcal{J}$ Set of collocation points

$n \in \mathcal{N}$ Set of well pairs

$s \in \mathcal{S}$ Set of scenarios

$t \in T$ Set of planning horizon

$w \in \mathcal{W}$ Set of well pads

Variables

$q^{is}_{w,n,i}$ Steam injection rate to well pad w, well n at time element i $(m^3/week)$

$q^{mo}_{n,i}$ Oil production rate from well pair n at time element i (m^3/day)

$q^{os}_{w,n,i}$ Oil produced in the producer well pad w, well n at time element i $(m^3/week)$

q^{o}_{n} Oil produced in the steam chamber for well n $(m^3/week)$

$q^{o}_{w,t}$ Oil produced from well pad w in year t $(m^3/year)$

$q^{st}_{w,t}$ Steam target to achieved by well w in year t $(m^3/year)$

$q^{s}_{n,i}$ Steam injection rate to well pair n at time element i (m^3/day)

$q^{ws}_{w,n,i}$ Water produced in the producer well pad w, well n at time element i $(m^3/week)$

q^{w}_{n} Water produced in the steam chamber for well n $(m^3/week)$

T^{p}_{n} Temperature of liquid pool at the producer well n (°C)

V^{m}_{n} Volume of mixture in liquid pool for well $n(m^3)$

V^{o} Volume of oil produced from the steam chamber (m^3)

V^{w} Volume of water produced from the steam chamber (m^3)

$z_{w,t}$ Binary variable to activate wells

Chapter 1

Introduction

1.1 Motivation

Canada has a large reserve of oil sands in Alberta at three locations: (i) Athabasca, (ii) Cold Lake and (iii) Peace River. Two commercially used in situ heat recovery methods are Cyclic Steam Stimulation (CSS) and Steam Assisted Gravity Drainage (SAGD). Steam allocation is an important decision to be made for bitumen thermo-recovery using Steam Assisted Gravity Drainage (SAGD) technique. This is due to the significant amount of steam requirement and often limited steam generation capacity. Profitable and safe extraction of oil from SAGD wells requires control on the amount of oil-water emulsion being extracted. Lack of reliable instrumentation to measure the volume of the liquid pool necessitates the estimation of the level using subcool. Subcool is defined as the difference between saturation temperature of water at the injector well and the temperature of the mixture extracted from the producer well. The level of liquid pool is directly proportional to the magnitude of subcool. High subcool can thus cause flooding in the injector well, while a very low subcool could cause steam breakthrough. Such situations lead to safety and economic concerns motivating the need for robust control [1, 2].

A SAGD facility consists of (i) the Central Processing Facility (CPF), (ii) the Surface Pads (SP's) and (iii) the Drainage Area (DA). CPF provides steam to each of the SP's through pipelines, and each SP has multiple pairs of parallel wells (or DA's) attached to it. The availability of revenue and steam in the planning horizon of a SAGD project allows us to strategically commission surface pads over the planning

horizon and simultaneously control the activated SP's.[3]. Higher profitability can be achieved by integrating the higher level scheduling horizon formulation with the lower level economic-NMPC formulation.

The SAGD process comprises pairs of horizontal wells drilled in the formation and vertically spaced a short distance apart. Steam is injected through the injector well (upper) while the producer well (lower) collects the condensate-bitumen mixture for delivering to the surface as shown in Figure 1.1. The SAGD process is shown to have various advantages over the use of CSS. The CSS process requires the injection of steam at high temperature and pressure, thus having a recovery factor of 20-25% which is not satisfactory for manufacturers. The high pressure and temperature of steam injection render it infeasible for use in regions with fine grain sands or thick bottom water. The SAGD process is shown to have higher extraction and recovery rates and is more environmentally friendly compared to other extraction processes [1].

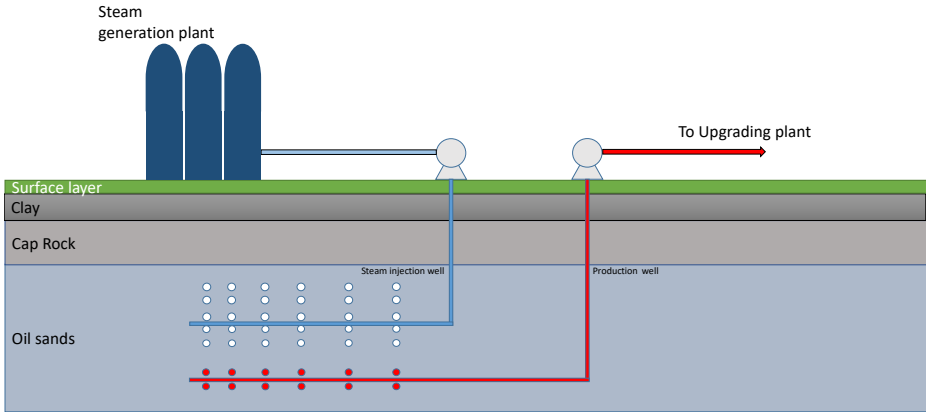

Figure 1.1: Typical SAGD plant

1.2 Literature survey on control methods

Gotawala et al.,[4] applied Proportional Integral Derivative (PID) control algorithms for subcool control and showed advantages in maintaining steam conformity. The use of such PID control algorithms in the context of gas-lifted wells shows oscillatory

characteristics. This oscillatory behavior was shown to be resolved by techniques such as partly closing choke (Schmidt et al.,[5]) or increasing the gas injection rate (Golan & Whitson, [6]). While the latter technique attenuates oscillation, it may not be the optimal solution. The use of model-based controllers would provide a smoother control performance and prevent issues such as overshoot and oscillatory behavior that are inherent to PID control algorithms.

Previous works by Eikrem et al.,[7] and Jahanshahi et al, [8] adopt simplified models for single well control. However, coupling of wells causes interaction across state variables and hence, it is important to understand the dynamics of the system. Dynamic optimization was implemented on a simple linear model by Codas et al [9]. The work of Krishnamoorthy et al[10] was based on a partial differential equation model for mass and momentum balances. Alali et al.[11] used partial differential equations to describe heat transfer in the steam chamber. Plenty of research has been done to develop transient models for long term steam chamber development [12, 13]. The use of complex reservoir models makes it difficult to implement model-based controllers in SAGD reservoirs. The simplified reservoir models have been derived previously and have similar dynamic response compared to commercial simulators like OLGA [7] and Petroleum Expert [14]. The research focuses on developing a simulator with PID control for subcool, based on first principle models. The author develops a comprehensive short term to long term SAGD simulator with first principle models generated and interconnected for steam generation, steam injection and reservoir. Purkayastha et al. [15] compared the performance of a multi-input multi-output (MIMO) model predictive controller with steam trap and oil rate controls with a multi-input single-output (MISO) MPC with only steam trap control. They showed that MIMO MPC offers better performance over the MISO MPC. Saputelli et al. [16] proposed a multiscale decision-making approach for real-time reservoir management which suggests an oilfield operations hierarchy that entails system identification, optimization, and control. The works mentioned above are solved in a deterministic setting while a lot of literature is not available for dealing with problems with uncertainty.

Krishnamoorthy et al. [17] derived first principle mathematical models for a gas-

lifted well network. The work addressed the uncertainty in gas-to-oil ratios using worst-case and scenario tree based optimization techniques. Performance for nominal, worst-case and scenario tree based optimization techniques was compared. Real-time optimization in SAGD at the lowest level of operations is riddled with uncertainty from assumptions made in long-term and medium-term optimization plans. The open-loop method does not take into account the new information available within the control horizon after decisions are made. Closed-loop prediction involves anticipation of new solutions as new information becomes available within a single optimization problem. The optimization involved would thus not optimize fixed control inputs over the entire control horizon. Closed-loop optimization was introduced in literature with regulatory and supervisory control of well operations [18, 19]. Adaptive and gain-scheduled MPCs were used for real-time optimization [20]. Shen et al. [21] presented a robust optimization approximation method to solve chance constrained MPC problem in SAGD application, where they used a linear process model obtained through closed-loop identification.

Van Essen et al. [22] developed an approach termed as "robust reservoir management", which optimizes control action over a collection of model realizations similar to scenario tree based optimization. Hanssen et al. [23] developed a method to optimize a set of control policies rather than control inputs. Policies are defined as a set of affine functions whose parameters (slope and intercept) are optimized to get a set of closed-loop predictions.

The plant model has been used to predict the behavior of the system and compute the optimal control inputs for tracking a set-point objective function. The process of tracking a pre-defined set-point does not guarantee an efficient and profitable operation of the system as discussed in [24]. The operation of a system at its constraints could cause constraint violations if uncertainty is not accounted for while designing an NMPC. Different methods for addressing the uncertainty experienced in NMPC have been explained by Lucia et al. [25]. The work implements open-loop and closed-loop methods to address the multistage stochastic optimization problem. The NMPC was applied to a polymerization reactor model and the performances of different ap-

proaches were compared.

1.3 Literature survey for integrated optimization problem

Figure 1.2: Multiple well-pads are set up in lease area, each well-pad has multiple well pairs associated with them as seen from the branched structure from the main line. The figure is obtained from: link-picture, and is available to be reused.

Well pad positioning, planning and utility network optimization are important aspects in SAGD well operations, those decisions impact the available capital for growth, and profit generated by the facility. Several studies have been published on the aspects of development planning and strategic arrangement of well pads. Nasab et al. [26] developed an optimization framework for determining the optimal strategy to place well pads in a SAGD development area. Shahandeh et al. [3] developed a method to optimize the Net Present Value (NPV) of oil revenue generated subject to uncertainty in oil price and reservoir production rates. The authors utilized rigorous mathematical models to determine the production and injection capacities available for each well

pad. The work aims to schedule the commissioning and decommissioning of wells based on uncertainty realizations. Ortiz et al. [27] worked on formulating a mixed-integer multi-period problem for oilfield production. The authors built three mixed integer optimization models of varying complexity for oil production in a reservoir. The problem considers fixed parameters to determine oil production decisions and operational starting and ending time for different wells. Awasthi et al. [28] formulated a multi objective optimization model to maximize the NPV and total oil production in an oil field. They built a bi-criterion optimization model to determine the ideal compromise between the two objective functions, i.e., between maximizing NPV and total oil production. The work considers the uncertainty in market value of oil and production parameters to build a two-stage stochastic optimization model.

Enterprise-wide optimization is a popular field of study lying at the interface of process systems engineering and operations research[29, 30]. Well-pad development scheduling does not take into consideration the performance of control level problem hence, may give subpotimal or even infeasible operational targets. The key feature of enterprise-wide optimization is the integration of various levels of operations in an enterprise for better decision making using additional information. Biegler [31] worked on integrating scheduling and dynamic process operation for continuous processes. The method utilized discrete formulation for simultaneous optimization of scheduling and operating decisions. The integrated optimization was applied on a semi-batch process for the manufacturing of polyether polyols. Nystrom et al. [32] worked on solving a production optimization problem to determine transition trajectories, operating points and sequencing for manufacturing a set of products. The problem is split as solving a dynamic optimization problem at the lower level while solving a MIP problem at the upper level for scheduling. Nie et al. [33] worked on developing a general-purpose formulation for integration of scheduling and dynamic optimization for batch/continuous processes. The integrated problem is designed as an RTN based scheduling problem and process dynamic optimization with simultaneous collocation method.

In the current day, process systems must be able to respond to external factors such as changes in demand and in prices of produced commodities in the market. Engell et al. and Touretzky et al [34, 35] discussed the possibilities of integration between

scheduling, and advanced control. Harjunkoski et al. [36] reviews system environment where integration between planning, scheduling and control systems takes place. Chatzidoukas et al. [37] worked on generating an optimal grade transition trajectory for polymerization processes. Integrated approach for optimal production scheduling is presented in parallel with transition profiles using Mixed Integer Dynamic Optimization (MIDO) techniques. Paulus and Borggrefe [38] have used a European electricity market model to make long-term forecasts for market process using linear optimization models in order to bridge the gap between demand and production in the electricity market. Soroush and Chmielewski[39] worked on process systems engineering opportunities available in power generation, storage and distribution. The work considers the interaction of fuel, solar, wind and flow battery interactions with the smart grid. Yue & You [40] developed a general modeling framework that takes into account both economic and environmental criteria. The bi-criterion optimization model was formulated as a mixed-integer linear fractional program (MILFP) and solved using tailored reformulation-linearization method and Dinkelbach's algorithm. Gallestey et al. [41] worked on utilizing model predictive control to increase economic efficiency by optimally utilizing limited resources. The scheduling and control were done in a cascade fashion with outer loop providing targets while inner loop met the envisioned targets. Van Essen et al.[42] presented a two-level strategy to optimize life-cycle production optimization in an operational setting. The upper level problem was modeled as a first principle reservoir model to produce injection and producing profile. These optimal targets were achieved using a model predictive controller (MPC). Some previous works studied the closed loop optimization and control applications in the oil and gas sector. Van Essen et al.[43] worked on hierarchical economic optimization of oil production from petroleum reservoirs. The oil production problem was formulated as a hierarchical optimization problem that considers economic life-cycle performance as the primary objective with the daily optimization production as the secondary objective. Li et al. [44] presented a mixed integer simulation optimization method for shale gas hydraulic fracturing network design. They optimized the well placement, number of fracturing stages, and fracture lengths in a discrete shale gas reservoir model. Grema and Cao [45] proposed a receding horizon control based optimal control approach for waterflooding process optimization. More recently, Horsholt

et al. [46] introduced a model reduction method for oil production optimization to decrease the simulation run-time while maintaining the model fidelity.

Multiparametric programming is one powerful technique that can be used to bridge the gap between scheduling and control decision making. Burnak et al. [47] presented simultaneous strategies for the integration of scheduling and control via multiparametric programming. The continuous and binary scheduling decisions are explicitly taken into account in the multiparametric model predictive controllers. Zhuge et al. [48] proposed a framework for the integration of scheduling and control to reduce the complexity and computational time. They identified explicit control policy using multi-parametric programming and integrated it with the scheduling level problem. They applied this integrated approach to a CSTR problem and achieved control. Chu et al. [49] discussed the online integration of scheduling and control to cope with process uncertainties. The authors worked with a sequential batch process where they solved the integrated problem to determine controller references for the lower level optimization problem. To reduce computational burden, the authors solved a reduced integrated problem by implementing a moving horizon approach. Tlacuahuac and Grossmann [50] proposed a simultaneous scheduling and control optimization formulation applied, to a CSTR. The scheduling for the CSTR was modeled as a mixed integer dynamic optimization (MIDO) problem, while the dynamics were represented as a set of ordinary differential equations solved using orthogonal collocation. Baldea et al.[51, 52], proposed a novel framework to integrate production scheduling and model predictive control for continuous processes. The authors utilize low-dimensional time-scale bridging model (SBM) to capture process dynamics over longer time scales relevant to the scheduling problem.

1.4 Optimization under uncertainty

Optimization under uncertainty refers to the branch of optimization where uncertainties are associated with parameters or states used in the model. This uncertainty in parameters or states makes the mathematical model uncertain, presenting us with a class of optimization commonly called Stochastic Programming (SP). Stochastic programming requires the knowledge of probability distribution of uncertain parameters

or states. The probability distribution of uncertainty is considered to be known or can be estimated [53].

Another method to deal with uncertainty involves finding an optimal solution that is optimal at the worst-case of uncertainty realized for the considered set. Robust optimization requires the programmer to assume or have the knowledge of the uncertainty set for the considered problem. The figure 1.3 represents the summary of methods used for optimization under uncertainty, the literature survey for optimization under uncertainty with the formulations and tutorials are given in chapter 2.

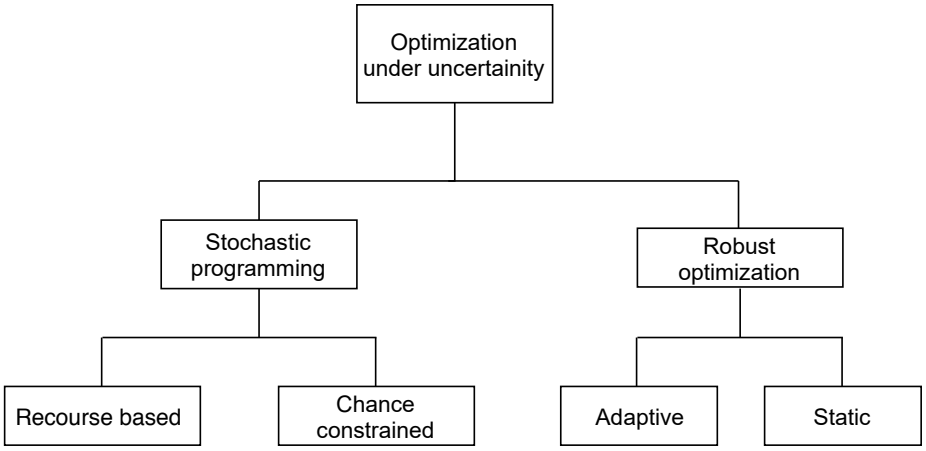

Figure 1.3: Summary of general methods for optimization under uncertainty

1.5 Thesis structure

In this thesis, SP methods and affine based policy have been applied to the case of NMPC for SAGD well pair control. Chapter 2, has a tutorial on the different methods used in the work. Chapter 3, shows the problem statement and modeling for SAGD case. The continuous ODE's utilized to describe the process and the NMPC are discretized utilizing direct collocation method using legendre polynomials. The allocation of limited steam to two different well pairs is shown while utilizing SP methods and Affine-policy based methods. The study compares the profit obtained from the same two wells using different methods while also considering the computational load to utilize each one of the above mentioned methods. Chapter 4, describes the

integrated optimization that solves the scheduling problem at the upper level while solving the control problem at the lower level. The scheduling problem was linearized to formulate a Mixed-Integer-Program(MIP) while the controller was a deterministic NLP. The study compares the performance of running the scheduler in closed-loop with a rolling horizon approach vs open-loop schedule with NMPC control. Chapter 5, gives the summary of the work done along with possible future work along similar lines to the work presented in the thesis.

Chapter 2

Tutorial

This section presents method formulations and simple example problem to show the implementation of various methods used in the thesis. Firstly, the chapter explains the theory and formations used to solve optimization problems under uncertainty. The generalized formulations are followed by explaining stochastic optimization methods using the simple example of a supply chain management problem. The problem deals with minimizing the cost of production, holding inventory and external purchases to satisfy customer demand. The demand is assumed to be uncertain, and the different formulations and results obtained are shown for the simple case.

2.1 Robust optimization

The robust optimization approach considers the uncertainty model to be deterministic and set-based. Robust optimization deals with finding an optimum solution that is viable for any realization of uncertainty in the assumed or given set. Robust optimization was first explored in early 1970 by Soyster [54]. The research exploration into robust optimization was popularized by the work of Ben-Tal and Nemirovski [55, 56, 57] in the late 1990s.

2.1.1 Static Robust Optimization

Static robust methods refers to the section of robust optimization where only a single stage optimization problem is considered. The decisions for such a problem are enforced simultaneously before the uncertainty is realized. Static robust methods are used when no further information of uncertainty is available in time, and the problem is solved for the worst-case realization of uncertainty. Such a solution, however is conservative. Consider a linear optimization problem represented as:

$$\begin{aligned} &\min\ c^\top x \\ &s.t \quad Ax \leq b \qquad \forall A \in \mathcal{U} \end{aligned}$$

where, $A \in \mathcal{U}$ indicates that the matrix A is affected by uncertainty, and thus, belongs to the uncertainty set $\mathcal{U}$. If a_i represents the i^{th} row of uncertainty matrix A and takes values in the uncertainty set $\mathcal{U}$, the static robust formulation can be represented by:

$$\begin{aligned} &\min\ c^\top x \\ &s.t \ \max_{\{a \in \mathcal{U}_\rangle\}} a_i^\top x \leq b \qquad \forall i \end{aligned}$$

This formulation thus chooses the maximum value of each a_i in row i of uncertain matrix A. The solution obtained would then satisfy the constraint for all possible realizations of uncertainty.

2.1.2 Adaptive robust optimization

The previous section talks about static robust optimization, where the decision-maker takes all the decisions at one stage, i.e. before the realization of uncertainty. In the adaptable setting, the decisions are taken stage wise and the decision taken in current stage would be dependent on the realization of uncertainty from the previous stages. If we consider a 3-stage problem:

$$\begin{aligned} &\min\ c^\top x \\ &s.t.\ A_1(u_1,u_2)x_1 + A_2(u_1,u_2)x_2(u_1) + A_3(u_1,u_2)x_3(u_1,u_2) \leq b, \quad \forall (u_1,u_2) \in \mathcal{U} \end{aligned}$$

The sequence of events in the above given problem is given as: 1) decision x_1 made, 2) uncertainty u_1 is realized after the first decision is made, the new decision x_2 is made, 3) uncertainty u_2 is realized after second decision is made, finally decision x_3 is made. Here x_1 would be the static decision taken before any uncertainty is realized, followed by decisions x_2 and x_3 that are the adaptable decisions made after uncertainty at the previous stage is realized.

2.2 Stochastic programming

Stochastic programming assumes the uncertainty in the problem has a probability distribution that is known or can be estimated. The idea was first introduced by Dantzig in his original paper dated back to 1955 [58]. This section explains in detail recourse-based SP, and gives a brief explanation of chance constraint-based SP.

2.2.1 Chance-constraint based SP

The constraints in an optimization problem can be defined as 1) constraints that have to be met at all costs, called the hard constraints, and 2) constraints that can be violated sometimes, called soft constraints. The hard constraints have no tolerance for violation, while soft constraints can tolerate a certain degree of violation. In the chance constrained approach, the soft constraints are modeled in a way such that they are met with a certain confidence limit α. The magnitude of confidence limit is inversely proportional to the probability of violation of the soft constraint. The formulation of a chance constrained model is as shown below:

$$\min_{x} \; c^{\top}x \tag{2.1}$$

$$s.t.\, \text{Prob}(A^{\top}(\xi)x \geq b(\xi)) \geq 1-\alpha \tag{2.2}$$

$$x \in X \tag{2.3}$$

In the formulation shown above, all the constraints given by the Equation 2.2 have to be satisfied with a certain probability greater than $1-\alpha$. This model expects all the constraints to be met with the same level of probability, and hence is referred to as a joint constrained problem. The more general model of a chance constrained problem can be given as:

$$\min_{x} \; c^{\top}x \tag{2.4}$$

$$s.t.\, \text{Prob}(a_i(\xi)x_i \geq b_i(\xi)) \geq 1-\alpha_i \quad i \in [1,2,..p] \tag{2.5}$$

$$x \in X \tag{2.6}$$

where p represents the number of constraints. The RHS of Equation 2.5, $1-\alpha_i$, represents the probability with which the i^{th} constraint has to be satisfied.

2.2.2 Recourse-based SP

The other way of solving stochastic optimization problems is through recourse based methods. The recourse based approach can be classified as two-stage or multi-stage recourse methods. The two-stage stochastic programming problem can be interpreted as, at the current time, the decision taken is without the uncertainty being realized called the here-and-now/first stage decisions. The decision taken after the uncertainty has been realized to mitigate the effect of the action taken at the first stage, called wait-and-see/second stage/recourse decision. The general form of a two-stage recourse stochastic programming problem is given below [59]

$$\min_{x,y(\xi)} c^\top x + E\left[q(\xi)^\top y(\xi)\right]$$
$$s.t.\, Ax \geq b$$
$$T(\xi)x + Wy(\xi) \geq h(\xi)$$
$$x \geq 0,\ y(\xi) \geq 0$$

The objective of the above described problem is to minimize the cost function. The first term of the cost function represents the cost of the first stage decision, before uncertainty has been realized. The second term of the cost function represents the expected cost of the second stage decision, taken after uncertainty has been realized. The expectation operator in the second term exists as the cost due to future decisions must be accounted for, while solving the optimization problem at the current instant. The above formulation can have infinite realizations of uncertainty and hence cannot be solved numerically.

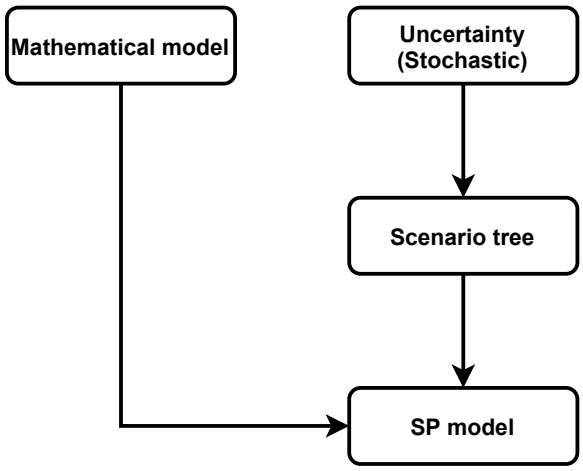

Figure 2.1: Utilizing scenario tree to represent stochastic program building in the presence of uncertainty

The assumption made to solve such an intractable model is that the primitive uncertainty vector (ξ) has a finite number of possible realizations called scenarios, represented as $\xi_1, ..., \xi_K$ with associated probabilities of $p_1, ..., p_K$. The primitive uncertainty is thus discretized to have K finite scenarios. The probability p_K represents the probability with which scenario k occurs. As the size of the primitive vector ξ increases, the number of scenarios required to represent the uncertainty vector sufficiently increases. For example, consider the components of the random vector $\xi \in \mathbb{R}^d$

are independent of each other, and we construct scenarios by assigning to each component 3 different possible scenarios. Then, we have the total number of scenarios equal to be $K = 3^d$. As the size of components increases, the growth of K is exponential and becomes computationally unmanageable to solve [60]. This problem of choosing the adequate number of scenarios for any primitive uncertainty set can be dealt with by randomizing the scenarios using Monte-Carlo sampling techniques. The general recourse-based SP using scenarios can be represented as:

$$\begin{aligned} \min_{x,y_1,y_2,..y_K} \; & c^\top x + \sum_{k=1}^{K} p_k q_k^\top y_k \\ s.t. \; & Ax \geq b \\ & T_k x + W y_k \geq h(\xi), \quad k \in [1, 2.., K] \\ & x \geq 0, \; y_k \geq 0 \quad k \in [1, 2.., K] \end{aligned}$$

The goal of recourse-based SP can be summarized in Figure 2.1. The nomenclature used in scenario tree representation is shown in Figure 2.2

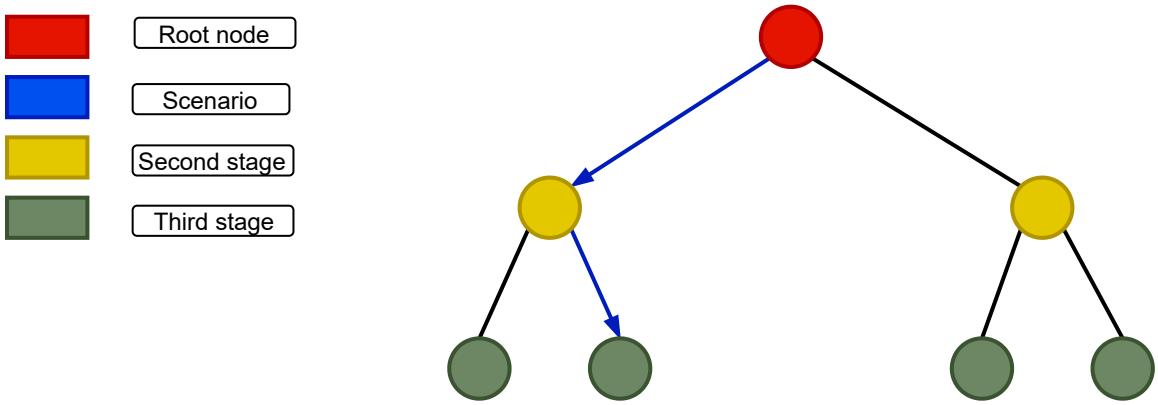

Figure 2.2: Nomenclature used in scenario tree

The root node represents the first stage without the uncertainty. The blue path represents one of the scenarios K, the yellow node represents the decision taken at the second stage, while the green node represents the third-stage decision. Consider the general formulation of a Nonlinear Model Predictive Control problem :

$$\min_{u_i} \quad \sum_{i=1}^{I} J(x_{i+1}, u_i) \tag{2.7a}$$

$$s.t. \quad x_{i+1} = f(x_i, u_i, \theta) \quad \forall i \tag{2.7b}$$

$$h(x_i, u_i) \leq 0 \quad \forall i \tag{2.7c}$$

where x_i represents system states, u_i represents control inputs, Equation 2.7a represents the cost function to be optimized, Equation 2.7b represents the system dynamic model, and Equation 2.7c represents the constraints associated with the system. The deterministic structure as shown in Equation 2.7a-2.7c is further exploited and extended to scenario tree based optimization to address uncertainty. We can express the evolution of states under uncertainty as: $x_{i+1,s} = f(x_{i,s}, u_{i,s}, \theta_s)$, where θ_s represents the parameter value of scenario s. Each new state $x_{i+1,s}$ is a function of the previous state $x_{i,s}$ and control input $u_{i,s}$ and the parameter value realized in the specific scenario s. The input $u_{i,s}$ for time instant i and scenario s is applied at the beginning of each time period to obtain the evolution of state. Scenario tree based methods require the use of non-anticipativity constraints as future decisions cannot be made at current time; hence the variables branching at the same node should assume the same value.

The goal of the optimization problem is to minimize the expected cost. If the probability of a particular scenario occurring can be given as ω_s, the scenario tree based multistage stochastic optimization formulation can be represented as:

$$\min_{u_{i,s}} \quad \sum_{s=1}^{S} \sum_{i=1}^{I} \omega_s J(x_{i+1,s}, u_{i,s}) \tag{2.8a}$$

$$s.t. \quad x_{i+1,s} = f(x_{i,s}, u_{i,s}, \theta_s) \quad \forall i, s \tag{2.8b}$$

$$h(x_{i,s}, u_{i,s}) \leq 0 \quad \forall i, s \tag{2.8c}$$

$$u_{i,s} = u(i, s') \quad \forall i, (s, s') \in SP \tag{2.8d}$$

Equation 2.8d represents the non-anticipativity condition, where SP defines the set where non-anticipative constraint should be applied. That is, at time i, the decision u_i is determined over scenarios s and s' that share the same path up to time i.

2.2.3 Affine policy based optimization

In adjustable robust optimization the decision is taken at the first instant without the realization of uncertainty. The decisions taken at the further stages are dependent on the uncertainty realized at the previous time instant. Ben-Tal, et al.[61] introduces the idea of affinely adjustable robust counterpart formulation for the recourse decisions in adjustable robust optimization. In a multi-stage problem, the method assumes the decisions taken from the second-stage of the optimization problem can be modeled as a linear function of either state or primitive uncertainty. When the decision variable is parameterized using states, the method is called closed-loop state feedback policy, whereas if the decision rule is parameterized using uncertainty the method is called

closed-loop uncertainty feedback policy. Consider a general two-stage optimization problem with uncertainty,

$$\begin{aligned}
&\min_{x,y(\xi)} c^\top x \\
&s.t.\, Ax \geq b \\
&\quad T(\xi)x + Wy(\xi) \geq h(\xi) \\
&\quad x \geq 0,\ y(\xi) \geq 0
\end{aligned}$$

In the above representation, the decision variable x is not affected by uncertainty (The first stage decision) and $y(\xi)$ is dependent on the primitive uncertainty ξ. The decision variable y is parametrized as an affine function of primitive uncertainty given as $y(\xi) = y_0 + y_1\xi$. The problem can now be represented as:

$$\begin{aligned}
&\min_{x,y(\xi)} c^\top x \\
&s.t.\, Ax \geq b \\
&\quad T(\xi)x + W(y_0 + y_1\xi) \geq h(\xi) \\
&\quad x \geq 0,\ y(\xi) \geq 0
\end{aligned}$$

The new problem is still a function of primitive uncertainty, causing a set of semi-infinite constraints for each realization of uncertainty making the problem intractable to solve. The solution to the above problem can be obtained by using robust dual counterpart. The methodology to obtain a computationally tractable model is obtained by Ben-Tal [61] and described below: Consider the stochastic programming problem:

$$\min_{x_1,x_2,y(\xi)} c_{x_1}x_1 + c_{x_2}x_2 + \mathbb{E}\left[c_y y(\xi)\right] \tag{2.9}$$

$$s.t.\ \ x_1 + y(\xi) \geq D(\xi) \quad \forall\, \xi \in \Xi \tag{2.10}$$

$$x_2 + y(\xi) = b_1 \quad \forall\, \xi \in \Xi \tag{2.11}$$

$$x_1, x_2 \geq 0 \tag{2.12}$$

$$y(\xi) \geq 0 \quad \forall\, \xi \in \Xi \tag{2.13}$$

Applying affine decision rule to the problem using the following formulations:

$$D(\xi) = \xi D_1 + (1-\xi)D_2$$

$$y(\xi) = y_0 + y_1\xi$$

Substituting $y(\xi)$ and $D(\xi)$ in Eq.(2.10) and Eq.(2.11) we have an intractable formulation given by:

$$\min_{x_1,x_2,y(\xi)} c_{x_1}x_1 + c_{x_2}x_2 + \mathbb{E}\left[c_y(y_0 + y_1\xi)\right] \tag{2.14}$$

$$
\begin{aligned}
s.t.\ \ & x_1 + y_0 + y_1\xi \geq \xi D_1 + (1-\xi)D_2 \quad \forall\, \xi \in \Xi && (2.15)\\
& x_2 + y_0 + y_1\xi = b_1 \quad \forall\, \xi \in \Xi && (2.16)\\
& x_1, x_2 \geq 0 && (2.17)\\
& y_0 + y_1\xi \geq 0 \quad \forall\, \xi \in \Xi && (2.18)
\end{aligned}
$$

where D_1 and D_2 are the extreme value realizations of uncertainty ξ. The tractable formulation of the above model is achieved by exploiting the duality property. Simplifying Eq.(2.15), to separate the terms with ξ and terms independent of ξ we have:

$$(x_1 + y_0 - D_2) + \xi(y_1 - D_1 + D_2) \geq 0 \quad \forall \xi \in \Xi$$

The primitive uncertainty set can be defined as a simple polyhedral set with the limits $\overline{\xi}$ and $\underline{\xi}$:

$$\underline{\xi} \leq \xi \leq \overline{\xi}$$

The uncertainty set Ξ is defined as $\mathbf{A}\xi \geq \mathbf{b}$
Using the matrix formulation $\mathbf{A}\xi \geq \mathbf{b}$ the constraint 2.15 can be rewritten as:

$$x_1 + y_0 - D_2 + \left\{ \begin{array}{c} \min_\xi \xi(y_1 - D_1 + D_2) \\ s.t\ \mathbf{A}\xi \geq \mathbf{b} \end{array} \right\} \geq 0$$

The term inside the parenthesis undergoes a dual transformation and hence we obtain:

$$x_1 + y_0 - D_2 + \left\{ \begin{array}{c} \max_{\lambda \geq 0} b^\top \boldsymbol{\lambda} \\ s.t\ \mathbf{A}^\top \boldsymbol{\lambda} = y_1 - D_1 + D_2 \end{array} \right\} \geq 0$$

where, the dimensions of $\boldsymbol{\lambda}$ is the same as that of $\mathbf{b}$. The max operator is then dropped to get the following set of constraints:

$$\left\{ \begin{array}{c} (x_1 + y_0 - D_2) + b^\top \boldsymbol{\lambda} \geq 0 \\ \mathbf{A}^\top \boldsymbol{\lambda} = y_1 - D_1 + D_2 \\ \boldsymbol{\lambda} \geq 0 \end{array} \right\}$$

The above set of constraints convert the semi-infinite intractable mathematical problem to a computationally tractable model that can be solved. The new model is shown below:

$$
\begin{aligned}
\min_{x_1, x_2, y(\xi)}\ & c_{x_1}x_1 + c_{x_2}x_2 + c_y(y_0 + y_1\mathbb{E}\left[\xi\right])\\
s.t.\ \ & x_1 + y_0 - D_2 + b^\top \boldsymbol{\lambda} \geq 0\\
& \mathbf{A}^\top \boldsymbol{\lambda} = y_1 - D_1 + D_2\\
& x_2 + y_0 - b_1 = 0\\
& y_0 + b^\top \lambda_y \geq 0
\end{aligned}
$$

$$A^\top \lambda_y = y_1$$
$$y_1 = 0$$
$$x_1, x_2 \geq 0$$
$$\boldsymbol{\lambda} \geq 0$$

2.3 Illustration Problem

The problem in this section has been taken from the book Optimization-Models [62]. The simple case of supply chain management has been considered to implement stochastic optimization techniques. The problem considers the supply-chain components that involve ordering costs, inventory handling costs and external order costs. The problem is solved over a finite time horizon, given as T. The objective of the problem is to minimize the costs of operation while satisfying demand. To derive an analogy between supply chain management problem and linear MPC, we can look at the following highlights of the analogy:

- The stock level of a certain product is analogous to the measured state in MPC. It is represented by the variable $x(k)$, stock level of product at time k
- The product bought at a certain time k is analogous to the control input given to a system at time k, in the case of MPC. The input is represented by $u(k)$ for time k
- The demand for a product is analogous to the demand of a certain product produced from the system under MPC control. The demand at time k is represented by $w(k)$

The mathematical representation for a supply chain model with one good and time period T is given below :
The stock level of the good at time $k+1$ is given as:

$$x(k+1) = x(k) + u(k) - w(k),\ k = 0, 1, ..., T-1$$

Here, $x(0) = x_0$ is the initial stock of goods in the inventory. The current level of stock is, thus the sum of level at the previous time instant and the products ordered in, while removing the stock that is sold to meet the demand $w(k)$. The holding cost for inventory is denoted by h, and the costs of meeting demand from external buying, and of buying the good are denoted by p and c, respectively. The objective cost to be minimized is given as:

$$cu(k) + max(hx(k+1), -px(k+1))$$

When the stock is positive, the holding cost $hx(k+1)$ is incurred. When the stock is negative, the stock has to be bought from an external supplier thus incurring an external cost of $-px(k+1)$. Considering an upper bound M on size of order. The T-stage optimization problem can be written as:

$$\min_{u(0),..,u(T-1)} \sum_{k=0}^{T-1} cu(k) + max\left(hx(k+1), -px(k+1)\right)$$
$$s.t.\ 0 \leq u(k) \leq M, \quad k = 0, 1, ..., T-1$$

Here, $x(k) = x_0 + \sum_{i=0}^{k-1}(u(i) - w(i)), \quad k = 1, ..., T$. Introducing slack variables, the max function in the objective function can be removed. The formulation now can be represented as:

$$\min_{u(0),..,u(T-1),y(0),...,y(T-1)} \sum_{k=0}^{T-1} y(k) \tag{2.19}$$
$$s.t.\ cu(k) + hx(k+1) \leq y(k) \quad k = 0, ..., T-1 \tag{2.20}$$
$$cu(k) - px(k+1) \leq y(k) \quad k = 0, ..., T-1 \tag{2.21}$$
$$0 \leq u(k) \leq M, \quad k = 0, ..., T-1 \tag{2.22}$$

Solving the above deterministic problem, we get the ordering schedule and stock levels as shown below:

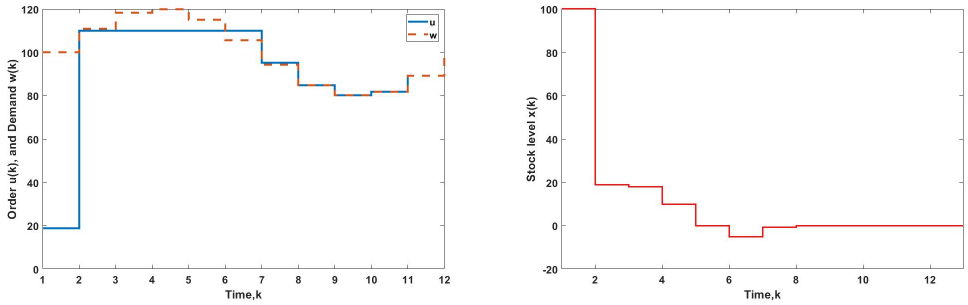

Figure 2.3: The plot on the left shows the plot for inputs of products over time, while the plot on the right shows the stock of the product over time

Since the demand of a given product is not certain, we assume there is a deviation of 15% on the upper and lower bounds of nominal demand. The lower and upper limit on the demand can be given as:

$$w_{lb} = (1-\rho)\hat{w}(k)$$
$$w_{ub} = (1+\rho)\hat{w}(k)$$

where, ρ can be defined as the assumed degree of deviation from the nominal case. The nominal case of demand can be defined by a sinusoidal function given as:

$$\hat{w}(k) = 100 + 20sin\left(2\pi\frac{k}{T-1}\right), \quad k = 0, .., T-1$$

The uncertainty in the model is solved using the methods discussed as follows:

2.4 Static Robust

The static robust method utilizes the worst-case limits on the uncertain parameters in order to convert the uncertainty problem into a deterministic problem that is solved at the extreme limits of the uncertain parameter.

Two new variables x_1 and x_2 are defined in order to get the correct stock for the case of extreme lower bound and extreme upper bound respectively. The formulation of the static robust problem is shown below:

$$\min_{u(0),..,u(T-1),y(0),...,y(T-1)} \sum_{k=0}^{T-1} y(k) \tag{2.23}$$

$$s.t.\ x_1(k) = x_1(0) + \sum_{i=0}^{k-1}(u(i) - w_{lb}(i)) \quad \forall k = 1, ..T-1 \tag{2.24}$$

$$x_2(k) = x_2(0) + \sum_{i=0}^{k-1}(u(i) - w_{ub}(i)) \quad \forall k = 1, ..T-1 \tag{2.25}$$

$$cu(k) + hx_1(k+1) \leq y(k) \quad k = 0, ..., T-1 \tag{2.26}$$

$$cu(k) - px_2(k+1) \leq y(k) \quad k = 0, ..., T-1 \tag{2.27}$$

$$0 \leq u(k) \leq M, \quad k = 0, ..., T-1 \tag{2.28}$$

Since each element of w belongs to an interval, Equation 2.20, $cu(k) + hx(k) \leq y$ will only be satisfied iff,

$$cu(k) + h(x_1(0) + \sum_{i=0}^{k-1}(u(i) - w_{lb}(i))) \leq y$$

The Equation 2.21, $cu(k) - px(k) \leq y$ is satisfied iff,

$$cu(k) - p(x_2(0) + \sum_{i=0}^{k-1}(u(i) - w_{ub}(i))) \leq y(k),$$

thus giving rise to the equations 2.24 to 2.27. The solution thus obtained will be based on the extreme limits of the demand, thus making the solution very conservative. The results obtained by static robust method is given below.

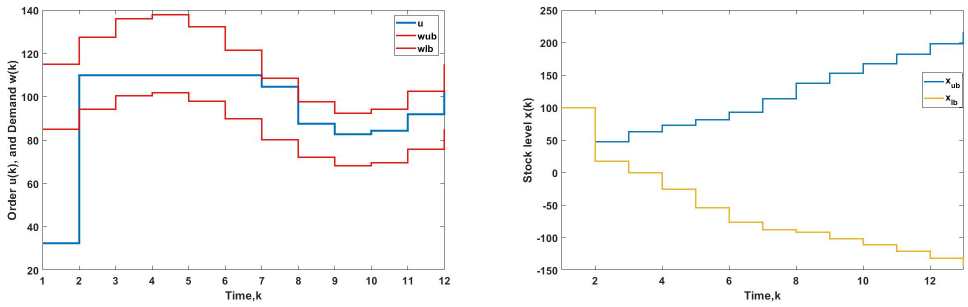

Figure 2.4: The plot on the left shows the plot for inputs of products over time while the plot on the right shows the stock of the product over time

The worst-case cost obtained for the static robust method is $\$11,392$.

2.5 Scenario-based method

The scenario-method was used to solve the uncertain model using robust horizon of 1. The scenario trees used to describe the demand parameter are shown below.

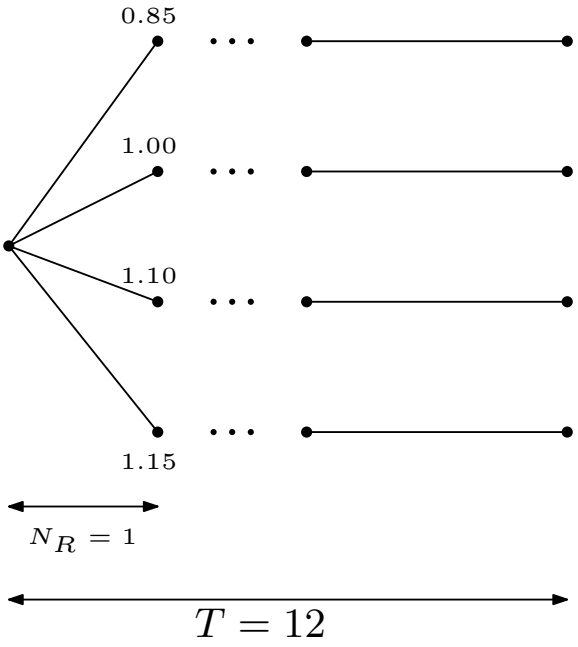

Figure 2.5: Scenario tree describing the deviation from nominal values in each one of the scenarios. Each scenario has the same probability of occurrence and hence a probability of 0.25 is assigned to each of the scenarios

The formulation for the scenario based method can be derived from the deterministic formulation such that a new index s is added in order to provide an input and

a stock level for each occurrence of a scenario. The formulation is given below:

$$\min_{u(0,s),..,u(T-1,s),y(0,s),...,y(T-1,s)} \sum_{s=1}^{S} \omega(s) \sum_{k=0}^{T-1} y(k,s) \tag{2.29}$$

$$s.t.\ x(k) = x(0,s) + Uu - Uw \tag{2.30}$$

$$cu(k) + hx_1(k+1) \leq y(k) \quad k = 0, ..., T-1 \tag{2.31}$$

$$cu(k) - px_2(k+1) \leq y(k) \quad k = 0, ..., T-1 \tag{2.32}$$

$$0 \leq u(k) \leq M, \quad k = 0, ..., T-1 \tag{2.33}$$

$$u(0,1) = u(0,2) = u(0,3) = u(0,4) \tag{2.34}$$

The U matrix here is defined as:

$$U = \begin{bmatrix} 1 & 0 & 0 & \cdots & 0 \\ 1 & 1 & 0 & \cdots & 0 \\ \vdots & \vdots & \ddots & \ddots & \vdots \\ 1 & 1 & 1 & \cdots & 1 \end{bmatrix}$$

The solution to the scenario tree problem can be given as:

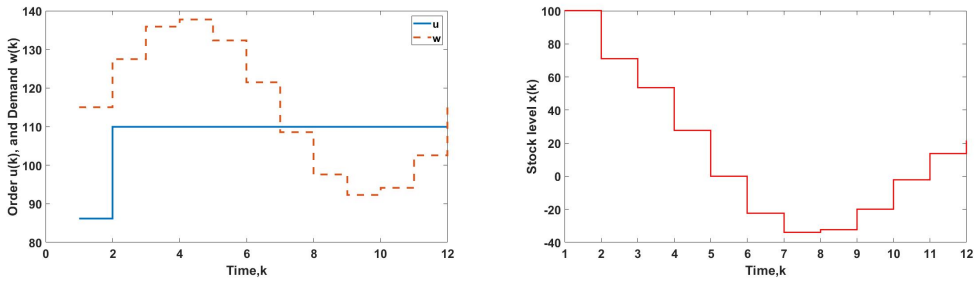

Figure 2.6: The plot on the left shows the plot for inputs of products over time while the plot on the right shows the stock of the product over time

The profit obtained using the scenario tree using expectation objective is $7959.8. The above figure shows only one scenario, and the performance of the methods can be compared only when they are being tested for a statistically significant number of generated scenarios. There were 1200 scenarios generated such that they have a mean that is the same as nominal demand, while the variance of the scenarios increased with increase in time given as:

$$\sigma_k^2 = (1+k)\bar{\sigma}^2, \quad k = 0, ..., T-1$$

where, $\bar{\sigma}^2 = 1$ The Figure 2.7 summarizes the results obtained from utilizing scenario tree method for 1200 scenarios.

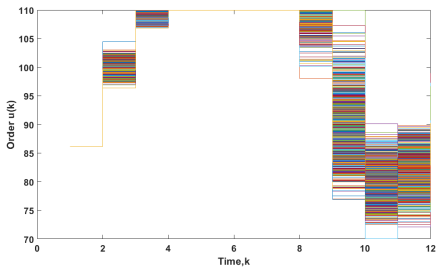

(a) Input for 1200 scenarios

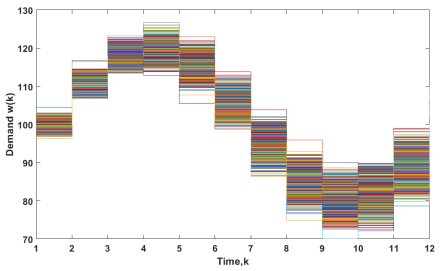

(b) Demand simulated for 1200 scenarios

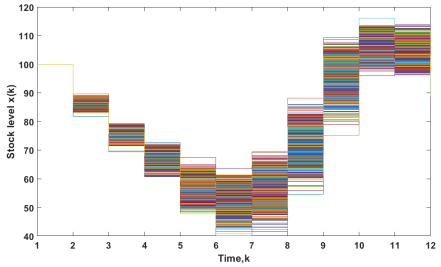

(c) Stock level for 1200 scenarios

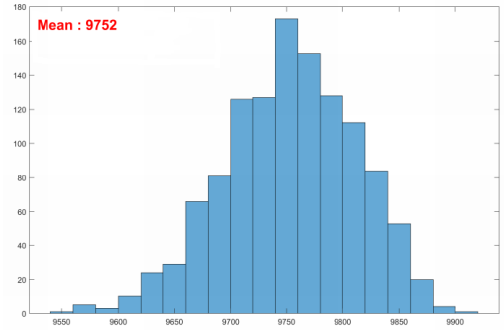

(d) Cost distribution for 1200 scenarios

Figure 2.7: Results obtained from simulating 1200 scenarios and applying scenario tree based method

2.6 Affine policy based method

Affine policy based method utilizes a closed-loop approach to address uncertainty. The input is parametrized with respect to uncertainty. The first stage decision is taken with no knowledge of uncertainty, while at consequent stages over the realization of uncertainty, the function output with respect to uncertainty gives the input at the current stage of optimization. Writing input as a function of uncertainty in demand we have $u = \bar{u} + A(w - \hat{w})$, where $\bar{u}$ represents the decision taken at current time, A represents the coefficients to be optimized, and the term $w - \hat{w}$ represents the deviation of actual demand from nominal case.

$$A = \begin{bmatrix} 0 & 0 & \cdots & 0 \\ \alpha_{1,0} & 0 & \cdots & 0 \\ \alpha_{2,0} & \alpha_{2,1} & \cdots & 0 \\ \vdots & \vdots & \ddots & \vdots \\ \alpha_{T-1,0} & \cdots & \alpha_{T-1,T-2} & 0 \end{bmatrix}$$

Representing the demand deviation by $\tilde{w}$, we have $\tilde{w} = w - \hat{w}$, which lies in the interval:

$$-\bar{w} \leq \tilde{w} \leq \bar{w}; \quad \bar{w} = \frac{\rho}{100}\hat{w} \geq 0$$

Substituting the parametrized input in place of u we have the formulation as given below:

$$\min_{\bar{u},y,A} 1^\top y \tag{2.35}$$

$$s.t \quad (c\bar{u} + cA\tilde{w}) + h(x_0 + U(\bar{u} + A\tilde{w}) - Uw) \leq y,\ \forall w \in W \tag{2.36}$$

$$(c\bar{u} + cA\tilde{w}) - p(x_0 + U(\bar{u} + A\tilde{w}) - Uw) \leq y,\ \forall w \in W \tag{2.37}$$

$$0 \leq \bar{u} + A\tilde{w} \leq M,\ \forall w \in W \tag{2.38}$$

Observe that, if ν is a vector, and $\bar{w} \geq 0$, the robust limits can be explained by:

$$\max_{-\bar{w} \leq \tilde{w} \leq \bar{w}} \nu^\top \tilde{w} = |\nu|^\top \bar{w}$$

$$\min_{-\bar{w} \leq \tilde{w} \leq \bar{w}} \nu^\top \tilde{w} = -|\nu|^\top \bar{w}$$

Applying the robust limits on Equations 2.36 and 2.37, we can reformulate the affine formulation as:

$$\min_{\bar{u},y,A} 1^\top y \tag{2.39}$$

$$s.t \quad c\bar{u} + hU\bar{u} + hx_0 - hU\hat{w} + |cA + hUA - hU|\,\bar{w} \leq y, \tag{2.40}$$

$$c\bar{u} - pU\bar{u} - px_0 + hU\hat{w} + |cA - pUA + pU|\,\bar{w} \leq y \tag{2.41}$$

$$\bar{u} + |A|\bar{w} \leq M, \tag{2.42}$$

$$\bar{u} - |A|\bar{w} \geq 0 \tag{2.43}$$

The above formulation is no longer defined on the deviation $\tilde{w}$ which is the uncertainty considered in our problem. The robust counterpart, thus, lets us consider the extreme limits of the uncertainty set $\tilde{w}$, removing the uncertain parameter $\tilde{w}$. The above problem is now simplified using slack variables, Z_1, Z_2 and Z_3.

$$\min_{\bar{u},y,A} 1^\top y \tag{2.44}$$

$$s.t \quad c\bar{u} + hU\bar{u} + hx_0 - hU\hat{w} + Z_1\bar{w} \leq y, \tag{2.45}$$

$$c\bar{u} - pU\bar{u} - px_0 + hU\hat{w} + Z_2\bar{w} \leq y \tag{2.46}$$

$$\bar{u} + Z_3\bar{w} \leq M, \tag{2.47}$$

$$\bar{u} - Z_3\bar{w} \geq 0, \tag{2.48}$$

$$|cA + hUA - hU| \leq Z_1, \tag{2.49}$$

$$|cA - pUA + pU| \leq Z_2, \tag{2.50}$$

$$|A| \leq Z_3 \tag{2.51}$$

The results obtained for 15% uncertainty is shown in Figure 2.8.

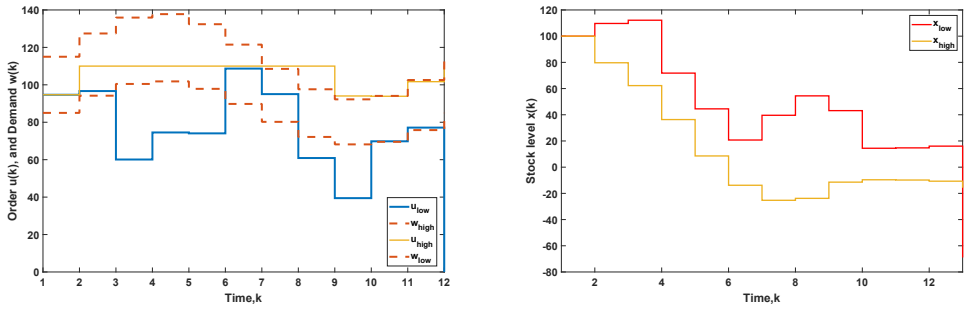

Figure 2.8: The plot on the left shows the plot for inputs of products over time, while the plot on the right shows the stock of the product over time

The ordering policy and stock can be derived as:

$$u = \bar{u} + A\tilde{w}$$

$$x = x_0 + U(\bar{u} - \hat{w}) + (UA - U)\tilde{w}$$

The above formulations give the right ordering policy as uncertainty is realized. The value of $\tilde{w}$ can be calculated at each stage to find the appropriate policy. The upper and lower limits for the orders and stock are derived as:

$$\begin{aligned} u_{lb} &= \bar{u} - |A|\bar{w}, \\ u_{ub} &= \bar{u} + |A|\bar{w}, \\ x_{lb} &= x_0 + U(\bar{u} - \hat{w}) - |UA - U|\bar{w}, \\ x_{lb} &= x_0 + U(\bar{u} - \hat{w}) + |UA - U|\bar{w} \end{aligned}$$

The limits are plotted in Figure 2.8 The above figure shows only one scenario, and the performance of the methods can be compared only when it is being tested for a statistically significant number of generated scenarios. Applying the method to the same 1200 scenarios generated for scenario tree method, we have the results summarized in Figure 2.9.

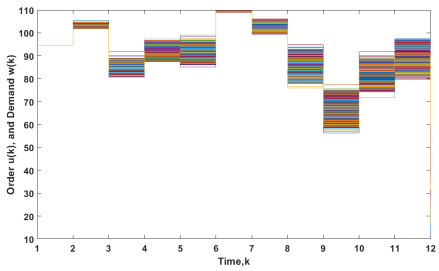

(a) Input for 1200 scenarios

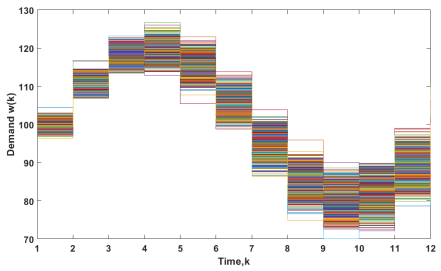

(b) Demand simulated for 1200 scenarios

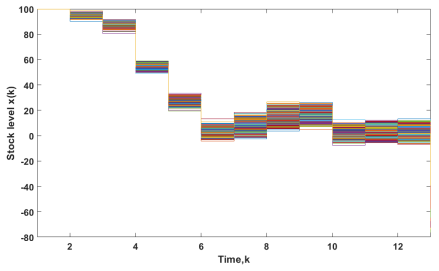

(c) Stock level for 1200 scenarios

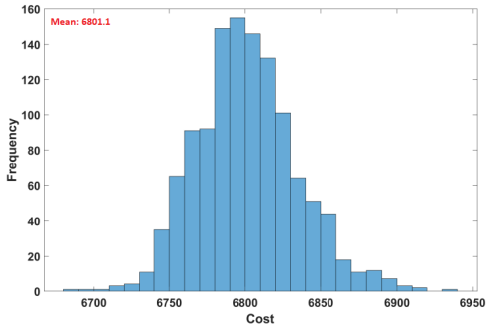

(d) Cost distribution for 1200 scenarios

Figure 2.9: The figure summarizes the results obtained from simulating 1200 scenarios and applying affine policy based method

The profiles were generated for the case where uncertainty was assumed to be $0.15\hat{w}$.

2.7 Conclusion

In the following chapter, we firstly discuss the origins and development of solutions to optimization under uncertainty. The section 2.1 describes the literature and formulations for static robust and adaptive robust optimization. The section 2.2 describes the literature and formulations for stochastic programming. The section describes the various formulations for stochastic programming that involves, chance constrained based in section 2.2.1 and recourse-based stochastic programming in section 2.2.2. The above formulations are shown in a problem illustration based on supply chain management, given in section 2.3.

Chapter 3

Steam allocation and oil production optimization in SAGD reservoir under SOR uncertainty

In this chapter, the steam allocation and oil production optimization under Steam-to-Oil-Ratio(SOR) uncertainty is discussed. The model was SAGD reservoir was adopted and modified from the work by Rashedi, et al. [14]. The steam chamber is modeled by first principle models containing heat and mass balances for liquid pool, described as a system of Ordinary Differential Equations (ODE's). These equations in continuous time are discretized and solved as a system of coupled non-linear algebraic equations. Section 3.1 describes the assumptions made in the model and the first principle equations that describe the model. Section 3.2 describes the deterministic formulation of the SAGD problem. Section 3.3 presents the general stochastic optimization problem and describes the formulation techniques for the different methods used. Section 3.4 presents the obtained results and compares the performance among them.

3.1 Mathematical modeling of SAGD reservoir

The SAGD reservoir model used for optimization is derived below. The assumptions made in the model are listed as follows:

- Only the ramp up stage is modelled, as the time frame considered is for short term SAGD ($\approx days$) and evolution to plateau stage takes approximately 0.5 - 2 years.
- The change in chamber height is slow compared to change in temperature and level. Hence, we assume that the volume of the steam chamber is constant.

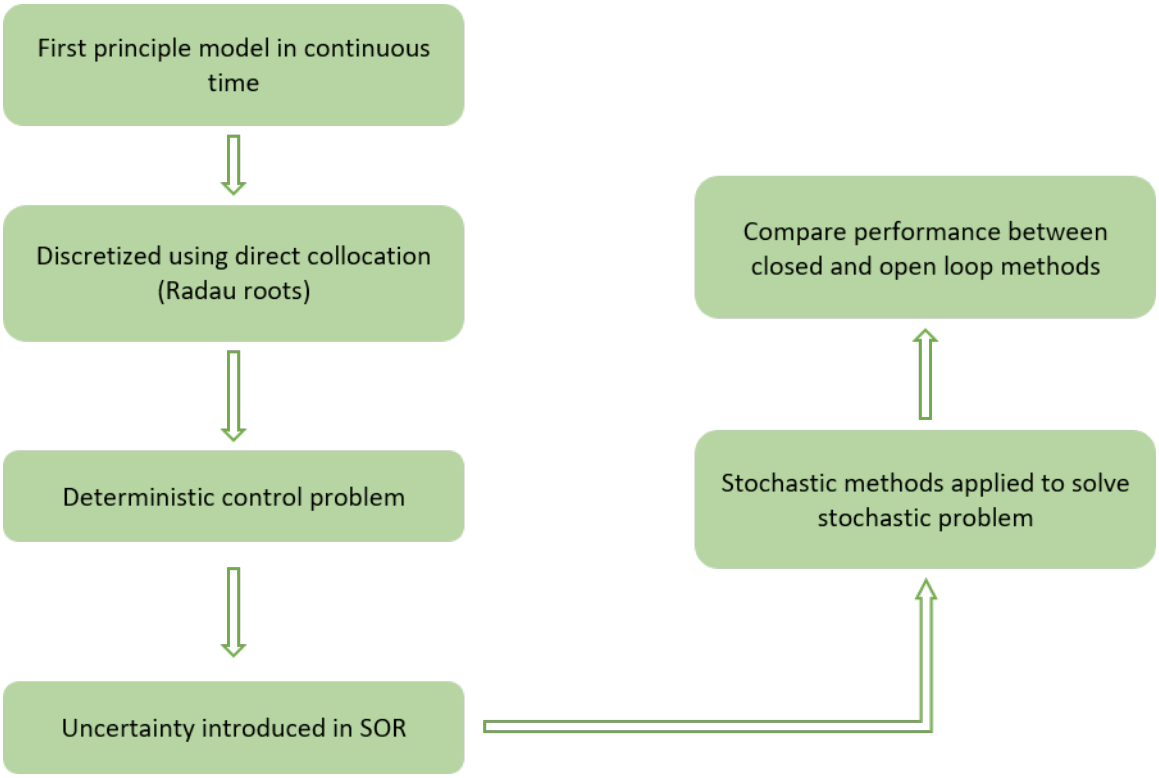

Figure 3.1: The figure describes the work-flow of conducted research

- The volume ratio of water and oil in the liquid pool is approximately equal to the flow ratio of water and oil that feeds the liquid pool, $\frac{V^w}{V^o} = \frac{q^w}{q^o}$
- The heat loss from the liquid pool to the reservoir is negligible compared to the heat gained by the liquid pool from the reservoir.
- The oil drained from the reservoir into the liquid pool is estimated as $q^o = q^s/SOR$. The SOR used here is not a cumulative steam-to-oil ratio but instantaneous steam-to-oil ratio used to estimate oil production from reservoir.

The SAGD model used in this work is applicable only for the ramp-up stage (i.e., the reservoir has not reached the cap rock). This limitation in the model can be overcome by modifying the model for the other stages of SAGD process. However, the proposed method for addressing uncertainty in NMPC can still be applied to the modified model.
The model consists of the mass balance in the liquid pool and the energy balance in the liquid pool. First, the mass balance equation can be written as:

$$\frac{d}{dt}\left[\rho^o V^o + \rho^w V^w\right] = \rho^o(q^o - q^{os}) + \rho^w(q^w - q^{ws}) \tag{3.1}$$

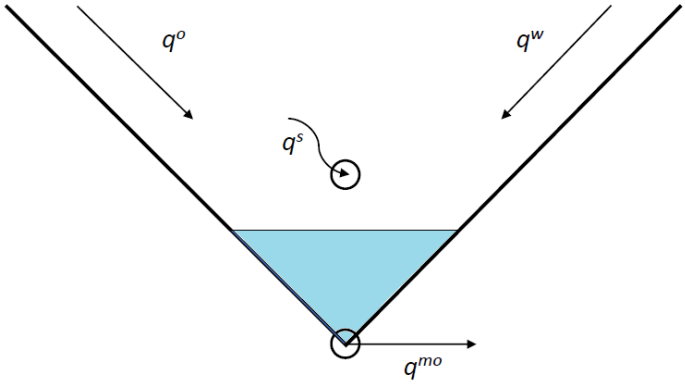

Figure 3.2: The figure shows the cross section of steam chamber

where the inlet mass flows include heated bitumen and condensed water from steam chamber, and the outlet mass flows include bitumen and water to producer well.

Energy balance over the liquid pool during the ramp up stage can be formulated as

$$\begin{aligned}\frac{d}{dt}\left[(\rho^o V^o C^{po} + \rho^w V^w C^{pw})(T^p - T^r)\right] = \hat{Q}(t) + \rho^o q^o C^{po}(T^s - T^r) \\ +\rho^w q^w C^{pw}(T^s - T^r) - \rho^o q^{os} C^{po}(T^p - T^r) - \rho^w q^{ws} C^{pw}(T^p - T^r)\end{aligned} \tag{3.2}$$

where the first term of the right hand side represents heat transfer from steam chamber to liquid pool $\hat{Q}(t) = 128.3P - 669.1$, which is an empirical relation that defines heat transfer between steam chamber and liquid pool to be directly proportional to steam injection pressure. The second and third term represent the heat carried by condensed steam and heated bitumen from steam chamber to liquid pool. The fourth term denotes the heat carried by produced water and oil through the production well and the last term represents the heat loss from liquid pool to surrounding reservoir (considered to be too small and hence ignored).

The mixture of oil and water produced from the reservoir can be modeled as

$$\rho^m q^{mo} = \rho^o q^{os} + \rho^w q^{ws} \tag{3.3}$$

For oil sands reservoir without any trap zones, it can be approximated that the oil drained from reservoir to the pool from reservoir temperature to saturated steam temperature requires an equivalent amount of heat from condensed steam, thus giving the relation:

$$\rho^w q^w = \frac{\rho^o q^o C^{po}(T^s - T^r)}{\eta^{eff} X^s \lambda^s} \tag{3.4}$$

Combining Eq(3.4) and Eq(3.1) we get the following relation:

$$\frac{dV^m}{dt} = \frac{\rho^o q^o + \rho^w q^w}{\rho^m} - q^{mo} \tag{3.5}$$

Solving equation Eq(3.2) we have:

$$\frac{dT^p}{dt} = \frac{\hat{Q}}{\rho^m C^{pm} V^m} + \left[\frac{\rho^o q^o C^{po} + \rho^w q^w C^{pw}}{\rho^m C^{pm} V^m}\right](T^s - T^r) - \frac{1}{V^m}\left[q^{mo} + \frac{dV^m}{dt}\right](T^p - T^r) \tag{3.6}$$

where the observed states are V^m and T^p. The flow rate of condensed oil is given as:

$$q^o = \frac{q^s}{SOR} \tag{3.7}$$

The volume of the oil in the liquid pool is given as:

$$V^o = \frac{V^m q^o}{q^o + q^w} \tag{3.8}$$

The volume of water in the liquid pool is given by:

$$V^w = \frac{V^m q^w}{q^o + q^w} \tag{3.9}$$

The level of the liquid can be calculated as:

$$l = \left[\frac{0.955 V^m}{e^2}\right]^{\frac{1}{3}} \tag{3.10}$$

The heat capacity of the mixture is calculated as:

$$C^{pm} = \frac{\rho^o V^o}{M^o(\frac{\rho^o V^o}{M^o} + \frac{\rho^w V^w}{M^w})} C^{po} + \frac{\rho^w V^w}{M^w(\frac{\rho^o V^o}{M^o} + \frac{\rho^w V^w}{M^w})} C^{pw} \tag{3.11}$$

The density of the mixture is calculated as:

$$\rho^m = \frac{V^o \rho^o + V^w \rho^w}{V^o + V^w} \tag{3.12}$$

The differential equations Eq(3.5) and Eq(3.6) are represented by the generalized equation

$$\dot{x}_n = f(x_n, z_n, u_n, p_n, \theta_n) \tag{3.13}$$

The algebraic equations from Eq(3.7) to Eq(3.12) can be represented as

$$g(x_n, z_n, u_n, p_n) = 0 \tag{3.14}$$

where n is the well index, and the differential states (x_n), algebraic states (z_n), input variables (u_n), deterministic parameters (θ_n) and uncertain parameter (p_n) are given by:

$$x_n = [V_n^m \quad T_n^p]^T$$

$$
\begin{aligned}
z_n &= [V_n^o \;\; l_n \;\; C_n^{pm} \;\; V_n^w \;\; \rho_n^m \;\; q_n^o \;\; q_n^w]^T \\
u_n &= [q_n^s \;\; q_n^{mo}]^T \\
\theta_n &= [\rho_n^o \;\; \rho_n^w \;\; e_n \;\; T_n^s \;\; X^s \;\; T_n^r \;\; C_n^{pw} \;\; C_n^{po} \;\; \lambda_n^s]^T \\
p_n &= [SOR_n]
\end{aligned}
$$

3.2 Deterministic formulation

The steam allocation and oil production optimization problem is represented mathematically as:

$$
\begin{aligned}
\min_{q_n^s, q_n^{mo}} \quad & \sum_n \int_0^T [\sigma_c q_n^s(t) - \sigma_p q_n^{mo}(t)]\, dt && \text{(3.15a)} \\
s.t. \quad & \dot{x}_n = f(x_n, z_n, u_n, p_n, \theta_n) \quad \forall n && \text{(3.15b)} \\
& g(x_n, z_n, u_n, p_n) = 0 \quad \forall n && \text{(3.15c)} \\
& \underline{A}_n \leq q_n^{mo} \leq \overline{A}_n \quad \forall n && \text{(3.15d)} \\
& \underline{B}_n \leq q_n^s \leq \overline{B}_n \quad \forall n && \text{(3.15e)} \\
& \sum_{n=1}^{N} q_n^s \leq \bar{C} \quad \forall n && \text{(3.15f)} \\
& \underline{\gamma_n} \leq V_n^m \leq \overline{\gamma_n} \quad \forall n && \text{(3.15g)} \\
& \underline{D}_n \leq T_n^p - T_n^s \leq \overline{D}_n \quad \forall n && \text{(3.15h)}
\end{aligned}
$$

The objective function represents the cost of steam and revenue from oil production to be optimized. Constraint Eq(3.15d) provides the upper limit on the oil production rate in a well pair whereas constraint Eq(3.15e) provides the limit on steam injection rate into a particular well pair. Constraint Eq(3.15f) limits the available steam capacity and constraint Eq(3.15h) limits the subcool temperature to prevent steam breakthrough.

Discretization

The orthogonal collocation technique is presented, used to discretize the continuous ODE's, and is adopted from a numerical example from Beigler [63]. The general representation of an ODE is written as:

$$
\frac{dz}{dt} = f(z(t), t), \quad z(0) = z_o \tag{3.16}
$$

The Equation 3.16 is continuous in time and can be solved as an initial value problem using various numerical techniques (polynomial approximation) or by utilizing

analytical methods to integrate between set limits. For a finite element, the polynomial approximation for state z is shown in Fig 3.3. To develop the NLP formulation,

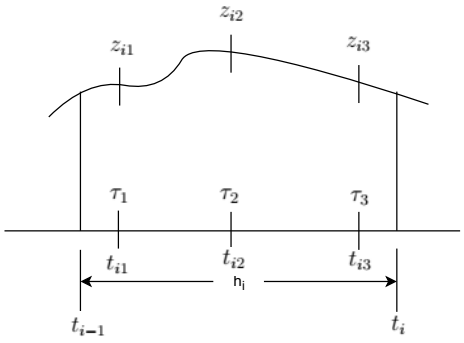

Figure 3.3: Polynomial approximation of state profile across finite element

most often, Lagrange interpolation polynomials are used. The time elements are represented as i, where each time element is split into K intervals using $K+1$ interpolation points, and the size of the interval is represented by h_i. The state in a given element is given as:

$$\begin{bmatrix} t = t_{i-1} + h_i\tau \\ z^K(t) = \sum_{j=0}^{K} l_j(\tau) z_{ij} \end{bmatrix} \quad \forall t \in [t_{i-1}, t_i]\,,\ \tau \in [0,1] \tag{3.17}$$

where, $l_j(\tau) = \prod_{k=0,\neq j}^{K} \frac{\tau-\tau_K}{\tau_j-\tau_k}$, $t_{ij} = t_{i-1} + \tau_j h_i$ and $z^K(t) = z_{ij}$. So the time derivative of the state can be represented by the Lagrangian polynomial as shown below:

$$z^K(t) = z_{i-1} + h_i \sum_{j=1}^{K} \Omega_j(\tau) \dot{z_{ij}} \tag{3.18}$$

The Equations 3.17 and 3.18 are normalized over time and represented as functions of τ. The collocation equation can now be represented as:

$$\sum_{j=0}^{K} z_{ij} \frac{dl_j(\tau_k)}{d\tau} = h_i f(z_{ik}, t_{ik}), \quad k = 1, ..., K \tag{3.19}$$

If Legendre roots are utilized to get the placement of collocation points, terminal conditions have to be enforced to maintain continuity of the state profiles. With Lagrange interpolation profiles, the terminal conditions are:

$$z_{i+1,0} = \sum_{j=0}^{K} l_j(1) z_{ij}, \ \ i = 1, ..., N-1 \tag{3.20}$$

$$z_f = \sum_{j=0}^{K} l_j(1) z_{Nj}, \ \ z_{1,0} = z_0 \tag{3.21}$$

Utilizing radau roots as collocation points eliminates the need for terminal conditions, as the last collocation point lies on the initial point for the next time element. The collocation roots are given in the Table 3.1

Degree K	Legendre Roots	Radau Roots
1	0.5	1.0
2	0.211325	0.3333
	0.788675	1.0000
3	0.112702	0.155051
	0.5	0.644949
	0.887298	1.0000

Table 3.1: The roots to be used as collocation points τ_k

The solution to the following example problem can be utilized to understand the method of orthogonal collocation: Consider the ODE [63],

$$\frac{dz}{dt} = z^2 - 2z + 1, z(0) = -3$$

We can split the time interval into N elements, the interval size is defined as $h = 1/N$, and we use collocation of the order 3 i.e, K=3.

$$\sum_{j=0}^{K} z_{ij} \frac{dl_j(\tau_k)}{d\tau} = h_i \left(z_{ik}^2 - 2z_{ik} + 1\right), \quad k = 1, ..., 3, \; i = 1, .., N \tag{3.22}$$

Using radau collocation of third order we have,

$$\tau_0 = 0, \; \tau_1 = 0.155051, \tau_2 = 0.644949, \; \tau_3 = 1$$

For $N = 1$ and $z_0 = -3$ and expanding on Equation 3.22 we have:

$$\begin{aligned} & z_0(-30\tau_k^2 + 36\tau_k - 9) + z_1(46.7423\tau_k^2 - 51.2592\tau_k + 10.0488) \\ & + z_2(-26.7423\tau_k^2 + 20.5925\tau_k - 1.38214) + z_3\left(10\tau_k^2 - \frac{16}{3}\tau_k + \frac{1}{3}\right) \\ & = (z_k^2 - 2z_k + 1), \quad k = 1, 2, 3 \end{aligned} \tag{3.23}$$

The three simultaneous equations then can be solved to obtain the solution for the three variables z_1, z_2, z_3.

The optimization problem defined above includes a set of continuous time differential algebraic equations. This infinite dimensional optimal control problem can be discretized and solved as a finite dimensional problem. The direct collocation technique using Legendre interpolation polynomials of third order is used in this work for

the purpose of discretization.
The given time interval is split into P equal sampling intervals. Legendre collocation scheme of third order is chosen and hence we have $C+1$ points in each interval: $0, ..., C$. The discretized states can be represented as:
$X_{i,j} = \left[V^m_{1,i,j}, \cdots V^m_{N,i,j}, T^p_{1,i,j}, \cdots T^p_{N,i,j}\right]^T$

$$Z_{i,j} = [V^o_{1,i,j}, \cdots V^o_{N,i,j}, l_{1,i,j}, \cdots l_{N,i,j}, C^{pm}_{1,i,j}, \cdots C^{pm}_{N,i,j}, V^w_{1,i,j}, \cdots V^w_{N,i,j}, \\ \rho^m_{1,i,j}, \cdots \rho^m_{N,i,j}, q^o_{1,i,j}, \cdots q^o_{N,i,j}, q^w_{1,i,j}, \cdots q^w_{N,i,j}]^T$$

where $X_{i,j}$ represents the combined states for n wells at time instant i and collocation point j in the interval $\left[i, i+1\right]$. For the sake of continuity in state variables, we have the relation that $X_{i,C}$ and initial conditions of the next time interval $X_{i+1,0}$ should be equal.

Deterministic optimization model

The intermediate equations were removed by substituting them into the ODE's. The new model is presented below.

$$\min_{q^s_{n,i}, q^{mo}_{n,i}} \quad \sum_{n=1}^{N}\sum_{i=1}^{I}[\sigma_c \cdot q^s_{n,i} - \sigma_p \cdot q^{mo}_{n,i}] + \sum_{n=1}^{N}\sum_{i=1}^{I}\gamma_1|q^s_{n,i+1} - q^s_{n,i}| + \sum_{n=1}^{N}\sum_{i=1}^{I}\gamma_2|q^{mo}_{n,i+1} - q^{mo}_{n,i}| \tag{3.24a}$$

$$s.t. \quad \sum_{j=0}^{C} V^m_{n,i,j}\frac{dl_j}{d\tau}(\tau_k) = h\left[q^o_{n,i} + q^w_{n,i} - q^{mo}_{n,i}\right] \quad \forall n, i \tag{3.24b}$$

$$Q_{1n,i,j,k}\sum_{j=0}^{C} T^p_{n,i,j,s}\frac{dl_j}{d\tau}(\tau_k) = h\left[L_i(q^o_{n,i} + q^w_{n,i})\hat{Q} + Q_{2n,i,j,k} - Q_{3n,i,j,k}(T^p_{n,i,k} - T^r)\right] \quad \forall n, i, j, k \tag{3.24c}$$

$$Q_{1n,i,j,k} = (\rho^o q^o_{n,i} C^{po}_n M^w + \rho^w q^w_{n,i} C^{pw}_n M^o)(\rho^o_n q^o_{n,i} + \rho^w_n q^w_{n,i})V^m_{n,i,k} \quad \forall n, i, j, k \tag{3.24d}$$

$$Q_{2n,i,j,k} = L_{n,i}(q^o_{n,i} + q^w_{n,i})(\rho^o_n q^o_{n,i} C^{po}_n + \rho^w_n q^w_{n,i} C^{pw}_n)(T^s_n - T^r) \quad \forall n, i, j, k \tag{3.24e}$$

$$Q_{3n,i,j,k} = (\rho^o_n q^o_{n,i} + \rho^w_n q^w_{n,i})(\rho^o_n q^o_{n,i} C^{po}_n M^w + \rho^w_n q^w_{n,i} C^{pw}_n M^o)(q^o_{n,i} + q^w_{n,i}) \quad \forall n, i, j, k \tag{3.24f}$$

$$q^o_{n,i} = \frac{q^s_{n,i}}{SOR_n} \quad \forall i, n \tag{3.24g}$$

$$q^w_{n,i} = \frac{\rho^o q^o_{n,i} C^{po}_n (T^s - T^r)}{\eta^{eff} X^s \lambda^s} \quad \forall i, n \tag{3.24h}$$

$$L_{n,i} = \rho^o_n q^o_{n,i} M_w + \rho^w_n q^w_{n,i} M_o \quad \forall i, n \tag{3.24i}$$

$$V^m_{n,i+1,0} = V^m_{n,i,C} \quad \forall i, n \tag{3.24j}$$

$$T^p_{n,i+1,0} = T^p_{n,i,C} \quad \forall i, n \tag{3.24k}$$

$$\underline{A_n} \leq q^{mo}_{n,i} \leq \overline{A_n} \quad \forall n, i \tag{3.24l}$$

$$\underline{B_n} \leq q^{s}_{n,i} \leq \overline{B_n} \quad \forall n, i \tag{3.24m}$$

$$\sum_{n=1}^{N} q^s_{n,i} \leq \bar{C} \quad \forall i \tag{3.24n}$$

$$\underline{\gamma} \leq V^m_{n,i,j} \leq \overline{\gamma} \quad \forall i, n, j \tag{3.24o}$$

$$\underline{D_n} \leq T^p_{n,i,j} - T^s_{n,i,j} \leq \overline{D}_n \quad \forall i, n, j \tag{3.24p}$$

where the second and third terms in equation 3.24a represent the penalty for change in successive inputs, which prevents the big change in control action, thus making the control inputs smooth. The usage of Radau roots simplifies the optimization problem as the final collocation point corresponds to the initial point of the next element.

3.3 Stochastic Optimization Problem

In this work, we consider the uncertainty related to SOR. The state variables will be uncertainty dependent. In an open-loop optimization model, the control variables will be independent of uncertainty. On the other hand, the control variables will be also uncertainty dependent in a closed-loop optimization formulation as presented in this section. The overall stochastic optimization model is given as following:

$$\min_{q^s_{n,i}, q^{m}o_{n,i}} \quad \mathbb{E}\Big[\sum_{n=1}^{N}\sum_{i=1}^{I}\left[\sigma_s \cdot q^s_{n,i}(\zeta) - \sigma_p \cdot q^{mo}_{n,i}(\zeta)\right] + \sum_{n=1}^{N}\sum_{i=1}^{I}\gamma_1 |q^s_{n,i+1}(\zeta) - q^s_{n,i}(\zeta)| + \sum_{n=1}^{N}\sum_{i=1}^{I}\gamma_2 |q^{mo}_{n,i+1}(\zeta) - q^{mo}_{n,i}(\zeta)|\Big] \tag{3.25a}$$

$$s.t. \quad \sum_{j=0}^{C} V^m_{n,i,j}(\zeta)\frac{dl_j}{d\tau}(\tau_k) = h\Big[q^o_{n,i}(\zeta) + q^w_{n,i}(\zeta) - q^{mo}_{n,i}(\zeta)\Big] \quad \forall n, i \tag{3.25b}$$

$$Q_{1n,i,j,k}(\zeta)\sum_{j=0}^{C} T^p_{n,i,j,s}(\zeta)\frac{dl_j}{d\tau}(\tau_k) = h\Big[L_i(q^o_{n,i}(\zeta) + q^w_{n,i}(\zeta))\hat{Q} + Q_{2n,i,j,k}(\zeta) - Q_{3n,i,j,k}(\zeta)(T^p_{n,i,k}(\zeta) - T^r)\Big] \quad \forall n, i, j, k \tag{3.25c}$$

$$Q_{1n,i,j,k}(\zeta) = (\rho^o q^o_{n,i}(\zeta) C^{po}_n M^w + \rho^w q^w_{n,i}(\zeta) C^{pw}_n M^o)(\rho^o_n q^o_{n,i}(\zeta) + \rho^w_n q^w_{n,i}(\zeta)) V^m_{n,i,k}(\zeta) \quad \forall n, i, j, k \tag{3.25d}$$

$$Q_{2n,i,j,k}(\zeta) =$$
$$L_{n,i}(q^o_{n,i}(\zeta) + q^w_{n,i}(\zeta))(\rho^o_n q^o_{n,i}(\zeta) C^{po}_n + \rho^w_n q^w_{n,i}(\zeta) C^{pw}_n)(T^s_n - T^r) \quad \forall n, i, j, k \tag{3.25e}$$

$$Q_{3n,i,j,k}(\zeta) =$$
$$(\rho^o_n q^o_{n,i}(\zeta) + \rho^w_n q^w_{n,i}(\zeta))(\rho^o_n q^o_{n,i}(\zeta) C^{po}_n M^w + \rho^w_n q^w_{n,i}(\zeta) C^{pw}_n M^o)(q^o_{n,i}(\zeta) + q^w_{n,i}(\zeta)) \quad \forall n, i, j, k \tag{3.25f}$$

$$q^o_{n,i}(\zeta) = \frac{q^s_{n,i}(\zeta)}{SOR_{n,i}(\zeta)} \quad \forall i, \ n \tag{3.25g}$$

$$q^w_{n,i}(\zeta) = \frac{\rho^o q^o_{n,i}(\zeta) C^{po}_n (T^s - T^r)}{\eta^{eff} X^s \lambda^s} \quad \forall i, \ n \tag{3.25h}$$

$$L_{n,i} = \rho^o_n q^o_{n,i}(\zeta) M_w + \rho^w_n q^w_{n,i}(\zeta) M_o \quad \forall i, \ n \tag{3.25i}$$

$$V^m_{n,i+1,0}(\zeta) = V^m_{n,i,C}(\zeta) \quad \forall i, \ n \tag{3.25j}$$

$$T^p_{n,i+1,0}(\zeta) = T^p_{n,i,C}(\zeta) \quad \forall i, \ n \tag{3.25k}$$

$$\underline{A}_n \leq q^{mo}_{n,i}(\zeta) \leq \overline{A}_n \quad \forall n, i \tag{3.25l}$$

$$\underline{B}_n \leq q^s_{n,i}(\zeta) \leq \overline{B}_n \quad \forall n, i \tag{3.25m}$$

$$\sum_{n=1}^{N} q^s_{n,i}(\zeta) \leq \bar{C} \quad \forall i \tag{3.25n}$$

$$\underline{\gamma} \leq V^m_{n,i,j} \leq \overline{\gamma} \quad \forall i, n, j \tag{3.25o}$$

$$\underline{D}_n \leq T^p_{n,i,j}(\zeta) - T^s_{n,i,j} \leq \overline{D}_n \quad \forall i, n, j \tag{3.25p}$$

For simplicity in presenting the above model, we ignored the condition that every constraint must be satisfied for a pre-defined uncertainty set: $\forall \xi \in \Xi$.

Scenario tree based optimization

In the scenario tree based formulation, a scenario tree is used to model the uncertainty. A scenario corresponds to a full path of SOR uncertainty realization over the prediction horizon. With ω_s being the probability of occurrence of a particular scenario s, we have the final optimization problem represented as:

$$\min_{q^s_{n,i,s}, q^{mo}_{n,i,s}} \quad \sum_{s=1}^{S} \omega_s \cdot \left(\sum_{n=1}^{N} \sum_{i=1}^{I} [\sigma_c \cdot q^s_{n,i,s} - \sigma_p \cdot q^{mo}_{n,i,s}] + \sum_{n=1}^{N} \sum_{i=1}^{N} \gamma_1 |q^s_{n,i+1,s} - q^s_{n,i,s}| + \sum_{n=1}^{N} \sum_{i=1}^{N} \gamma_2 |q^{mo}_{n,i+1,s} - q^{mo}_{n,i,s}| \right) \tag{3.26a}$$

$$s.t. \quad \sum_{j=0}^{C} V^m_{n,i,j,s} \frac{dl_j}{d\tau}(\tau_k) = h\Big[q^o_{n,i,s} + q^w_{n,i,s} - q^{mo}_{n,i,s}\Big] \quad \forall n, i, s \tag{3.26b}$$

$$Q_{1n,i,j,k,s}\sum_{j=0}^{C}T^{p}_{n,i,j,s}\frac{dl_j}{d\tau}(\tau_k)=h\Big[L_i(q^{o}_{n,i,s}+q^{w}_{n,i,s})\hat{Q}+Q_{2n,i,j,k,s}-Q_{3n,i,j,k,s}(T^{p}_{n,i,k,s}-T^{r})\Big]$$
$$\forall n,i,j,k,s \tag{3.26c}$$

$$Q_{1n,i,j,k,s}=(\rho^{o}q^{o}_{n,i,s}C^{po}_{n}M^{w}+\rho^{w}q^{w}_{n,i,s}C^{pw}_{n}M^{o})(\rho^{o}_{n}q^{o}_{n,i,s}+\rho^{w}_{n}q^{w}_{n,i,s})V^{m}_{n,i,k,s}$$
$$\forall n,i,j,k,s \tag{3.26d}$$

$$Q_{2n,i,j,k,s}=L_{n,i,s}(q^{o}_{n,i,s}+q^{w}_{n,i,s})(\rho^{o}_{n}q^{o}_{n,i,s}C^{po}_{n}+\rho^{w}_{n}q^{w}_{n,i,s}C^{pw}_{n})(T^{s}_{n}-T^{r})$$
$$\forall n,i,j,k,s \tag{3.26e}$$

$$Q_{3n,i,j,k,s}=(\rho^{o}_{n}q^{o}_{n,i,s}+\rho^{w}_{n}q^{w}_{n,i,s})(\rho^{o}_{n}q^{o}_{n,i,s}C^{po}_{n}M^{w}+\rho^{w}_{n}q^{w}_{n,i,s}C^{pw}_{n}M^{o})(q^{o}_{n,i,s}+q^{w}_{n,i,s})$$
$$\forall n,i,j,k,s \tag{3.26f}$$

$$q^{o}_{n,i,s}=\frac{q^{s}_{n,i,s}}{SOR_{n,i,s}}\qquad \forall i,\ n,\ s \tag{3.26g}$$

$$q^{w}_{n,i,s}=\frac{\rho^{o}q^{o}_{n,i,s}C^{po}_{n}(T^{s}-T^{r})}{\eta^{eff}X^{s}\lambda^{s}}\qquad \forall i,\ n,\ s \tag{3.26h}$$

$$L_{n,i,s}=\rho^{o}_{n}q^{o}_{n,i,s}M_{w}+\rho^{w}_{n}q^{w}_{n,i,s}M_{o}\qquad \forall i,\ n,\ s \tag{3.26i}$$

$$V^{m}_{n,i+1,0,s}=V^{m}_{n,i,C,s}\qquad \forall i,\ n,\ s \tag{3.26j}$$

$$T^{p}_{n,i+1,0,s}=T^{p}_{n,i,C,s}\qquad \forall i,\ n,\ s \tag{3.26k}$$

$$\underline{A}_{n}\le q^{mo}_{n,i,s}\le\overline{A}_{n}\quad \forall n,i,s \tag{3.26l}$$

$$\underline{B}_{n}\le q^{s}_{n,i,s}\le\overline{B}_{n}\quad \forall n,i,s \tag{3.26m}$$

$$\sum_{n=1}^{N}q^{s}_{n,i,s}\le\bar{C}\quad \forall i,\ s \tag{3.26n}$$

$$\underline{\gamma}\le V^{m}_{n,i,j,s}\le\overline{\gamma}\quad \forall i,n,j,s \tag{3.26o}$$

$$\underline{D}_{n}\le T^{p}_{n,i,j,s}-T^{s}_{n}\le\overline{D}_{n}\quad \forall i,n,j,s \tag{3.26p}$$

$$u_{n,i,s}=u_{n,i,s'}\quad \forall n,i,(s,s')\in SP \tag{3.26q}$$

The notation $u_{i,s}$ represents input u at sample i and s scenario.

Affine policy based method

The uncertainty in SOR is modeled as a function of a primitive uncertainty ξ in N wells.

$$SOR_{n,i}(\xi)=A(n)\xi_{n,i}+(1-\xi_{n,i})B(n)\qquad \forall n,i \tag{3.27}$$

where the lower bound of SOR is represented as $A(n)$, the upper bound is represented as $B(n)$, and ξ satisfies

$$0 \leq \xi_{n,i} \leq 1 \qquad \forall n, i \tag{3.28}$$

The uncertainty from the parameters in N wells can be summarized in a vector as: $\zeta = [1, \xi_{1,1}, ..., \xi_{1,P}, \xi_{2,1}, ..., \xi_{2,P}, ..., \xi_{N,1}, ..., \xi_{N,P}]$. The uncertainty set can be defined as as: $\Xi = \{\zeta : \quad Eqs..3.28\}$. The above set Ξ can be simplified and written as

$$\Xi = \{\xi : W \cdot \zeta \geq h^u\}$$

where W and h^u are a matrix and a vector of known coefficients from the mentioned equations in the uncertainty set, respectively.

Robust counterpart constraint derivation

For those constraints with only input variables, while the constraint satisfaction is enforced for a given uncertainty set, robust counterparts of the constraints are derived. As an example, the procedure for robust counterpart constraints derivation is described below:

1. Consider the stochastic constraint 3.25l :

$$q^{mo}_{n,i}(\zeta) \leq \overline{A}_n \quad \forall i,\ n,\ \zeta \in \Xi$$

2. Apply the LDR and factor $\zeta_{[t-1]}$:

$$\left(\mathbf{q}^{mo}_{n,i}\right)^\top \cdot \boldsymbol{\zeta_{[i-1]}} \leq \overline{A}_n \qquad \forall i, n, \zeta \in \Xi$$

3. Derive the robust counterpart and introduce the truncate operator $P^{\zeta}_{n,mo}$:

$$\left\{ \max_{\zeta \in \Xi} \left(\left(\boldsymbol{q}^{mo}_{n,i}\right)^\top \cdot \boldsymbol{P^{\zeta}_i} \right) \cdot \boldsymbol{\zeta} \right\} \leq \overline{A}_n \qquad \forall i,\ n$$

4. Use the uncertain set definition:

$$\left\{ \begin{array}{l} \max \left(\left(\boldsymbol{q}^{mo}_{n,i}\right)^\top \cdot \boldsymbol{P^{\zeta}_i} \right) . \boldsymbol{\zeta} \\ s.t. \ -\boldsymbol{W} . \boldsymbol{\zeta} \leq -\boldsymbol{h}^u \end{array} \right\} \leq \overline{A}_n \qquad \forall i, n$$

5. Introduce a dual variable $\Lambda^{mo}_{n,i}$ and apply duality to inner LP problem:

$$\left\{ \begin{array}{l} \min \ -\left(\boldsymbol{h}^u\right)^\top \Lambda^{mo1}_{n,i} \\ s.t. \ -\boldsymbol{W}^\top \Lambda^{mo1} = \left(\left(\boldsymbol{q}^{mo}_{n,i}\right)^\top \cdot \boldsymbol{P}^{\zeta}_i \right)^\top \\ \quad \Lambda^{mo1}_{n,i} \geq 0 \end{array} \right\} \leq \overline{A}_n \qquad \forall i, n$$

6. Drop the minimization operator

$$\begin{cases} -\left(\boldsymbol{h}^{u}\right)^{\top}\Lambda_{n,i}^{mo1} \leq \overline{A}_{n} \\ -\boldsymbol{W}^{\top}\Lambda_{n,i}^{mo1} = \left(\left(\boldsymbol{q}_{n,i}^{mo}\right)^{\top}\cdot\boldsymbol{P}_{i}^{\zeta}\right)^{\top} \qquad \forall i,\ n \\ \Lambda_{n,i}^{mo1} \geq 0 \end{cases}$$

The optimization problem is represented as:

$$\begin{aligned}
\min_{q_{n,i}^{s},q_{n,i}^{mo}} \quad & \sum_{n=1}^{N}\sum_{i=1}^{I}\left[\sigma_{c}\cdot\boldsymbol{q}_{n,i}^{s}\mathbb{E}_{\zeta\in\Xi}[\boldsymbol{\zeta}]-\sigma_{p}\cdot\boldsymbol{q}_{n,i}^{mo}\mathbb{E}_{\zeta\in\Xi}[\boldsymbol{\zeta}]\right]+ \\
& \sum_{n=1}^{N}\sum_{i=1}^{I}\gamma_{1}|\boldsymbol{q}_{n,i+1}^{s}\mathbb{E}_{\zeta\in\Xi}[\boldsymbol{\zeta}]-\boldsymbol{q}_{n,i}^{s}\mathbb{E}_{\zeta\in\Xi}[\boldsymbol{\zeta}]|+ \qquad (3.29a) \\
& \sum_{n=1}^{N}\sum_{i=1}^{I}\gamma_{2}|\boldsymbol{q}_{n,i+1}^{mo}\mathbb{E}_{\zeta\in\Xi}[\boldsymbol{\zeta}]-\boldsymbol{q}_{n,i}^{mo}\mathbb{E}_{\zeta\in\Xi}[\boldsymbol{\zeta}]| \\
s.t. & \sum_{j=0}^{C}V_{n,i,j,s}^{m}\frac{dl_{j}}{d\tau}(\tau_{k})=h\Big[q_{n,i,s}^{o}+q_{n,i,s}^{w}-q_{n,i}^{mo}\cdot P_{i}^{\zeta}\zeta\Big] \quad \forall n,i,s \qquad (3.29b) \\
& Q_{1n,i,j,k,s}\sum_{j=0}^{C}T_{n,i,j,s}^{p}\frac{dl_{j}}{d\tau}(\tau_{k})=h\Big[L_{i}(q_{n,i,s}^{o}+q_{n,i,s}^{w})\hat{Q}+Q_{2n,i,j,k,s}-Q_{3n,i,j,k,s}(T_{n,i,k,s}^{p}-T^{r})\Big] \\
& \qquad \forall n,i,j,k,s \qquad (3.29c) \\
& Q_{1n,i,j,k,s}=(\rho^{o}q_{n,i,s}^{o}C_{n}^{po}M^{w}+\rho^{w}q_{n,i,s}^{w}C_{n}^{pw}M^{o})(\rho_{n}^{o}q_{n,i,s}^{o}+\rho_{n}^{w}q_{n,i,s}^{w})V_{n,i,k,s}^{m} \\
& \qquad \forall n,i,j,k,s \qquad (3.29d) \\
& Q_{2n,i,j,k,s}=L_{n,i,s}(q_{n,i,s}^{o}+q_{n,i,s}^{w})(\rho_{n}^{o}q_{n,i,s}^{o}C_{n}^{po}+\rho_{n}^{w}q_{n,i,s}^{w}C_{n}^{pw})(T_{n}^{s}-T^{r}) \\
& \qquad \forall n,i,j,k,s \qquad (3.29e) \\
& Q_{3n,i,j,k,s}=(\rho_{n}^{o}q_{n,i,s}^{o}+\rho_{n}^{w}q_{n,i,s}^{w})(\rho_{n}^{o}q_{n,i,s}^{o}C_{n}^{po}M^{w}+\rho_{n}^{w}q_{n,i,s}^{w}C_{n}^{pw}M^{o})(q_{n,i,s}^{o}+q_{n,i,s}^{w}) \\
& \qquad \forall n,i,j,k,s \qquad (3.29f) \\
& q_{n,i,s}^{o}=\frac{q_{n,i}^{s}\cdot P_{i}^{\zeta}\zeta}{SOR_{n,i,s}} \quad \forall i,\ n,\ s \qquad (3.29g) \\
& q_{n,i,s}^{w}=\frac{\rho^{o}q_{n,i,s}^{o}C_{n}^{po}(T^{s}-T^{r})}{\eta^{eff}X^{s}\lambda^{s}} \quad \forall i,\ n,\ s \qquad (3.29h) \\
& L_{n,i,s}=\rho_{n}^{o}q_{n,i,s}^{o}M_{w}+\rho_{n}^{w}q_{n,i,s}^{w}M_{o} \quad \forall i,\ n,\ s \qquad (3.29i) \\
& V_{n,i+1,0,s}^{m}=V_{n,i,C,s}^{m} \quad \forall i,\ n,\ s \qquad (3.29j) \\
& T_{n,i+1,0,s}^{p}=T_{n,i,C,s}^{p} \quad \forall i,\ n,\ s \qquad (3.29k)
\end{aligned}$$

$$\begin{cases} -\left(\boldsymbol{h}^u\right)^\top \Lambda^{mo1}_{n,i} \leq \bar{A}_n \\ -\boldsymbol{W}^\top \Lambda^{mo2}_{n,i} = \left(\left(\boldsymbol{q}^{mo}_{n,i}\right)^\top \cdot \boldsymbol{P}^\zeta_i\right)^\top \qquad \forall i,\ n \\ \Lambda^{mo1}_{n,i} \geq 0 \end{cases} \tag{3.29l}$$

$$\begin{cases} -\left(\boldsymbol{h}^u\right)^\top \Lambda^{mo2}_{n,i} \leq -\underline{A}_n \\ -\boldsymbol{W}^\top \Lambda^{mo2}_{n,i} = \left(\left(-\boldsymbol{q}^{mo}_{n,i}\right)^\top \cdot \boldsymbol{P}^\zeta_i\right)^\top \qquad \forall i,\ n \\ \Lambda^{mo2}_{n,i} \geq 0 \end{cases} \tag{3.29m}$$

$$\begin{cases} -\left(\boldsymbol{h}^u\right)^\top \Lambda^{s1}_{n,i} \leq \bar{B}_n \\ -\boldsymbol{W}^\top \Lambda^{s1}_{n,i} = \left(\left(\boldsymbol{q}^{s}_{n,i}\right)^\top \cdot \boldsymbol{P}^\zeta_i\right)^\top \qquad \forall i,\ n \\ \Lambda^{s1}_{n,i} \geq 0 \end{cases} \tag{3.29n}$$

$$\begin{cases} -\left(\boldsymbol{h}^u\right)^\top \Lambda^{s2}_{n,i} \leq -\underline{B}_n \\ -\boldsymbol{W}^\top \Lambda^{s2}_{n,i} = \left(\left(-\boldsymbol{q}^{s}_{n,i}\right)^\top \cdot \boldsymbol{P}^\zeta_i\right)^\top \qquad \forall i,\ n \\ \Lambda^{s2}_{n,i} \geq 0 \end{cases} \tag{3.29o}$$

$$\begin{cases} -\left(\boldsymbol{h}^u\right)^\top \Lambda^{st}_{i} \leq \overline{C} \\ -\boldsymbol{W}^T \Lambda^{st}_{i} = \left(\sum_{n=1}^{N}\left(\boldsymbol{q}^{s}_{n,i}\right)^\top \cdot \boldsymbol{P}^\zeta_i\right)^\top \qquad \forall i, n \\ \Lambda^{st}_{n,i} \geq 0 \end{cases} \tag{3.29p}$$

$$\underline{\gamma} \leq V^m_{n,i,j,s} \leq \overline{\gamma} \quad \forall i, n, j,\ s \tag{3.29q}$$

$$\underline{D}_n \leq T^p_{n,i,j,s} - T^s_n \leq \overline{D}_n \quad \forall i, n, j,\ s \tag{3.29r}$$

where equations 3.29l - 3.29p are the robust counterpart constraints, which correspond to the stochastic constraints 3.26l - 3.26p, respectively. Note that explicit nonanticipativity constraints are not needed here since the affine decision rule covers this condition.

Robust optimization was developed by [64, 65]. They consider an uncertainty set without full probability distribution information. Finally, both the scenario tree model and the affine policy model are nonlinear optimization problem. They are solved using the NLP solver IPOPT in this work.

3.4 Simulations and results

The discretized NLP is implemented in GAMS for a system of two well pairs. The reservoir parameters of the two wells are shown in Table 3.2. Radau collocation of order 3 is chosen.

Table 3.2: Well parameters

	Well 1	Well 2
$\rho_o(kg/m^3)$	1005	920
$\rho_w(kg/m^3)$	920	827.32
SOR	3.65	4.15
$P(kPa)$	2000	3000
$T_r(^\circ C)$	4	4
$T_s(^\circ C)$	212	233
$C_{po}(J/kg/^\circ C)$	1.9	1.98
$C_{pw}(J/kg/^\circ C)$	4.57	4.71
$\sigma_c(\$/m^3)$	95	95
$\sigma_p(\$/m^3)$	373	373

The simulations were carried out on a 4-core Intel i5-6500 CPU@3.2 GHz with 8GB RAM. The process model was solved on MATLAB 2018b using ODE45, and the optimization problem is solved on GAMS 25.1.1.

The initial condition is supplied to GAMS through MATLAB. The solution to the algebraic equations provides the initial condition to the next element. The steam injection and oil production rate are obtained for the entire prediction horizon. Only the first input is applied to the process model; the state obtained is then sent as the initial condition for optimizer. Using ode45 and the inputs provided from GAMS, the process is integrated in the same interval length as set in GAMS. The Fig. 3.4 represents the methodology of integration and inputs applied.

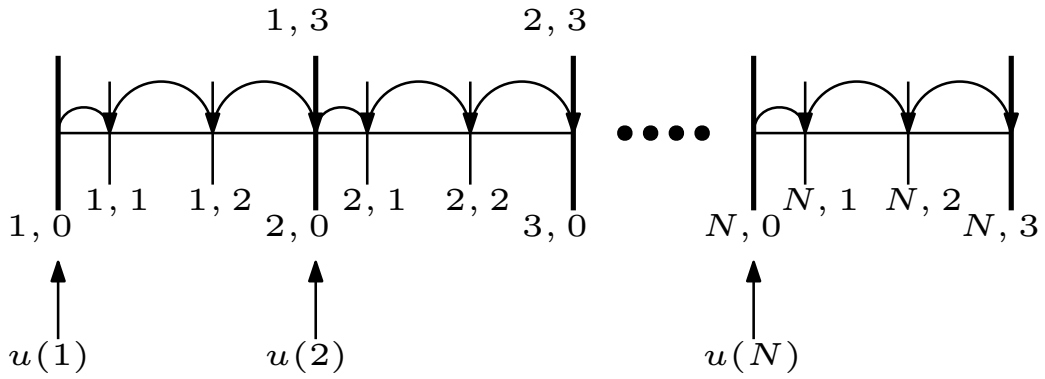

Figure 3.4: The figure shows the timeline for implementing optimal inputs at time i. The input $u(1)$ stays constant over the collocation points and is applied at the beginning of period 1. The state is then integrated within the time element i between collocation points j. The state evolves as $x_{i,j}...x_{i,c}$ where i represents time element and j represents the collocation point.

The simulation and the process were initialized with the same set of SOR's and the

optimal controller kept the temperature and volume profiles under the set constraints as shown in Fig. 3.27a. Three representative scenarios were picked to capture the uncertainty in the parameters. The three scenarios are represented by Fig. 3.5.

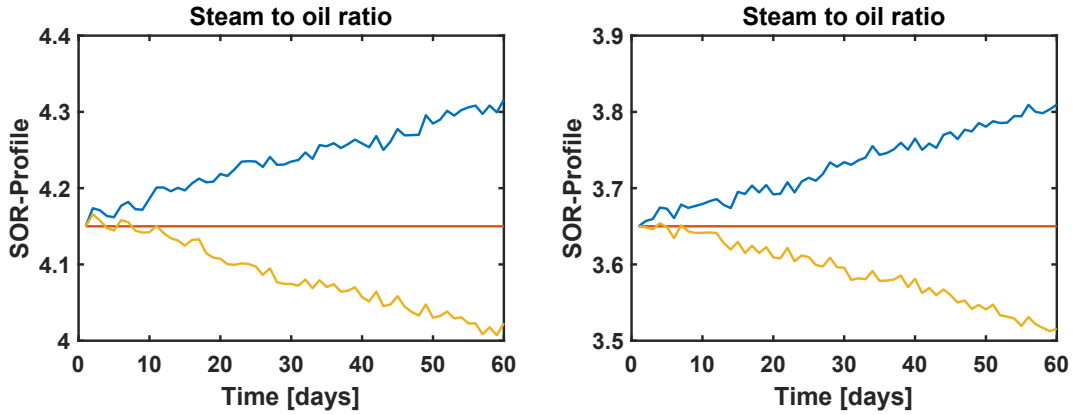

Figure 3.5: Three representative SOR Profiles well 1(left) and well 2(right)

Monte-Carlo simulations were used to generate 100 scenarios with a normal distribution, mean set at 0 and standard deviation 1. The formula to generate the scenario is given as: $SOR_{n,i+1} = SOR_{n,i} + R_n$ where, R_n represents the random number generated from the normal distribution. Fig. 3.6 shows the SOR profile generated for two separate SAGD wells.The SOR used here is instantaneous SOR (ISOR). The oil produced from the reservoir, draining into the liquid pool in the steam chamber is calculated based on the steam injection and the ISOR. The deviation assumed on ISOR reflect the daily basis non-constant oil production rate caused by the reservoir geological condition change as the production goes on. The deviations from the nominal value are not of large magnitude in the short term (± 0.3 dimensionless units).

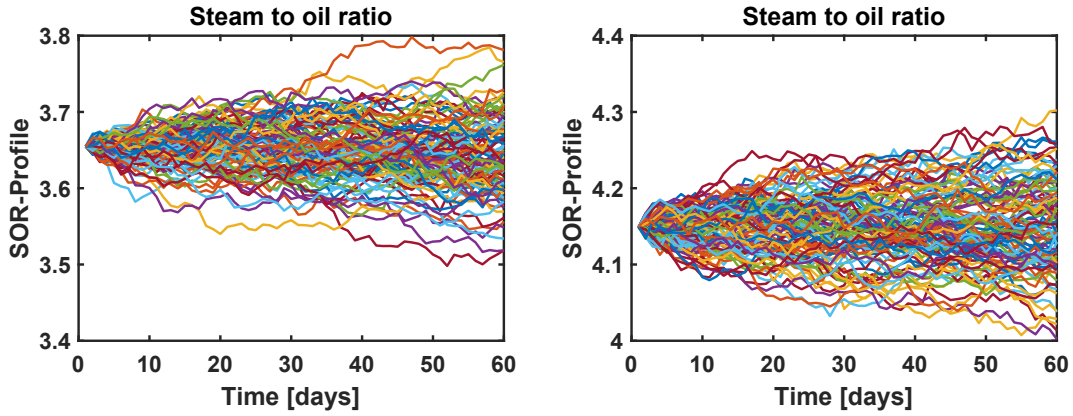

Figure 3.6: SOR Profiles generated using monte-carlo simulations for 100 different scenarios. Well 1(left) and well 2(right)

Deterministic optimization

For the deterministic case, the process model with the optimizer was solved with a static nominal value for SOR. The rolling horizon approach was implemented by using the same SOR for the process and optimization model, and the initialization for the next time instant was obtained from the process model's previous state. When

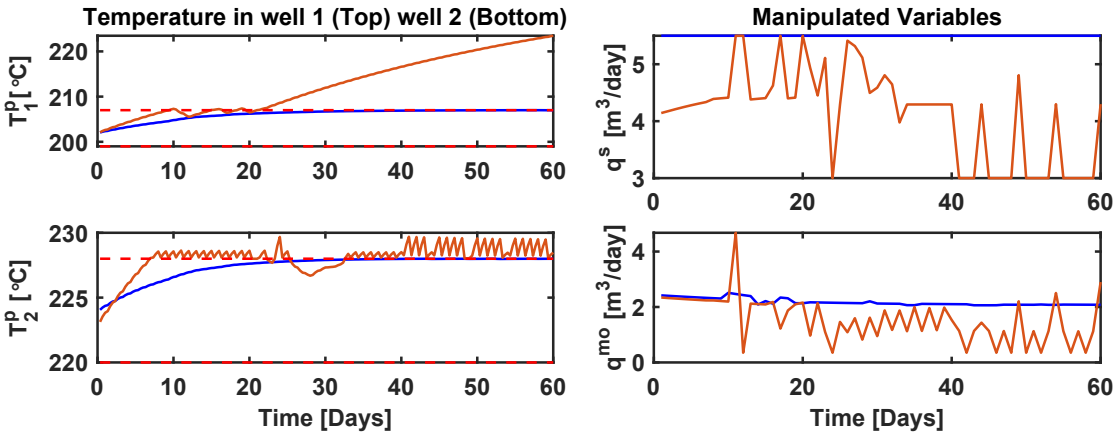

(a) Temperature profile (b) Manipulated variables

Figure 3.7: (a) The figure represents the temperature profile for deterministic case(Blue) and the case where there is a slight mismatch in the SOR parameter(Orange). The dotted-red lines represent the constraints on sub-cool which are clearly violated when there is a mismatch in the parameter. (b) This figure represents the 1)Steam injection rate on the top and 2) Oil production rate on the bottom. The steam allocation was set to a maximum value of $5.5m^3/day$ that was constantly achieved in the deterministic case, the case with the mismatch however does not use the max allowed allocation

SOR is slightly perturbed from its normal constant value, the nominal value of SOR is supplied to the optimizer whereas the increasing scenario profile is supplied to the process as the true SOR. The slight mismatch causes the temperature to overshoot by a big margin and violate the constraint as shown in Fig. 3.27a. The figure shows that, for NMPC, lack of addressing the uncertainty involved with parameters can lead to solution that violates the constraints and cause operational difficulties.

Worst-case open-loop optimization

Worst-case optimization is performed by feeding the most conservative realization of SOR for both wells. The increasing random profiles of SOR are being fed to the process model, whereas the optimizer works only with the constant conservative value supplied to it. The temperature of liquid pool is shown in Fig. 3.8. The results are

shown for completely optimal solutions by the optimizer. The temperature profiles of all the scenarios stayed well within the constraints with the steam allocation constraint active. The worst-case method utilizing the most conservative parameter to obtain the solution does not give a very profitable estimate of control inputs as shown in Fig. 3.9. This use of an open-loop method does not take into consideration the availability of new information for the next time step. Such a static solution thus would not give an optimal solution.

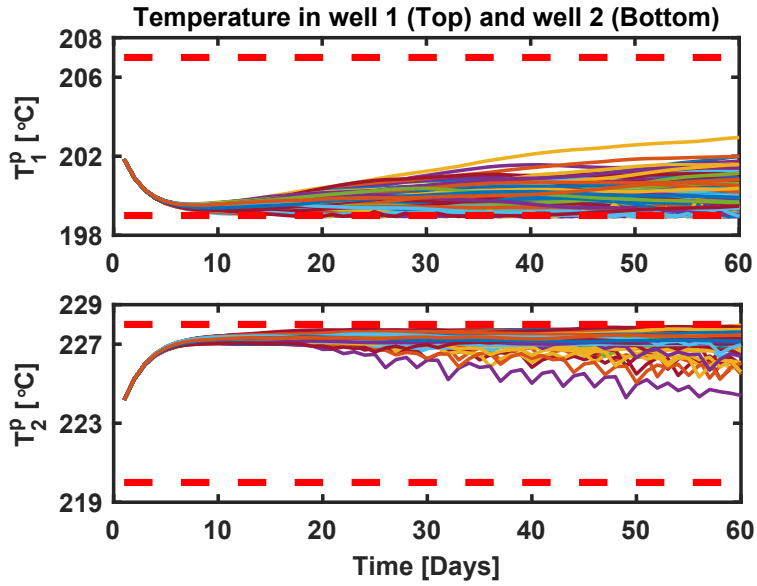

Figure 3.8: The temperature of liquid pool in well 1 and 2 for 100 scenarios using worst-case optimization. The dotted red lines represent the constraints for sub-cool and the controller does not violate the set constraints.

Scenario tree based optimization

The scenario tree used for addressing the uncertainty is given in Fig. 3.10. The robustness of the solution to the uncertainty from SOR can be offset by presenting the extreme values in the scenario tree. The temperature and steam injection of scenario tree based optimization for three representative scenarios are shown in Fig. 3.11 respectively for a robust horizon 1. The states for the extreme scenarios stay well within the set constraints with the steam allocation constraint active. The profit obtained for the three representative scenarios is given in Fig. 3.12. The profits increase from scenario 1 to scenario 3. As the SOR continues to decrease, there is an increase in the obtained profit.

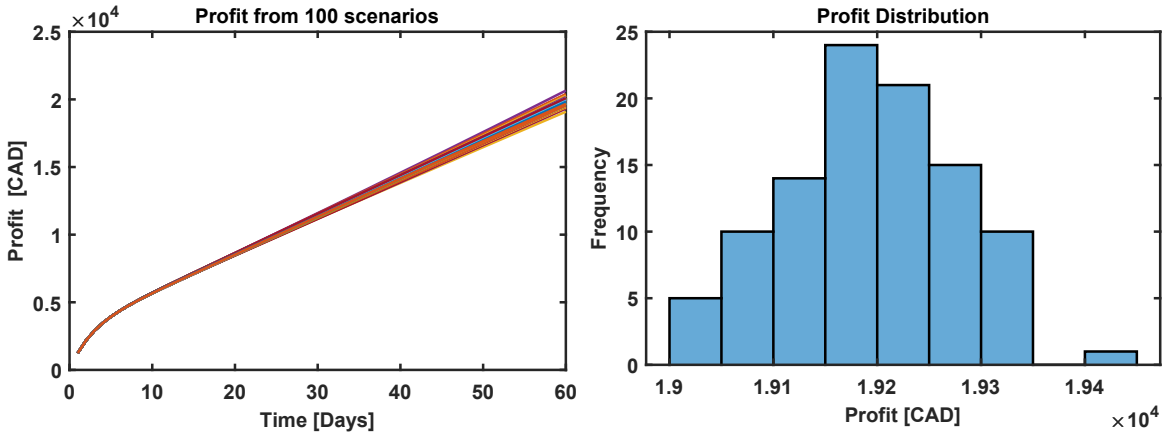

(a) Cumulative profit plot (b) Histogram of profits obtained

Figure 3.9: (a) The figure represents the cumulative profits obtained from worst-case method. The plot has representative profits for 100 scenarios.(b) The histogram gives a frequency of profits obtained from 100 scenarios. The mean cumulative profit obtained over 60 days is $19212.

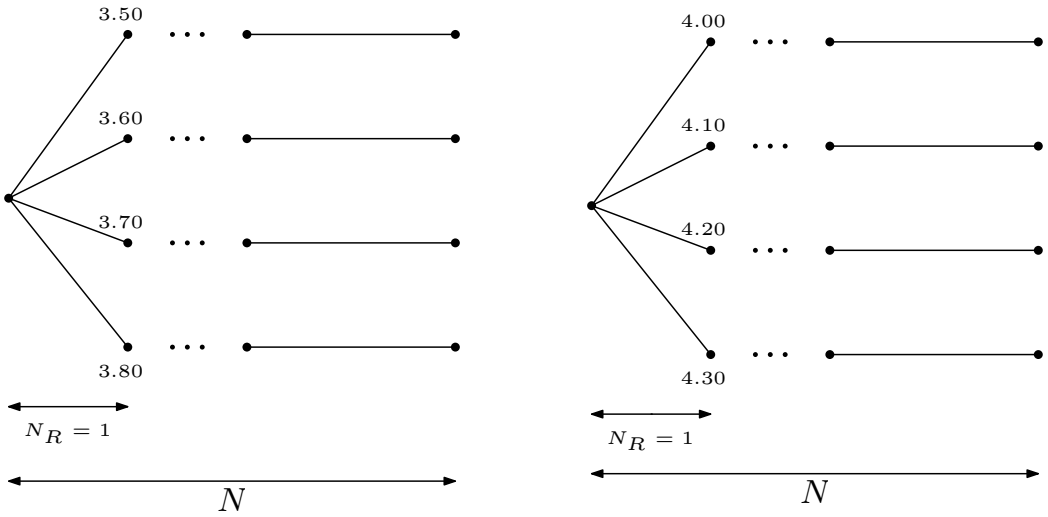

(a) Scenario tree well-pair 1 (b) Scenario tree well-pair 2

Figure 3.10: (a) The figure shows the scenarios considered for well pair 1 with a nominal value at the first node and the highest possible value of SOR at the 4th node (b) The figure shows the scenarios considered for well pair 2 with a nominal value at the first node and the highest possible value of SOR at the 4th node. Both the scenario trees have a robust horizon of 1 as the branching stops at time instant 1.

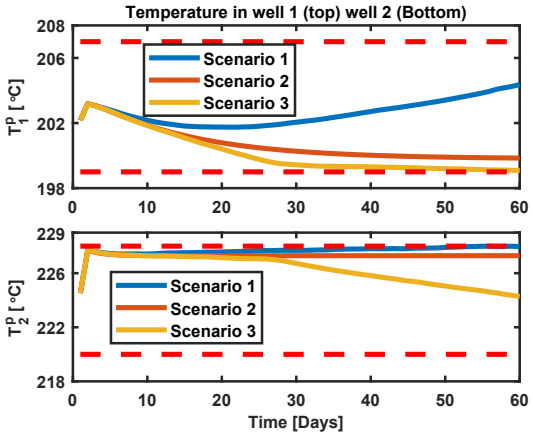

(a) Temperature profile for 3 scenarios

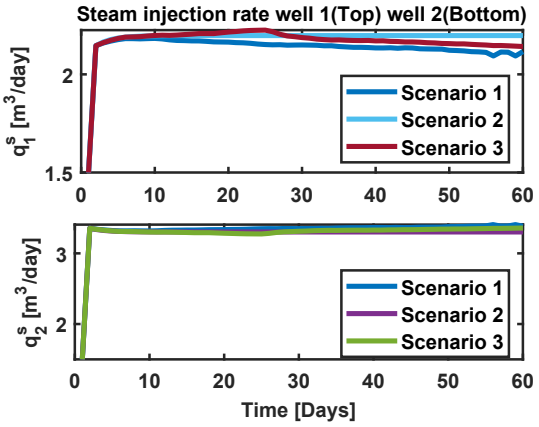

(b) Steam injection rate for 2 well pairs

Figure 3.11: (a) The figure shows the temperature for the three extreme scenarios chosen, the sub-cool constraints are not violated. (b) The manipulated variables for well 1(Top) and well 2(Bottom)

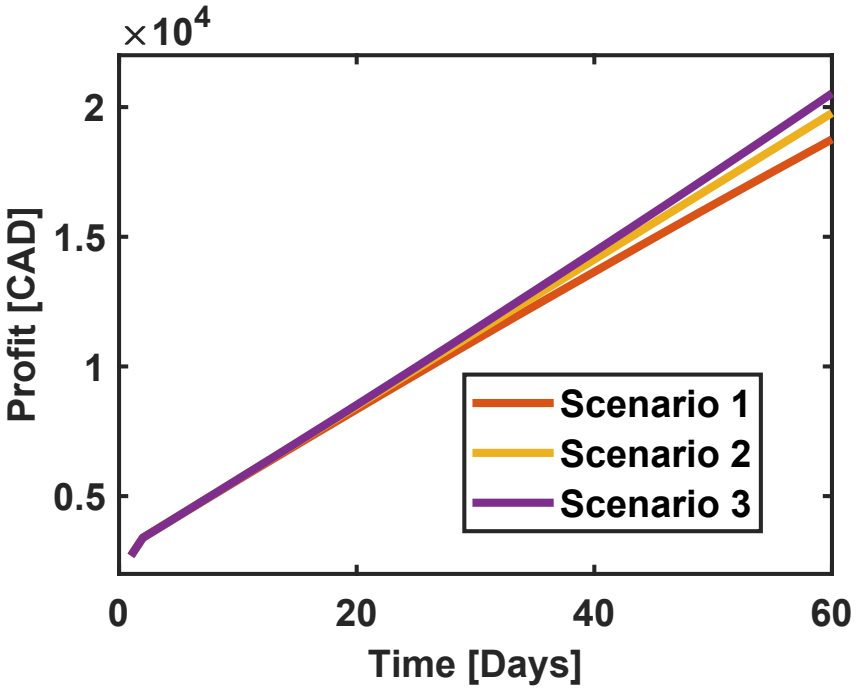

Figure 3.12: Cumulative profits obtained from 3 scenarios

The method applied to the 100 scenarios gave a statistically significant result for the said method. [66]The scenario tree with a robust horizon 1 was enough to address the deviations presented by the 100 scenarios as seen in Fig. 3.13. The cumulative profit plot for the 100 scenarios and the histogram are represented in Fig. 3.14.

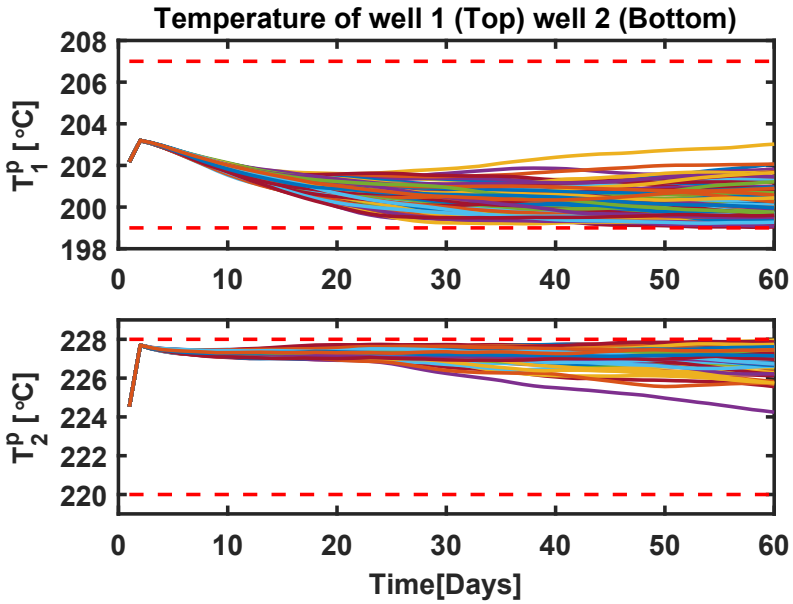

Figure 3.13: The temperature of liquid pool in well 1 and 2 for 100 scenarios using scenario tree based optimization. The dotted red lines represent the constraints for sub-cool and the controller does not violate the set constraints.

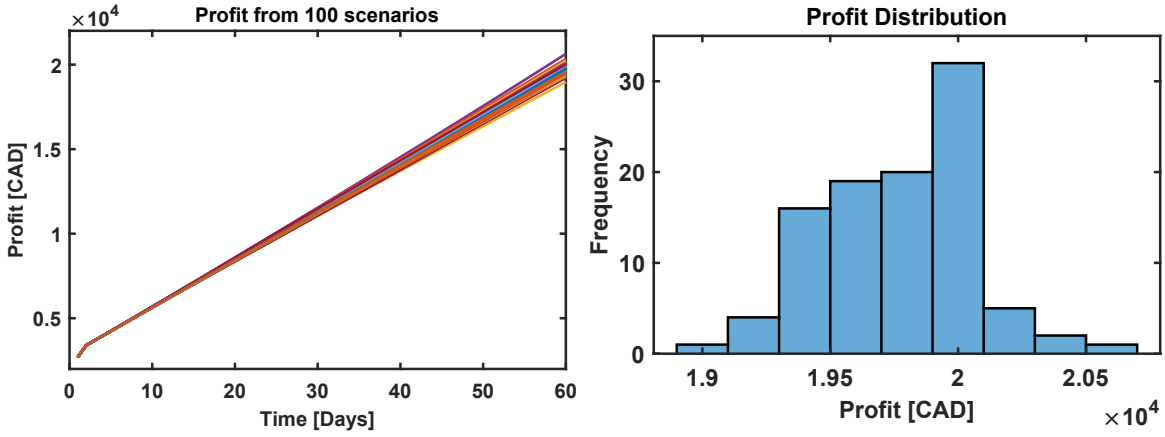

(a) Cumulative profit plot

(b) Histogram of profits obtained

Figure 3.14: (a) The figure represents the cumulative profits obtained from scenario tree based method. The plot has representative profits for 100 scenarios.(b) The histogram gives a frequency of profits obtained from 100 scenarios. The mean cumulative profit obtained over 60 days is \$19770.

The robust horizon being 1 prevents the excessive branching, and hence provides a solution quicker than that of a robust horizon 2. The computational load increases as the number of scenarios and corresponding branching increases. The scenario tree with robust horizon 2 is shown in Fig. 3.15. The extreme values of the parameters are used in designing the scenario tree to ensure feasibility at points not represented

explicitly in the scenario tree.

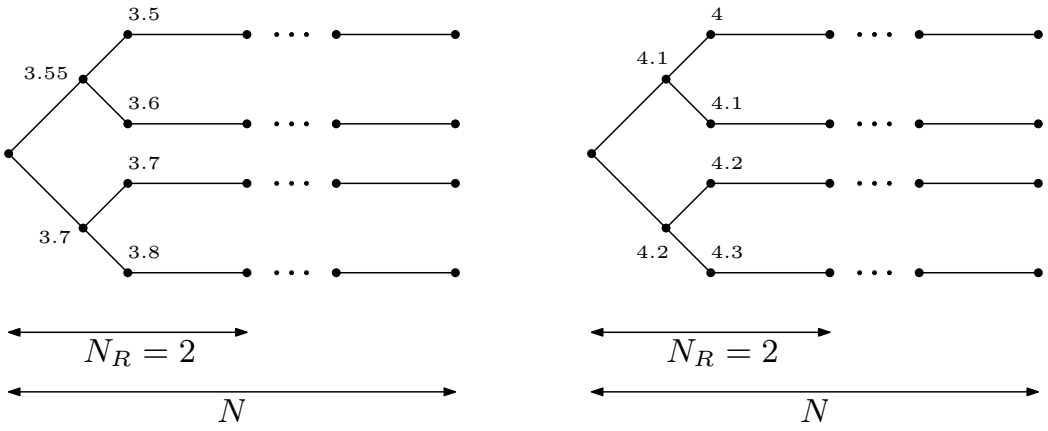

(a) Scenario tree well-pair 1 (b) Scenario tree well-pair 2

Figure 3.15: (a) The figure shows the scenarios considered for well pair 1 with a nominal value at the first node and the highest possible value of SOR at the 4th node (b) The figure shows the scenarios considered for well pair 2 with a nominal value at the first node and the highest possible value of SOR at the 4th node. Both the scenario trees have a robust horizon of 2 as the branching stops at time instant 2.

The results for scenario tree based optimization with robust horizon 2 are shown in Fig. 3.16. The profits obtained for three representative scenarios is shown in Fig. 3.17. The states for the three scenarios stay well within the constraints for the nominal, and the two extreme cases. The profits increase as the SOR decreases with time as expected.

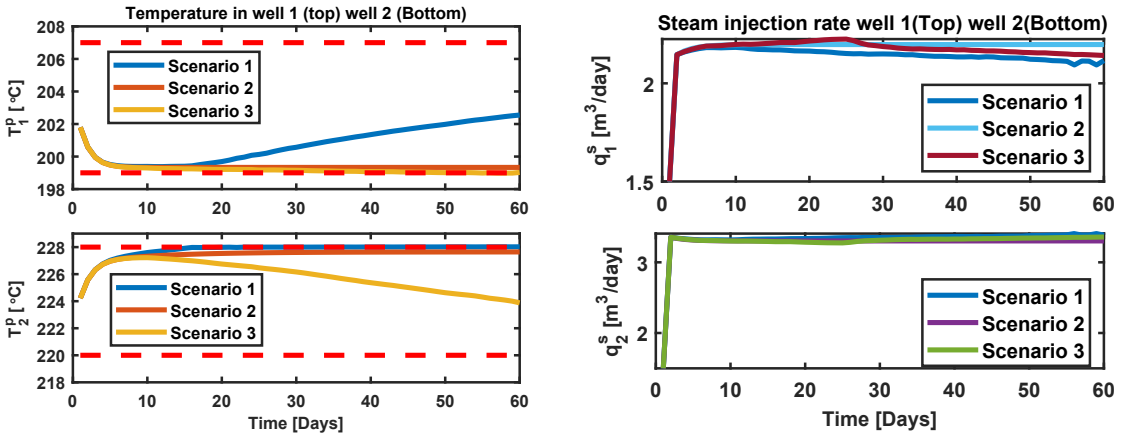

(a) Temperature profile for 3 scenarios (b) Steam injection rate for 2 well pairs

Figure 3.16: (a) The figure shows the temperature for the three extreme scenarios chosen, the sub-cool constraints are not violated. (b) The manipulated variables for well 1(Top) and well 2(Bottom)

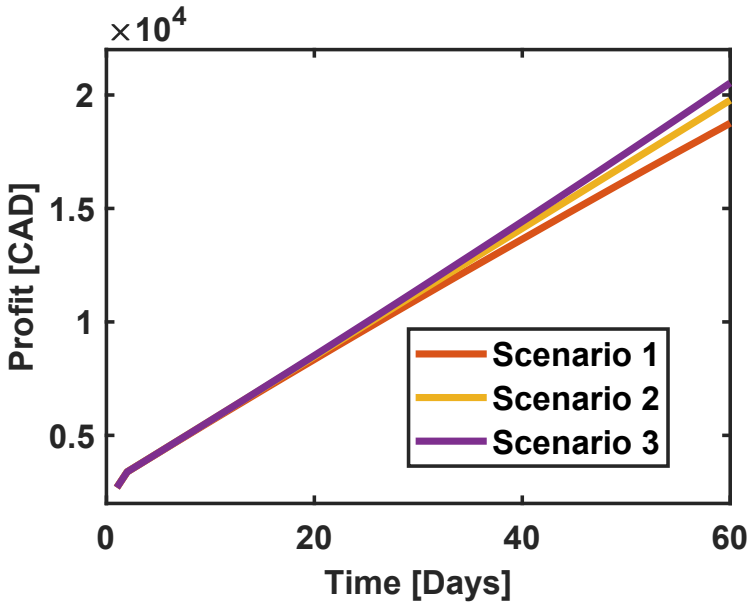

Figure 3.17: Cumulative profits obtained from 3 scenarios

Scenario tree based method with a robust horizon 2 was applied to the 100 scenarios. The states and cumulative profit obtained for 100 scenarios are given below. The results obtained by $N_R = 1$ and $N_R = 2$ do not vary as much and either one can be used provided the number of scenarios remains constant.

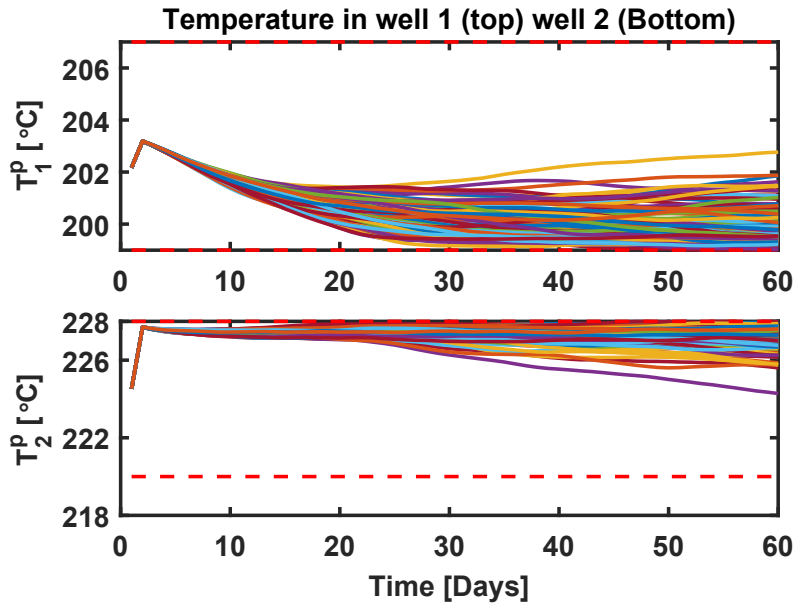

Figure 3.18: The temperature of liquid pool in well 1 and 2 for 100 scenarios using scenario tree based optimization for a robust horizon of 2. The dotted red lines represent the constraints for sub-cool and the controller does not violate the set constraints.

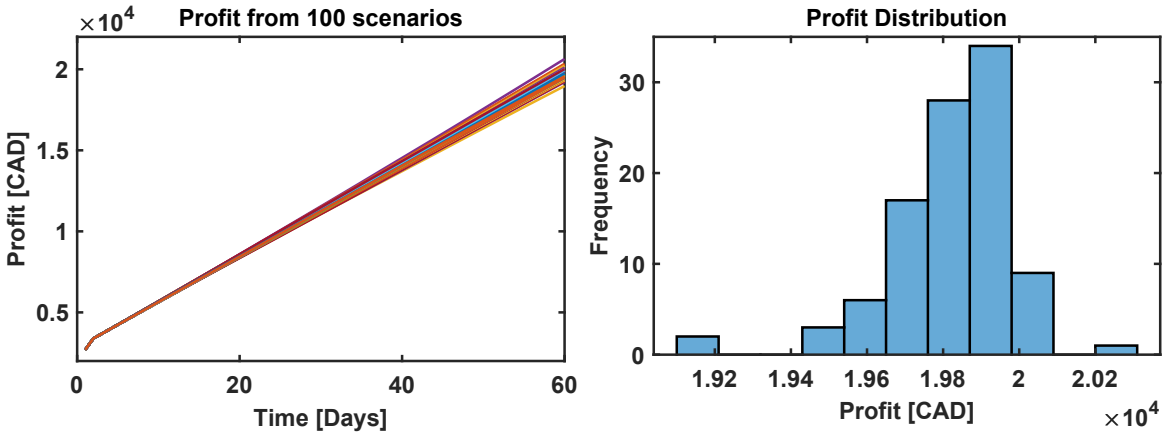

(a) Cumulative profit plot

(b) Histogram of profits obtained

Figure 3.19: (a) The figure represents the cumulative profits obtained from scenario tree based method (Robust horizon 2). The plot has representative profits for 100 scenarios.(b) The histogram gives a frequency of profits obtained from 100 scenarios. The mean cumulative profit obtained over 60 days is $19838.

Scenario tree method with robust horizon 2 requires 24.35% more time to compute than scenario tree method with robust horizon 1 without enough economic profitability as shown in Table 3.3.

Affine policy based optimization

Next, the affine method is applied to bring in feedback to the control loop. This method was applied in two ways: 1) Rolling-horizon fashion and 2) Re-optimization after prediction horizon. In rolling horizon fashion the inputs obtained at the first sample instant is applied, after which the problem is re-optimized. In the latter however, the policy obtained is utilized to obtain inputs until the prediction horizon after which the problem is re-optimized.

The affine policy based method brings in feedback control thus making it a closed-loop method [25]. The scenario tree with a robust horizon of 1 is used along with affine policy in a rolling-horizon fashion. The states and manipulated variables are as shown in Fig. 3.20. The profits for three representative scenarios are given in Fig. 3.21.

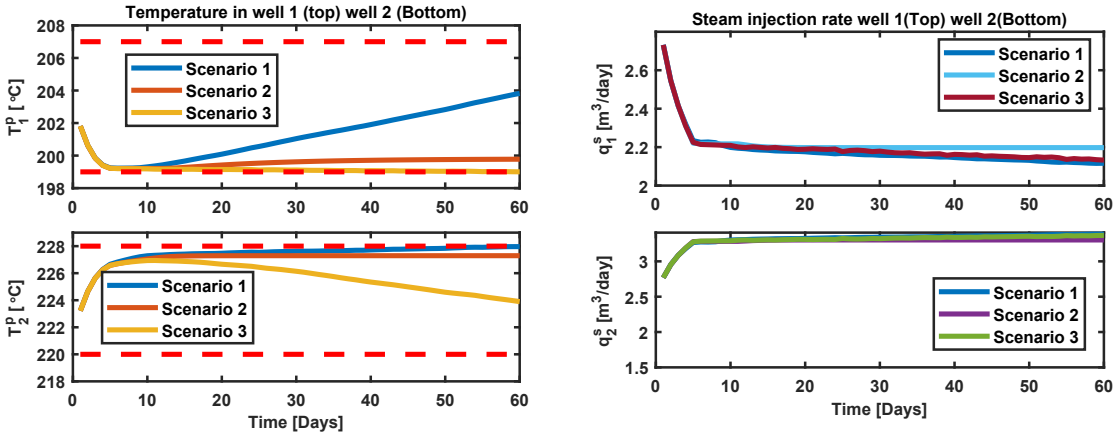

(a) Temperature profile for 3 scenarios (b) Steam injection rate for 2 well pairs

Figure 3.20: (a) The figure shows the temperature for the three extreme scenarios chosen, the sub-cool constraints are not violated, using affine policy based method with rolling horizon (b) The manipulated variables for well 1(Top) and well 2(Bottom)

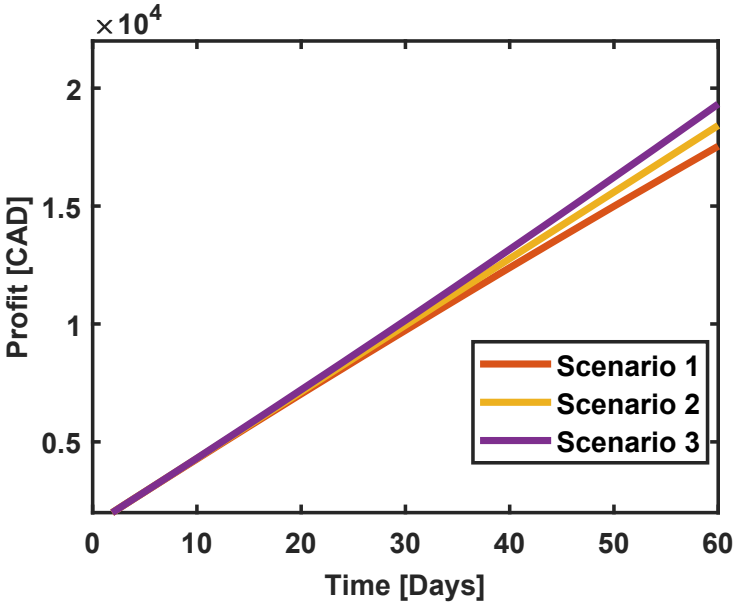

Figure 3.21: Cumulative profit obtained for 3 scenarios

The state and manipulated variables for the three scenarios resemble the ones presented by scenario tree method $N_R = 1$. The profits obtained, however, are less than that obtained from the open-loop method as the policy obtained is optimal for the entire prediction horizon whereas, only the input obtained at first instant is applied and the problem is re-optimized. To get a statistically significant difference between profits obtained between scenario tree and affine methods, the same is applied on 100 scenarios. The state for 100 scenarios are given in Fig .3.22.

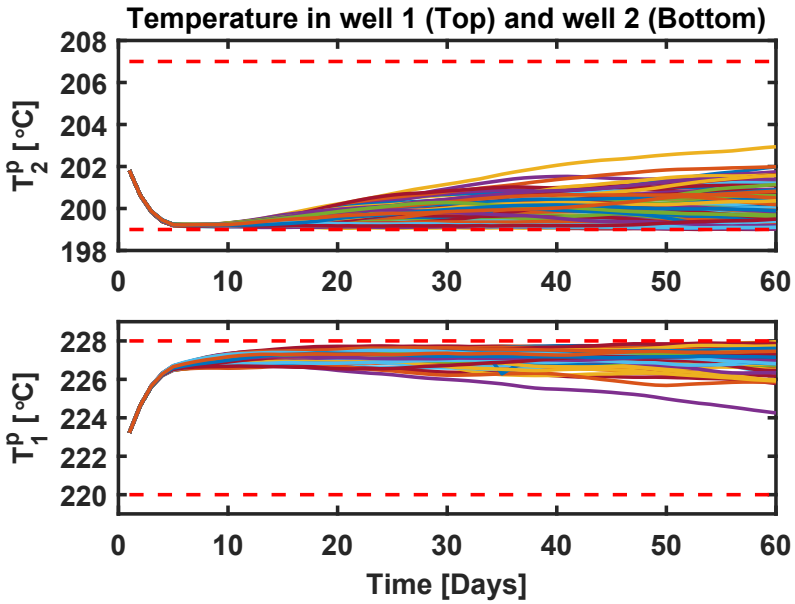

Figure 3.22: The temperature of liquid pool in well 1 and 2 for 100 scenarios using affine policy based optimization in a rolling horizon fashion. The dotted red lines represent the constraints for sub-cool and the controller does not violate the set constraints.

The profit obtained for 100 scenarios and the distribution is shown in Fig. 3.23.

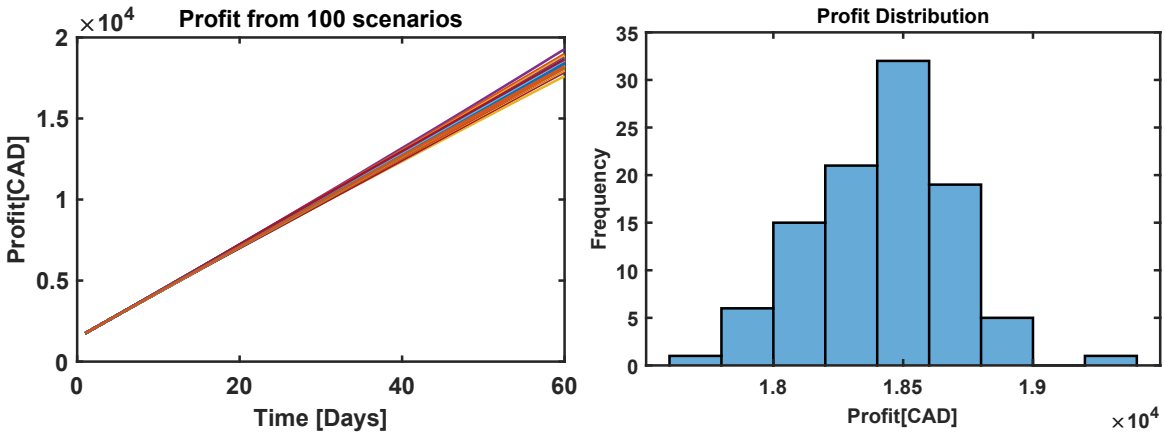

(a) Cumulative profit plot (b) Histogram of profits obtained

Figure 3.23: (a) The figure represents the cumulative profits obtained from affine policy based method with rolling horizon. The plot has representative profits for 100 scenarios.(b) The histogram gives a frequency of profits obtained from 100 scenarios. The mean cumulative profit obtained over 60 days is \$18417.

As seen from the histogram, the obtained mean over 100 scenarios has a sub-par performance when compared to the scenario tree method as well as static robust(worst-case) method.

The above results show that applying affine policy in a rolling horizon manner and re-optimize the policy at every step does not lead to superior solution performance. Next, we apply the affine policy method but re-optimization at the end of the prediction horizon (denoted as "no-rolling horizon"), the results obtained show a very different trend than the ones obtained with open-loop methods. The results for 3 scenarios with rolling-horizon after the prediction horizon are given in Fig. 3.24 for states and Fig. 3.25 shows the profit obtained. The profits are summarized in Table 3.4.

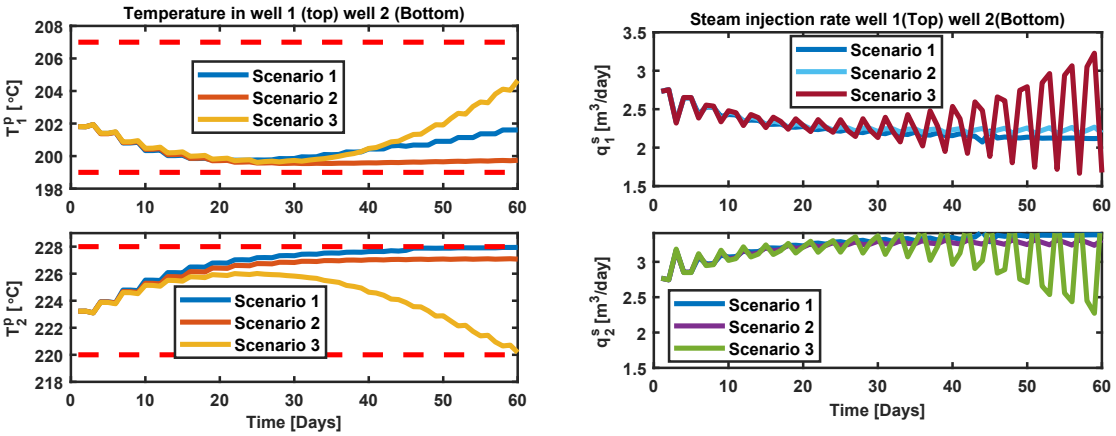

(a) Temperature profile for 3 scenarios

(b) Steam injection rate for 2 well pairs

Figure 3.24: (a) The figure shows the temperature for the three extreme scenarios chosen, the sub-cool constraints are not violated, using affine policy based method without rolling horizon (b) The manipulated variables for well 1(Top) and well 2(Bottom)

The states as seen above stay well within the set constraints. The profits obtained from the three methods show a much higher profit compared to that of the other methods.

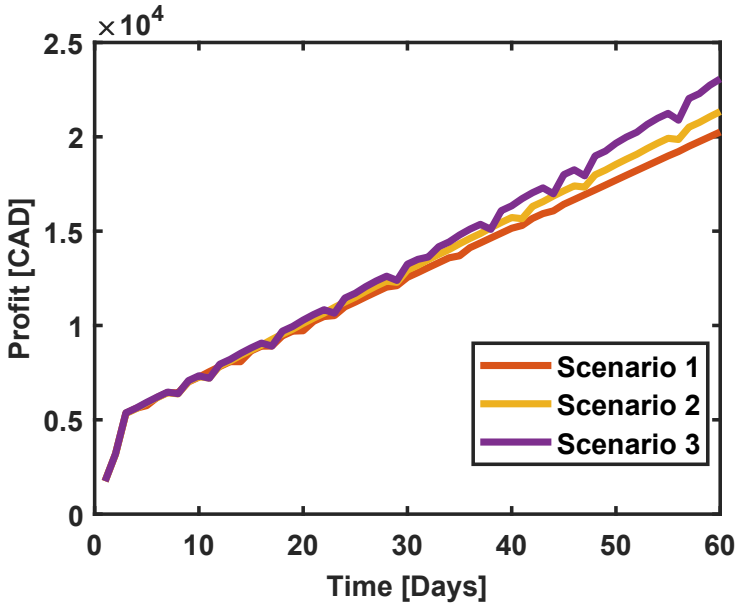

Figure 3.25: Cumulative profit obtained for 3 scenarios

The same method is applied for 100 scenarios to show statistically significance in performance. The subcool state for 100 scenarios is shown in Fig. 3.26. The profit obtained for 100 cumulative scenarios and the distribution is given in Fig. 3.27. The profits statistics are summarized in Table 3.3.

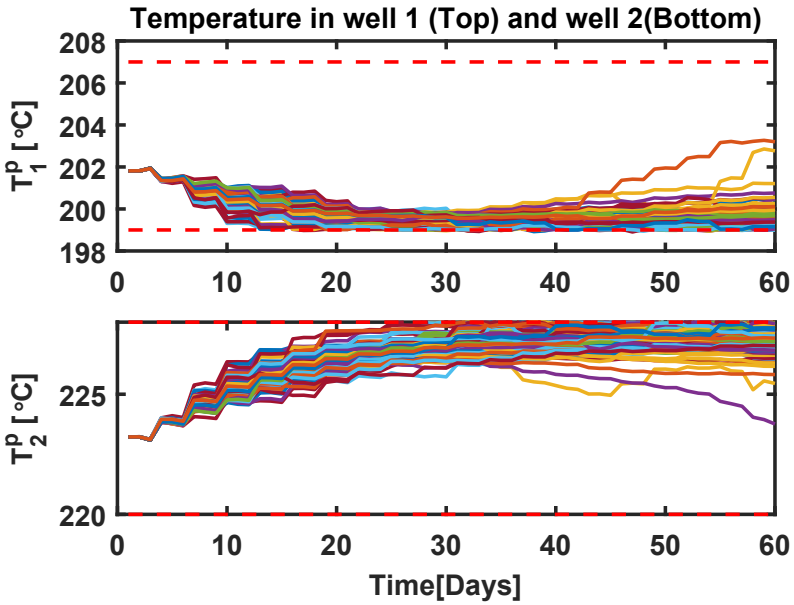

Figure 3.26: Temperature of liquid pool in well 1 and well 2

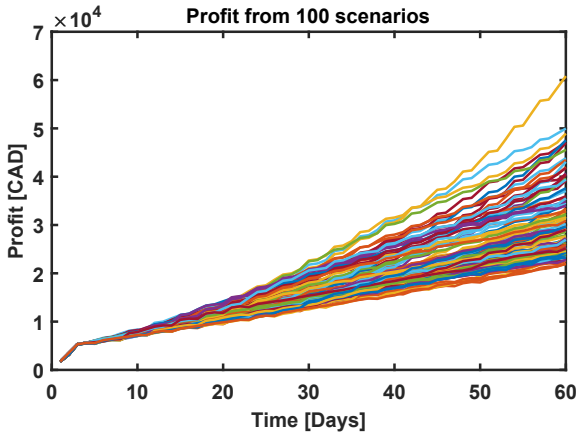

(a) Temperature profile for 3 scenarios

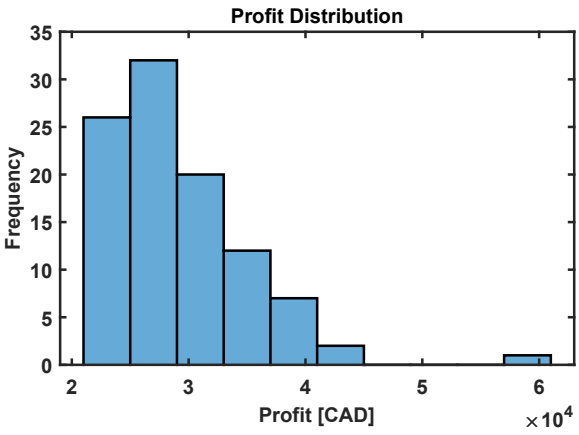

(b) Steam injection rate for 2 well pairs

Figure 3.27: (a) The figure shows the temperature for 100 scenarios generated by monte carlo method, the sub-cool constraints are not violated, using affine policy based method without rolling horizon (b) The histogram gives a frequency of profits obtained from 100 scenarios. The mean cumulative profit obtained over 60 days is \$30988.

	Static Robust	Scenario ($N_R = 1$)	Scenario ($N_R = 2$)	Affine (Rolling horizon)	Affine (No-rolling horizon)
Mean	19212	19770	19838	18417	30988
Standard deviation	91.7	282.3	156.8	282.3	7655.1
Time taken	3804.7s	4331.4s	5386.1s	17050s	5993.7s

Table 3.3: The table represents the mean and variance for profits obtained using different methods for 100 scenarios. The time taken for each method to compute 60 days of input was averaged out over 100 scenarios and is presented in seconds.

	Static Robust	Scenario ($N_R = 1$)	Scenario ($N_R = 2$)	Affine (Rolling horizon)	Affine (No-rolling horizon)
Scenario 1	18594	18891	19050	17538	20255
Scenario 2	19519	19770	19906	18417	21337
Scenario 3	20333	20684	20776	19326	23069

Table 3.4: Profits obtained from 3 representative scenarios

3.5 Conclusion

In this work, we presented an optimization method for SAGD reservoir steam allocation and oil production optimization considering SOR uncertainty. First principles model of the SAGD process is used for NMPC problem formulation. The uncertainty in SOR is dealt with using multistage stochastic optimization technique. The use of an evolving scenario tree to model uncertainty helps make an intractable problem tractable in real-time optimization. The scenario tree method with a robust horizon performs well compared to worst-case static robust method. Furthermore, when the

affine policy method is implemented with a rolling-horizon method after the end of each prediction horizon, it provides the highest operating profits compared to the other methods. The computational time required for affine policy based method using rolling horizon at the end of rolling horizon, utilizes 38.3% more time than scenario tree based method but gives a profit that is higher by 56.74%. The closed-loop method also shows superiority in handling the states close to their constrained values.

Chapter 4

Integrated well pad development scheduling with steam allocation optimization in Steam Assisted Gravity Drainage

In this work, we consider a linear mathematical model to schedule multiple well pairs over the planning horizon. Nonlinear SAGD model has been adopted from Gotawala and Gates [67] and implemented in the NMPC setup. The integrated problem is solved hierarchically in a shrinking horizon fashion for the scheduling level and in a rolling horizon mode for the control level. The NMPC achieved perfect control on all the active well pads while minimizing an economic objective. The scheduler used relevant information from the lower level control problem in order to reschedule and commission the adequate number of wells to provide highest profit. The section 4.1 introduces the problem statement tackled in this chapter. The section 4.2 introduces the mathematical model used for the upper and lower level problem. The section 4.3 portrays the methodology used in the chapter. The section 4.4 portrays and explains the results obtained.

4.1 Problem statement

SAGD development involves developing and positioning well pads in the area leased from the government. The optimal positioning and development of well pads is an important area of study for the profitable execution of the project. The lack of information from the lower level operation make the target set by the scheduler to be sub-optimal, or even infeasible to be implemented on the ground level. This is a big drawback of isolated planning of well pad development.

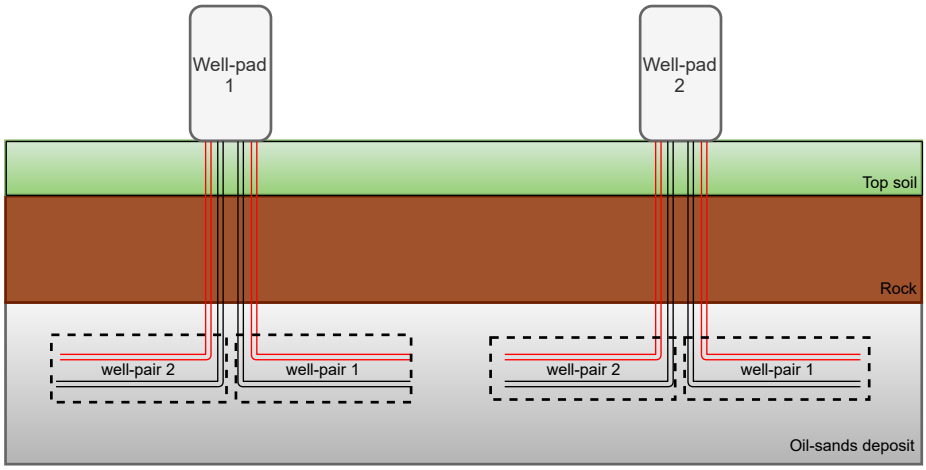

Figure 4.1: Representation of SAGD facility with two well-pads each having 2 well-pairs of injector and producer wells.

Usual SAGD facility has multiple well-pads each having multiple well pairs. The integrated optimization of scheduling and control of SAGD well-pads works on a two-fold objective. The first objective of the problem is to strategically develop the SAGD well-pads in the allocated region for the maximization of the NPV of the project in the scheduling horizon. The second objective of the problem is to control the process under its safe limits for optimal steam injection to the process. Solving the scheduling and control level problem using integrated optimization achieves the two fold objective in a pragmatic manner. The information available from the control level is utilized in the scheduling level in order to re-optimize the development of new well pads, while considering the restrictions imposed by the control level. The integrated optimization problem thus achieves a practical schedule while satisfying the constraints imposed by the lower level.

4.2 Mathematical Model

4.2.1 Scheduling level model

Miura and Wang [68], presented an improved model to predict cumulative steam to oil ratio (CSOR) for SAGD wells at the Japan Canada Oil Sands Limited (JACOS) Hangingstone project. The authors compared the obtained CSOR to the one predicted by the Edmonds and Peterson[69] model. The steam chamber growth with

time was developed by[68] by improving the model suggested by Butler[1] given as:

$$h_s = 2\left(\frac{kgk_t}{m\nu_s\phi\Delta S_o C_{vo}}\right)^{1/3} t^{2/3} \tag{4.1}$$

The analytic model for CSOR is obtained as:

$$CSOR = \frac{\Delta T(t)}{\Delta H(t)\phi\left(S_{oi} - \frac{b-1}{b}\left(\frac{\nu_s(t)\phi h_s(t)}{bkgt}\right)^{1/(b-1)}\right)} \times \left(C_{vr} + \frac{\sqrt{k_t C_{vo} t}}{\beta h_s(t)}\right) \tag{4.2}$$

where β represents sweep efficiency factor that varies in the range of 50% to an economic limit of 85%, and $h_s(t)$ represents the change in steam chamber height with time in Eq.4.1. The latent heat is obtained from the difference between enthalpy of steam at chamber temperature and enthalpy of the condensate at producer well.

$$\begin{aligned}\Delta H(t) = {} & H(\text{steam at chamber temperature}) \\ & - H(\text{condensate at producing temperature})\end{aligned} \tag{4.3}$$

The instantaneous steam-to-oil ratio (ISOR) can be calculated as:

$$ISOR_{w,t} = \frac{CSOR_{w,t}}{\sum_{k=1}^{t-1} ISOR_{w,k}} \qquad \forall w \in \mathcal{W}, t \in T \tag{4.4}$$

The steam consumption model is formulated using heat consumption in the steam chamber. The heat consumption in SAGD well considers two components, heat inside steam chamber H_{inside} and cumulative heat loss H_{loss}. The heat outside the steam chamber is composed of heat losses from the chamber sides and under-burden which is considered to be one-third of heat losses from the overburden. The total heat consumption H_{total} and total required steam volume V_{steam} are calculated using the following equations:

$$H_{inside} = A\Delta T C_{vr} h \eta_s \tag{4.5}$$

$$H_{top} = \frac{4}{3} A\Delta T \sqrt{\frac{k_t C_{vo} t}{\pi}} \tag{4.6}$$

$$H_{loss} = H_{top} + \frac{1}{3} H_{top} \tag{4.7}$$

$$H_{total} = H_{inside} + H_{loss} \tag{4.8}$$

$$V_{steam}(t) = \frac{H_{total}}{H_{lv}} = \frac{A\Delta T}{H_{lv}}(C_{vr} h \eta_s + \sqrt{k_t C_{vo} t}) \tag{4.9}$$

Equations 4.5 to 4.9 are used to determine the cumulative volume of steam until the year t. The steam required to be injected in each year is determined using the formula $q_{w,\tau}^{smax} = V_{steam}(t) - V_{steam}(t-1)$. Using equations 4.5 to 4.9 the steam utilization

profile for a single well-pair is presented in figure 4.2. It is worth pointing out that the above steam injection plan is only based on geological model and ignores the lower level control restrictions. The steam injection and oil production model represents an ideal target which may not necessarily be achieved. This paper's objective is close the loop between scheduling level and control level such that the model can be updated timely based on the control level feedback.

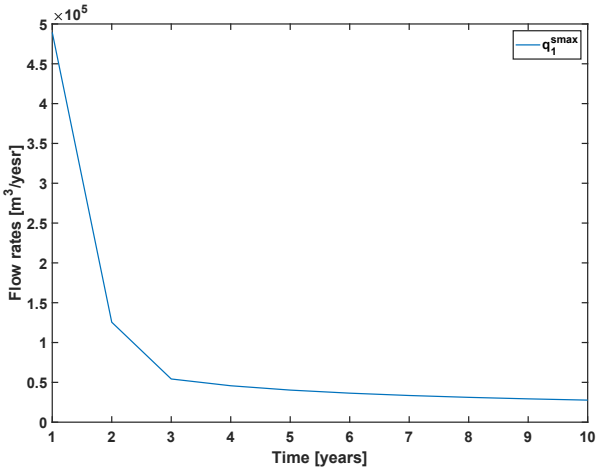

Figure 4.2: The figure represents the max steam injection rates to well-pad 1

The scheduling problem can then be described as:

$$\min \quad \sum_{t\in T}\sum_{w\in\mathcal{W}} \frac{1}{(1+DR)^t}[\alpha_t^{st} q_{w,t}^{st} - \alpha_t^{o} q_{w,t}^{o}] \tag{4.10a}$$

$$s.t. \quad t_w^{start} = \sum_{t\in T} z_{w,t}\cdot t \quad \forall w \in \mathcal{W} \tag{4.10b}$$

$$\sum_{t\in T} z_{w,t} \leq 1 \quad \forall w \in \mathcal{W} \tag{4.10c}$$

$$q_{w,t}^{o} = \sum_{\tau\in T^w} \frac{z_{w,t-\tau+1} q_{w,\tau}^{st}}{ISOR_{w,t}} \qquad \forall w \in \mathcal{W}, t \in T \tag{4.10d}$$

$$q_{w,t}^{st} \leq \sum_{\tau\in T^w} z_{w,t-\tau+1} q_{w,\tau}^{smax} \qquad \forall w \in \mathcal{W}, t \in T \tag{4.10e}$$

$$q_{w,t}^{st} \geq \sum_{\tau\in T^w} z_{w,t-\tau+1} q_{w,\tau}^{smin} \qquad \forall w \in \mathcal{W}, t \in T \tag{4.10f}$$

$$\sum_{w\in\mathcal{W}} q_{w,t}^{st} \leq q_t^{cpf} \quad \forall t \in T \tag{4.10g}$$

The scheduling problem aims to commission and decommission wells in a SAGD facility based on profitability. Equation (4.10c) ensures the wells can be commissioned

only once, equation (4.10f) sets the limits on maximum available steam due to mechanical restrictions and equation (4.10g) assures no shutdown takes place before a well reaches end of its lifetime. The equation (4.10g) offers limits on total steam available at the central processing facility (CPF) represented by q_t^{cpf}. The equation (4.10d) makes the above model from 4.10c to 4.10g a Mixed Integer Non-Linear Programming (MINLP) problem. The above model can be linearized and hence converted to a Mixed Integer Linear Programming (MILP) problem, as represented below.

$$\min \quad \sum_{t\in T}\sum_{w\in\mathcal{W}} \frac{1}{(1+DR)^t}[\alpha_t^{st} q_{w,t}^{st} - \alpha_t^{o} q_{w,t}^{o}] \tag{4.11a}$$

$$s.t. \quad t_w^{start} = \sum_{t\in T} z_{w,t}\cdot t \quad \forall w \in \mathcal{W} \tag{4.11b}$$

$$\sum_{t\in T} z_{w,t} \leq 1 \quad \forall w \in \mathcal{W} \tag{4.11c}$$

$$q_{w,t}^{o} = \sum_{\tau\in T^w} \frac{y_{w,t,t-\tau+1}^{st}}{ISOR_{w,t}} \qquad \forall w \in \mathcal{W}, t \in T \tag{4.11d}$$

$$q_{w,t}^{st} \leq \sum_{\tau\in T^w} z_{w,t-\tau+1} q_{w,\tau}^{smax} \qquad \forall w \in \mathcal{W}, t \in T \tag{4.11e}$$

$$q_{w,t}^{st} \geq \sum_{\tau\in T^w} z_{w,t-\tau+1} q_{w,\tau}^{smin} \qquad \forall w \in \mathcal{W}, t \in T \tag{4.11f}$$

$$\sum_{w\in\mathcal{W}} q_{w,t}^{st} \leq q_t^{cpf} \quad \forall t \in T \tag{4.11g}$$

$$y_{w,t,t-\tau+1}^{st} \leq q_{w,\tau}^{smax} z_{w,t-\tau+1} \qquad \forall w \in \mathcal{W}, t \in T, \tau \in T^w \tag{4.11h}$$

$$y_{w,t,t-\tau+1}^{st} \leq q_{w,t}^{st} \qquad \forall w \in \mathcal{W}, t \in T, \tau \in T^w \tag{4.11i}$$

$$y_{w,t,t-\tau+1}^{st} \geq q_{w,t}^{st} - q_{w,\tau}^{smax}(1 - z_{w,t-\tau+1}) \quad \forall w \in \mathcal{W}, t \in T, \tau \in T^w \tag{4.11j}$$

The equation (4.10d) is a product of a binary variable and a continuous variable, making the model nonlinear. This equation can be simplified by using an intermediate continuous variable $y_{w,t,t-\tau+1}^{st}$. Equations 4.11d,4.11h,4.11i and 4.11j show the linearization to convert MINLP to a MILP formulation.

4.2.2 Control level model

The mathematical model used for building the NMPC is adopted from Gotawala et al.[67]. The underlying assumptions made are as follows:

- The mass balance is assumed to be steady state
- The ramp-up stage model is sufficient to control sub-cool for the entire lifetime of SAGD well pads

- The ISOR is assumed to be constant within each year
- Control can be sufficiently achieved using just the steam injection rate q^{is} as the manipulated variable
- The ratio of volumes of oil and water contained in the pool is proportional to the ratio of the flow rates of oil and water that feed the pool: $\frac{V^w}{V^o} \approx \frac{q^w}{q^o}$

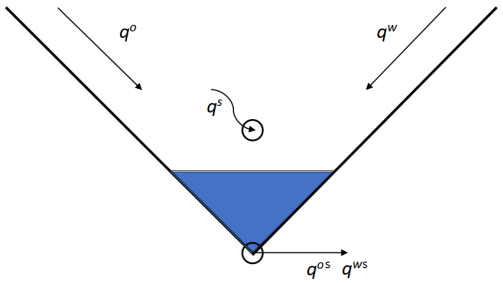

Figure 4.3: The steam chamber is assumed to have a triangular shape. q^s represents the input of steam to the chamber and is the manipulated variable, q^o and q^w represents the oil produced from the reservoir and condensed steam respectively. q^{os} and q^{ws} represent the produced oil and water pumped to the surface

The material balance around the liquid pool is given by:

$$\rho^{oil}q^o + \rho^{wa}q^w - \rho^{oil}q^{os} - \rho^{wa}q^{ws} = \frac{d}{dt}(\rho^{oil}V^o + \rho^{wa}V^w) \tag{4.12}$$

The water production rate from the liquid pool q^{ws} is related to the steam injection rate, expressed as :

$$q^{ws} = fq^{is} \tag{4.13}$$

where f can be between 0.9 and 1.1, and q^{is} is the steam injection rate. The oil produced from the well is given as:

$$q^{os} = \frac{q^{is}}{ISOR} \tag{4.14}$$

The oil drained from reservoir to the pool from reservoir temperature to saturated steam temperature requires equivalent amount of energy from condensed steam, thus giving us the relation:

$$\rho^{wa}q^w = \frac{\rho^{oil}q^oC^{po}(T^s - T^R)}{\eta^{eff}\eta^s\lambda^s} \tag{4.15}$$

Substituting equations 4.13, 4.14 and 4.15 in 4.12 and setting $\frac{dV_o}{dt} = 0$, we have

$$q^o = \frac{q^{is}\left(\frac{1}{ISOR} + \frac{\rho^{wa}}{\rho^{oil}} f\right)}{1 + \left(\frac{C_{po}(T^s - T^r)}{\eta^{eff}\eta^s\lambda^s}\right)} \tag{4.16}$$

The energy balance around the liquid pool can be written as:

$$\begin{aligned} &\rho^{oil} q^o C^{po}(T^s - T^R) + \rho^{wa} q^w C^{pw}(T^s - T^R) + \mathring{Q} \\ &- \rho^{oil} q^{os} C^{po}(T^P - T^R) - \rho^{wa} q^{ws} C^{pw}(T^P - T^R) \\ &= \frac{d}{dt}\left[(\rho^{oil} V^o C^{po} + \rho^{wa} V^w C^{pw})(T^p - T^R)\right] \end{aligned} \tag{4.17}$$

Simplifying the above equation and re-writing it, we have:

$$\frac{dT^p}{dt} + A\left(T^p - T^r\right) = B + Q \tag{4.18}$$

where,

$$A = \frac{1}{V^o}\left[q^o - \frac{q^{is}\left(\frac{1}{ISOR} + \frac{\rho^{wa}}{\rho^{oil}} f\right)}{1 + \left(\frac{C^{po}(T^s - T^r)}{\eta^{eff}\eta^s\lambda^s}\right)} + \frac{1}{ISOR}\left(\frac{q^{is}}{1 + \left(\frac{C^{pw}(T^s - T^r)}{\eta^{eff}\eta^s\lambda^s}\right)}\right)\right]$$

$$B = \frac{q^o}{V^o}(T^s - T^r) - \frac{f\rho^{wa}C^{pw}}{V^o\rho^{oil}C^{po}}\left[\frac{1}{1 + \left(\frac{C^{pw}(T^s - T^r)}{\eta^{eff}\eta^s\lambda^s}\right)}\right]$$

and,

$$Q = \frac{\mathring{Q}}{1 + \left(\frac{C^{pw}(T^s - T^r)}{\eta^{eff}\eta^s\lambda^s}\right)}$$

The heat lost from the steam chamber to the liquid pool $\mathring{Q}$ is given as [70]:

$$\mathring{Q} = 128.3P - 669.1 \tag{4.19}$$

The deterministic NMPC model is represented as:

$$\min \quad \int_n \int_i \alpha_s^{st} q^{is} - \alpha_s^o q^o \tag{4.20a}$$

$$s.t. \quad q^o = \frac{q^{is}\left(\frac{1}{ISOR} + \frac{\rho^{wa}}{\rho^{oil}} f\right)}{1 + \left(\frac{C_{po}(T^s - T^r)}{\eta^{eff}\eta^s\lambda^s}\right)} \tag{4.20b}$$

$$\frac{dT^p}{dt} + A\left(T^p - T^r\right) = B + Q \tag{4.20c}$$

$$A = \frac{1}{V^o}\left[q^o - \frac{q^{is}\left(\frac{1}{ISOR} + \frac{\rho^{wa}}{\rho^{oil}} f\right)}{1 + \left(\frac{C^{po}(T^s - T^r)}{\eta^{eff}\eta^s\lambda^s}\right)} + \frac{1}{ISOR}\left(\frac{q^{is}}{1 + \left(\frac{C^{pw}(T^s - T^r)}{\eta^{eff}\eta^s\lambda^s}\right)}\right)\right] \tag{4.20d}$$

$$B = \frac{q^o}{V^o}(T^s - T^r) - \frac{f\rho^{wa}C^{pw}}{V^o\rho^{oil}C^{po}}\left[\frac{1}{1+\left(\frac{C^{pw}(T^s-T^r)}{\eta^{eff}\eta^s\lambda^s}\right)}\right] \tag{4.20e}$$

$$Q = \frac{\mathring{Q}}{1+\left(\frac{C^{pw}(T^s-T^r)}{\eta^{eff}\eta^s\lambda^s}\right)} \tag{4.20f}$$

$$\mathring{Q} = 128.3P - 669.1 \tag{4.20g}$$

$$\int_n\int_i q^{is} \leq 3 \times \frac{q_w^{st} - q_{par}^{is}}{T^m - X} \tag{4.20h}$$

$$\int_n\int_i q^{is} \leq \bar{C} \tag{4.20i}$$

$$\underline{D} \leq T^p - T^s \leq \overline{D} \tag{4.20j}$$

The above model in continuous time is discretized using Radau collocation roots of third order as shown in Figure 4.4.

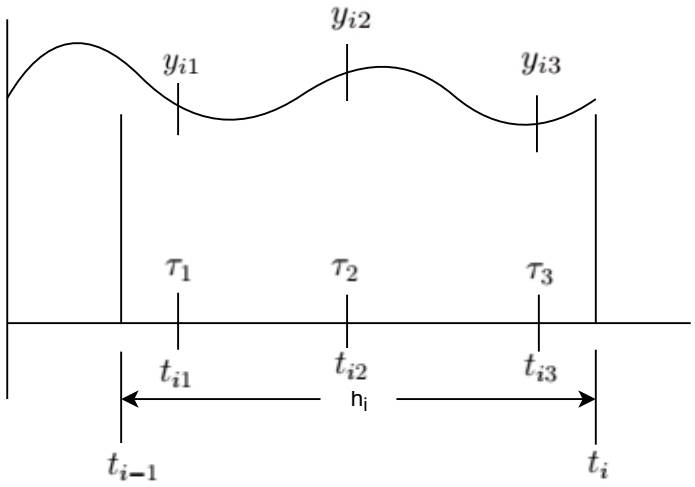

Figure 4.4: The figure shows the discretization method to convert an ODE. The points $\tau_1 - \tau_3$ show the three Legendre polynomial roots. The equations are solved at these discrete time intervals.

The discretized model used for control is given below:

$$\min \quad \sum_{n\in\mathcal{N}}\sum_{i\in\mathcal{I}} \alpha_s^{st} q_{w,n,i}^{is} - \alpha_s^o q_{w,n,i}^o \tag{4.21a}$$

$$s.t. \quad q_{w,n,i}^o = \frac{q_{w,n,i}^{is}\left(\frac{1}{ISOR_{w,s}} - \frac{\rho_w^{wa}}{\rho_w^{oil}}f\right)}{1+\left(\frac{C_w^{po}(T_w^s-T_w^r)}{\eta^{eff}\eta^s\lambda_w^s}\right)} \quad \forall n \in \mathcal{N}, i \in \mathcal{I} \tag{4.21b}$$

$$\sum_{j=0}^{3} T^{p}_{w,n,i,j} \frac{dl_j}{d\tau}(\tau_k) = h\left[Q_w + B_{w,n,i} - A_{w,n,i}\left(T^{p}_{w,n,i,k} - T^{r}_{w}\right)\right] \quad \forall n \in \mathcal{N}, i \in \mathcal{I}, k \in \mathcal{K} \tag{4.21c}$$

$$A_{w,n,i} = \frac{1}{V^{o}_{w}}\left[q^{o}_{w,n,i} - \frac{q^{is}_{w,n,i}\left(\frac{1}{ISOR_w} - \frac{\rho^{wa}_{w}}{\rho^{oil}_{w}} f\right)}{1 + \left(\frac{C^{po}_{w}(T^{s}_{w} - T^{r}_{w})}{\eta^{eff}\eta^{s}\lambda^{s}_{w}}\right)} + \frac{1}{ISOR_{w,s}}\left(\frac{q^{is}_{w,n,i}}{1 + \left(\frac{C^{pw}_{w}(T^{s}_{w} - T^{r}_{w})}{\eta^{eff}\eta^{s}\lambda^{s}_{w}}\right)}\right)\right] \quad \forall n \in \mathcal{N}, i \in \mathcal{I} \tag{4.21d}$$

$$B_{w,n,i} = \frac{q^{o}_{w,n,i}}{V^{o}_{w,n,i}}(T^{s}_{w} - T^{r}_{w}) - \frac{f\rho^{wa}_{w}C^{pw}_{w}}{V^{o}_{w}\rho^{oil}_{w}C^{po}_{w}}\left[\frac{1}{1 + \left(\frac{C^{pw}_{w}(T^{s} - T^{r})}{\eta^{eff}\eta^{s}\lambda^{s}_{w}}\right)}\right] \quad \forall n \in \mathcal{N}, i \in \mathcal{I} \tag{4.21e}$$

$$Q_w = \frac{128.3P_w - 669.1}{1 + \left(\frac{C^{pw}_{w}(T^{s}_{w} - T^{r}_{w})}{\eta^{eff}\eta^{s}\lambda^{s}_{w}}\right)} \tag{4.21f}$$

$$T^{p}_{w,n,i+1,0} = T^{p}_{w,n,i,'3'} \quad \forall n \in \mathcal{N}, i \in \mathcal{I} \tag{4.21g}$$

$$\underline{B_n} \leq q^{is}_{w,n,i} \leq \overline{B_n} \quad \forall n \in \mathcal{N}, i \in \mathcal{I} \tag{4.21h}$$

$$\sum_{n \in \mathcal{N}} q^{is}_{w,n,i} \leq \bar{C} \quad \forall i \in \mathcal{I} \tag{4.21i}$$

$$\sum_{n \in \mathcal{N}} \sum_{i \in \mathcal{I}} q^{is}_{w,n,i} \leq 3 \times \frac{q^{st}_{w} - q^{is}_{par,w}}{T^{m} - X} \tag{4.21j}$$

$$\underline{D_n} \leq T^{p}_{w,n,i,j} - T^{s}_{n} \leq \overline{D_n} \quad \forall n \in \mathcal{N}, i \in \mathcal{I}, j \in \mathcal{J} \tag{4.21k}$$

The usage of Radau roots simplifies the optimization problem as the final collocation point corresponds to the initial point of the next element. The above discretized model is solved for each well pad $w \in \mathcal{W}$.

4.3 Methodology

The scheduler solves the mixed integer linear programming problem from the start of the scheduling horizon. The binary variables schedule the commission of specific well-pads at specific years of the scheduling horizon, and provide the target values for the commissioned well-pads. The control level receives the target steam injection and well pad commissioning information. The NMPC provides optimal inputs to the process, thus keeping the subcool for the wells within the well pad under set safe limits. The total steam utilized in the control level is passed to the scheduling level in order to update the maximum amount of steam to inject into the process while keeping the process under control. The total steam utilized and the active well

pad information is passed as feedback to the scheduler in order to fix the variables and resolve at the next time instant (year). This method ensures the following: 1) The wells commissioned at the previous time instant stays commissioned while the scheduler re-optimizes at the current time, 2) The NPV calculated at the current time instant utilizes the information of actual steam injected from the control level, and 3) Updating the maximum steam for injection keeps the limits closer to the targets achievable by the lower level control problem.

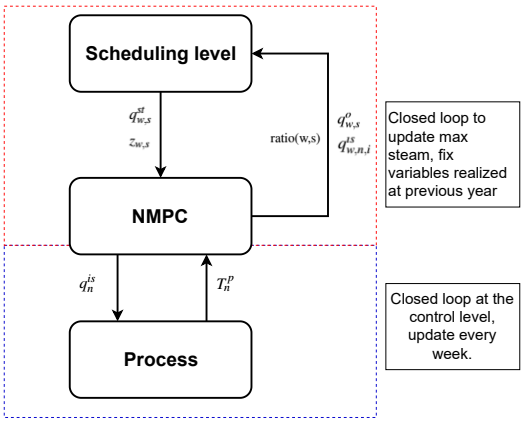

Figure 4.5: The flow-chart explains the hierarchical method to solve the integrated optimization problem. The variables passed from control level to scheduling level are used to fix the values of the variables that are realized and utilized after current year.

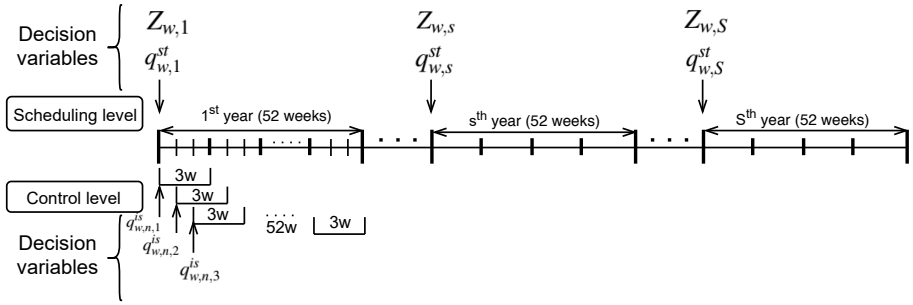

Figure 4.6: The time-line shows the integration of two optimization problems at very different time scales of years and weeks on the upper and lower level respectively. The shrinking horizon approach for the scheduling and rolling horizon approach for the control level are shown, where the control level utilizes a prediction horizon of 3 weeks.

During the start of the well pad, the growth of the steam chamber has not been achieved and hence the complete steam target provided by the scheduler is injected into the process without any control while producing all the bitumen produced in year one. The figure 4.5 shows the summary of the variables being passed in the

closed-loop operation. The time-line of the decisions taken by the upper level problem and the lower level problem is summarized in figure 4.6.

The methodology involves solving the integrated optimization problem in a hierarchical manner. Solving the scheduler problem and the control problem together, as one single problem requires solving a very large mixed integer nonlinear program. The problem takes a lot of computational effort to solve. In the presence of large number of well-pads (20 well-pads) with each well pad having 6 well-pairs, the size of the optimization problem would be too large to solve. In order to solve the integrated optimization model, we formulated a hierarchical optimization method: scheduler solved first at the upper level and control for the wells that have been activated by scheduler is performed at the lower level. Note that the maximum steam injection $q_{w,t}^{smax}$ is only a target to be applied, and it may not be realistic for control level operation since it is only evaluated based on geological model[68].

The control problem with the prediction horizon of 3 predicts optimal inputs for 3 weeks while implementing the control action at the first time instant. This rolling-horizon method is used to control the active well-pad until the end of year. The total steam utilized by the active well-pads in a given year $\sum_{n\in\mathcal{N}}\sum_{i\in\mathcal{I}} q_{w,n,i}^{is}$ is utilized to calculate the ratio between target given by the scheduler and actual steam given by

$$\text{ratio(w,t)} = \frac{q_{w,t}^{smax}}{\sum_{n\in\mathcal{N}}\sum_{i\in\mathcal{I}} q_{w,n,i}^{is}}$$

The ratio is passed back to the scheduler to update the $q_{w,t}^{smax}$ for all the wells at the previous time instant, which is calculated each year when new information is available from commissioning wells. Three methodologies were considered: 1) No-shrinking horizon implementation for scheduling level with no update, 2) Shrinking horizon implementation for scheduling level without update, and 3) Shrinking horizon implementation for scheduling level with update.

The process model was built in MATLAB R2018b, and the scheduling level was programmed in GAMS 25.1.1 and solved with CPLEX solver. The NMPC was programmed in GAMS 25.1.1 and solved with IPOPT solver. The simulations were carried out on Intel(R) Core(TM) i5-6500 CPU @ 3.2GHz with 4-cores and 8GB RAM.

4.4 Results and Discussion

The following section describes the results obtained from the integrated optimization technique utilizing the three methodologies as described above. The SAGD well development planning involves 20 well-pads, each having 6 pairs of wells. The well pads, when active, activates all the 6 well pairs pertaining to them. The well pairs have different geological parameters and injection pressure with a total available steam injection capacity constrained by $q_{w,t}^{smax}$ for each well pad in each year. The steam is allocated among the 6-well pairs in a well-pad by the control level.

The scheduling level utilizes a planning horizon of 25 years. The lifetime of all the well-pads were vary between 7 to 10 years. Each well-pad has a different lifetime. The number of wells that can be commissioned is limited by the amount of steam available at the central processing facility.

4.4.1 No-shrinking horizon implementation of scheduling level

In this methodology the scheduling level of the integrated optimization is solved only at year one to obtain the schedule for the entire scheduling horizon, without resolving at year t to end of planning horizon at year T as shown in figure 4.6. The schedule obtained by this method is described in figure 4.7, which shows the Gantt chart obtained by single solution of scheduling optimization.

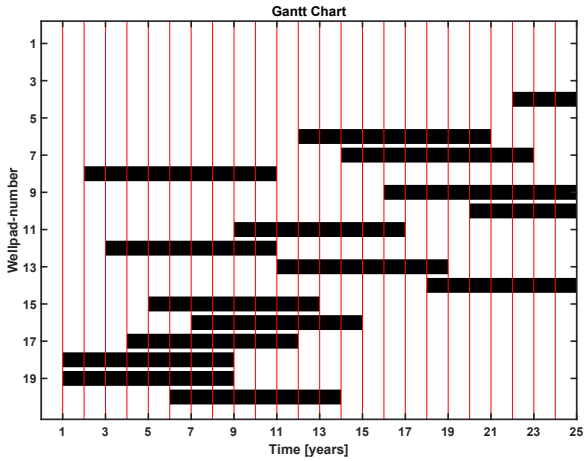

Figure 4.7: The gantt chart represents the commissioning of wells by the scheduling level formulation.

The gantt chart shows wells being commissioned at year 22, with very little time left of the scheduling horizon. This causes a capital investment at year 22 that is not very profitable for the enterprise. The information from the scheduling level is passed

down to the control level that can be used to control only the wells that are active. The results obtained from the control level are shown below.

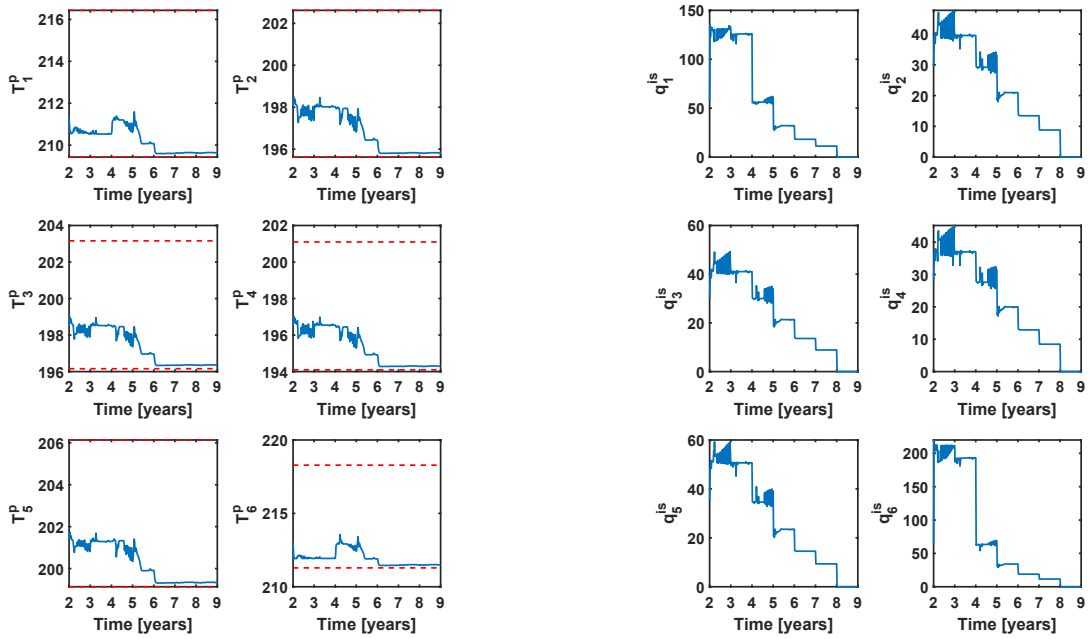

(a) Temperature profile for well-pad 18. The subplots represent the temperature of produced emulsions in each well given by T_n^p

(b) Steam injection profiles for well-pad 18. The subplots represent the steam injection rate in each well given by q_n^{is}

Figure 4.8: The figure shows the control profiles obtained from control level for a single well-pad

As shown in figure 4.8 the control profiles stay well within their set constraints. The produced steam however does not match the targets set by the scheduling level.

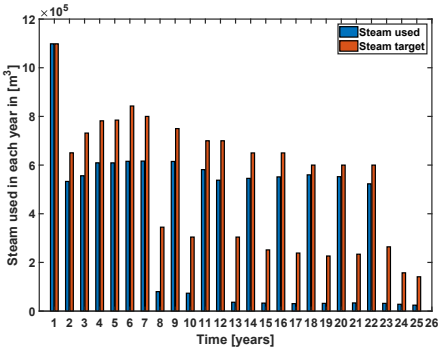

(a) Steam target to be achieved by control level, obtained from the scheduling level.

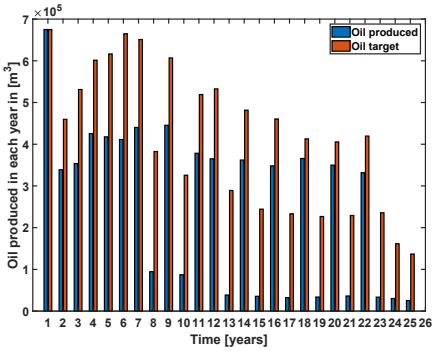

(b) Oil target to be achieved by control level, obtained from the scheduling level.

Figure 4.9: The figure shows the steam and oil produced by the control level on the ground vs the targets envisioned by scheduling level.

The figure 4.9 shows the difference in the levels of steam utilized by the lower-level control problem versus the targets envisioned by the scheduling level. The steam utilized at the first year meets the steam target given by the scheduling level because, at the year of commissioning of a well no control action takes place and the entire steam available is utilized by the well pad. The vast difference in the target and level achieved in the remaining time is due to the fact that the solution is obtained from an open-loop method. The NPV obtained from this method is $\$1.2885\mathrm{E}+09$.

4.4.2 Shrinking horizon implementation of scheduling level

In this methodology, the scheduling level of the integrated optimization is solved at the end of each year to obtain the schedule for the current year of production as shown in figure 4.6. The schedule obtained by this method is described in figure 4.10, which shows the Gantt chart obtained by single solution of scheduling optimization for selected years 1,9,16, and 25.

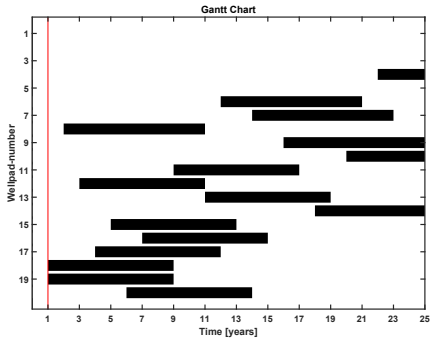

(a) Gantt chart to show the schedule obtained at year 1 of the scheduling horizon

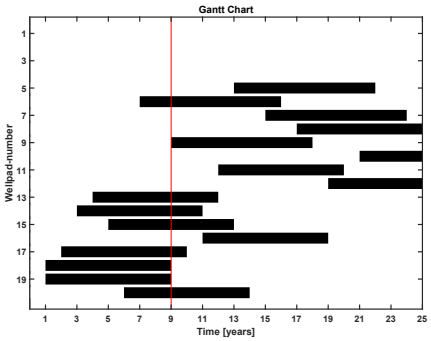

(b) Gantt chart to show the schedule obtained at year 9 of the scheduling horizon

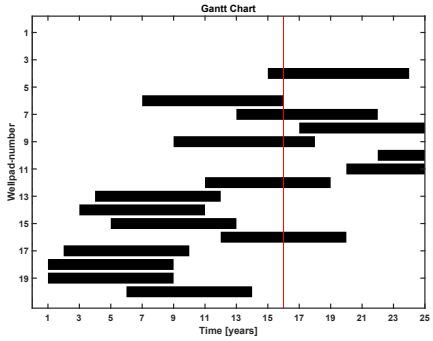

(c) Gantt chart to show the schedule obtained at year 16 of the scheduling horizon

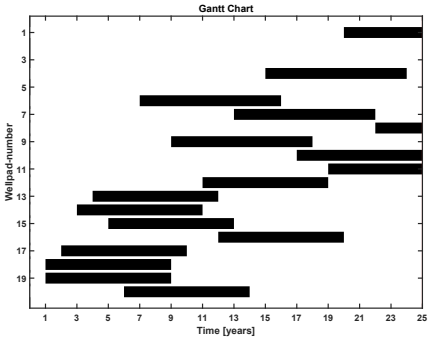

(d) Gantt chart to show the schedule obtained at year 25 of the scheduling horizon

Figure 4.10: The figure shows the gantt charts for scheduling level at different years of the scheduling horizon

The Gantt chart shows wells being commissioned at year 22, with very little time left of the scheduling horizon. This causes a capital investment at year 22 not very profitable. The information from the scheduling level is passed down to the control level. The results obtained from the control level are shown below.

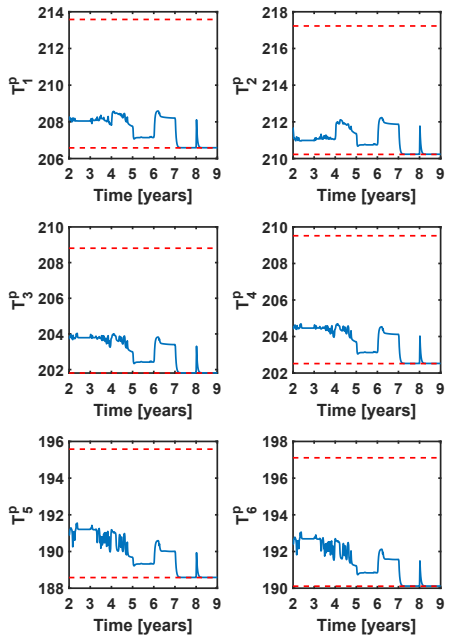

(a) Temperature profile for well-pad 19. The subplots represent the temperature of produced emulsions in each well given by T_n^p

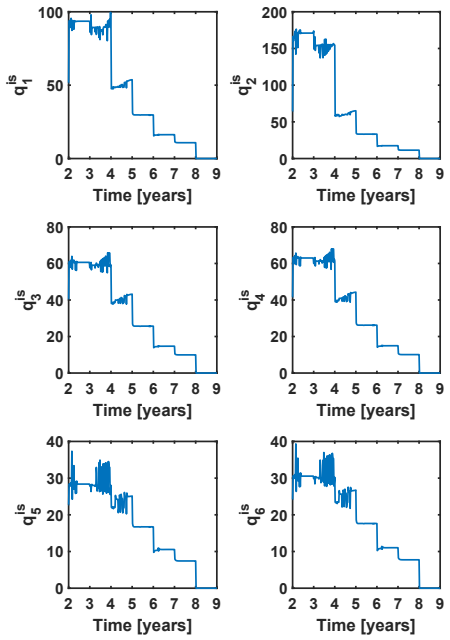

(b) Steam injection profiles for well-pad 19. The subplots represent the steam injection rate in each well given by q_n^{is}

Figure 4.11: The figure shows the control profiles obtained from control level for a single well-pad

As shown in the figure 4.11 the control profiles stay well within their set constraints. The injected steam however does not match the targets set by the scheduling level.

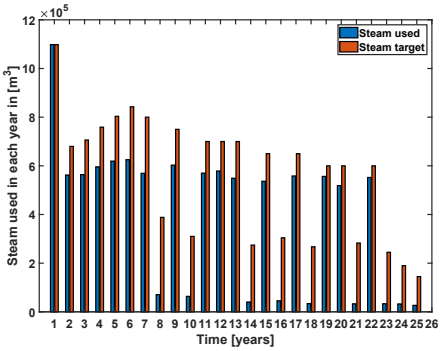

(a) Steam target to be achieved by control level, obtained from the scheduling level.

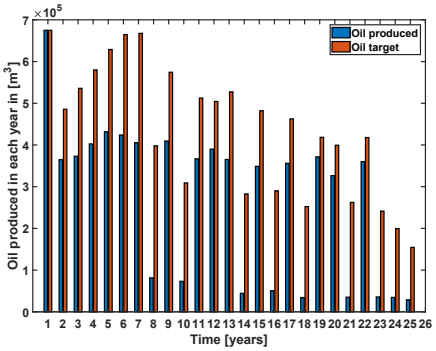

(b) Oil target to be achieved by control level, obtained from the scheduling level.

Figure 4.12: The figure shows the steam and oil produced by the control level on the ground vs the targets envisioned by scheduling level.

The figure 4.12 shows the difference in the levels of steam utilized by the lower-level control problem vs the targets envisioned by the scheduling level. The vast difference in the target and level achieved is due to the fact that the solution is obtained from an open-loop method without updating the max steam injection as new information is available. The NPV obtained from this method is $\$1.3277\mathrm{E}+09$ which is better than the NPV obtained by no-shrinking horizon implementation of scheduling level by 3.92%.

4.4.3 Shrinking horizon implementation of scheduling level with update

In this methodology, the scheduling level of the integrated optimization is solved at the end of each year to obtain the schedule for the current year of production as shown in figure 4.6. The ratio of target to actual steam injected is updated such that the max possible steam injection for all the wells at that year are updated using the ratio. The ratio is updated at the end of each year of operation, with the consideration of ratios obtained from all the active and decommissioned wells, with respect to the lifetime of wells active at the current time instant . The schedule obtained by this method is described in figure 4.13, that shows the Gantt chart obtained by single solution of scheduling optimization for the years (1,9,16,25).

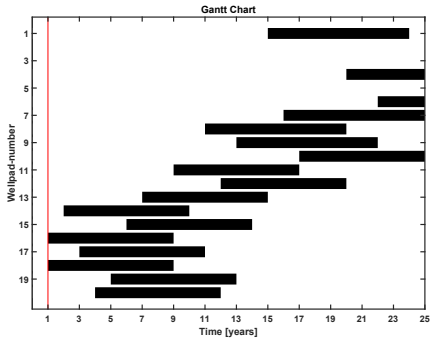

(a) Gantt chart to show the schedule obtained at year 1 of the scheduling horizon

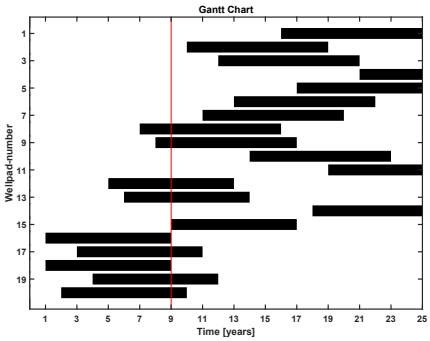

(b) Gantt chart to show the schedule obtained at year 9 of the scheduling horizon

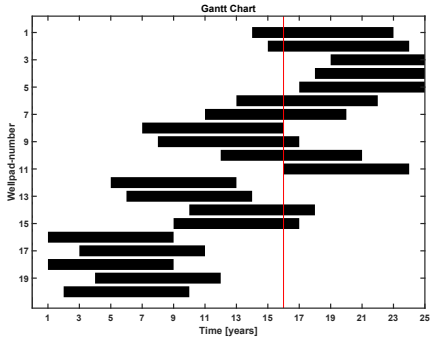

(c) Gantt chart to show the schedule obtained at year 16 of the scheduling horizon

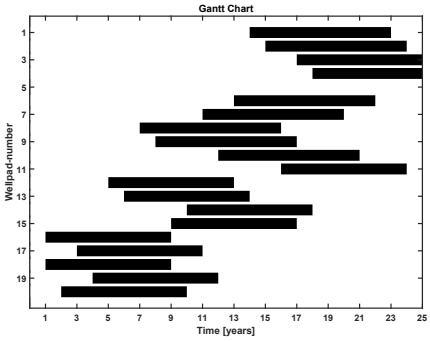

(d) Gantt chart to show the schedule obtained at year 25 of the scheduling horizon

Figure 4.13: The figure shows the gantt charts for scheduling level at different years of the scheduling horizon

The Gantt charts here show the scheduling optimizer to commission the last well-pad by year 19, thus not commissioning wells at a year much later than that to prevent capital investments towards the end of the lifetime of the SAGD project. This increases the profitability by a very good margin.

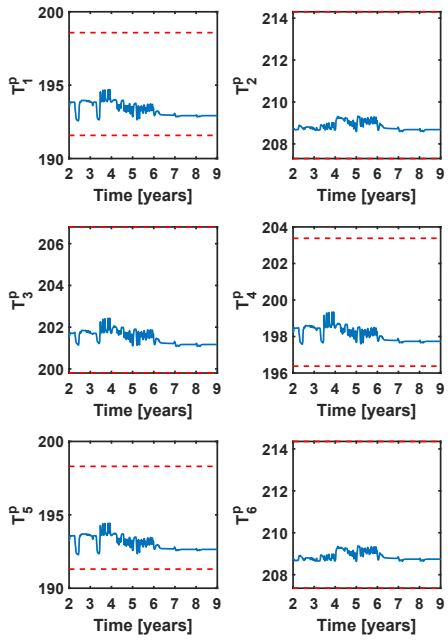

(a) Temperature profile for well-pad 16. The subplots represent the temperature of produced emulsions in each well given by T_n^p

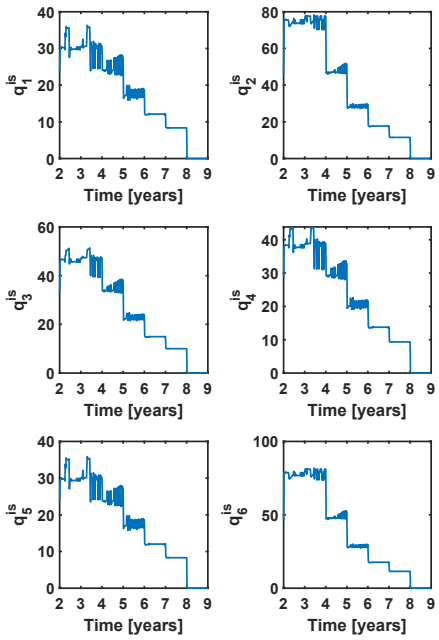

(b) Steam injection profiles for well-pad 16. The subplots represent the steam injection rate in each well given by q_n^{is}

Figure 4.14: The figure shows the control profiles obtained from control level for a single well-pad

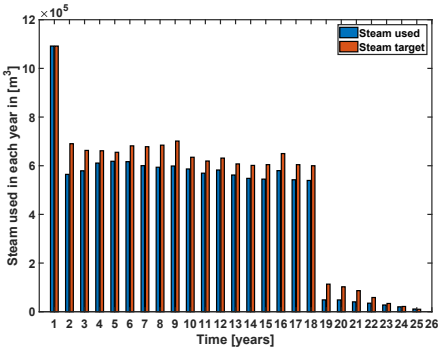

(a) Steam target to be achieved by control level, obtained from the scheduling level.

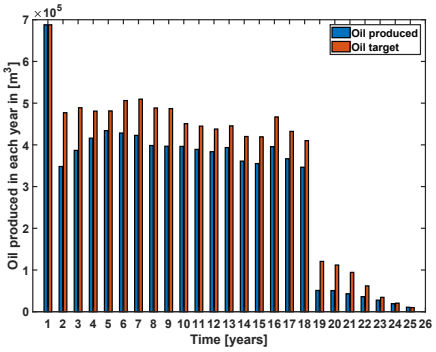

(b) Oil target to be achieved by control level, obtained from the scheduling level.

Figure 4.15: The figure shows the steam and oil produced by the control level on the ground vs the targets envisioned by scheduling level.

The figure 4.15 shows the difference in the levels of steam utilized by the lower-level control problem vs the targets envisioned by the scheduling level. The difference in the target and level achieved is minimized due to the fact that the solution is

obtained from an closed-loop method by updating the max steam injection as new information is available. This form of communication between the ground reality and targets envisioned by the scheduler increases the NPV of the SAGD project. The NPV obtained from this method is $\$1.5170E+09$ which is better than the NPV obtained by shrinking horizon implementation of scheduling level without update by 18.93%. The comparison plot of NPV obtained by three different methods shows the percentage improvement from one method to another in figure 4.16.

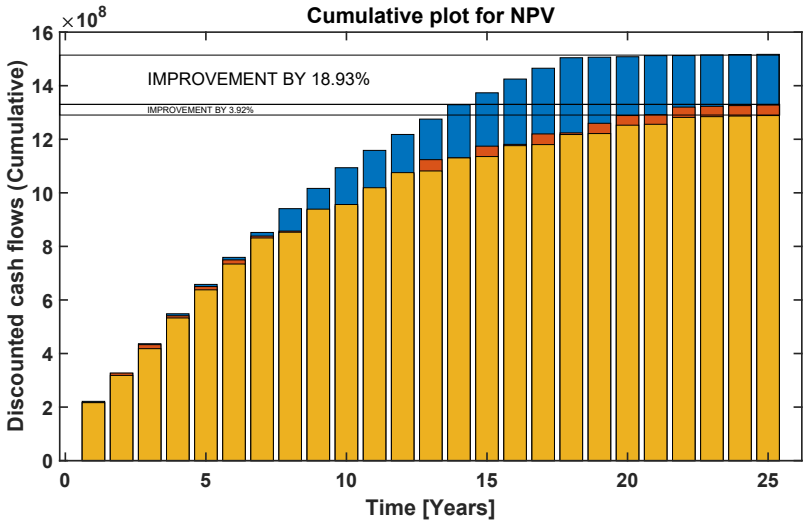

Figure 4.16: The plot compares the performance of different methodologies, the blue bar represents NPV obtained from the shrinking horizon with update, orange represents shrinking horizon without update and yellow represents no-shrinking horizon implementation of scheduling level

4.5 Conclusion

In this chapter, we study the problem of integrated well pad development scheduling with nonlinear model predictive control in steam-assisted gravity drainage. This integration decision-making problem addresses the long term resource allocation (investment on well pad development) and short term resource allocation (steam injection allocation) problem in an integrated manner. The scheduling problem has been modeled as a mixed integer program. The deterministic problem is then solved while considering fixed parameters based on geographical location of well pads. The commissioning inputs as well as steam targets for the commissioned wells are passed onto

the control level optimizer. The lower level NMPC utilizes the targets obtained from the scheduling level in order to inject steam into the process optimally thus maintaining sub-cool within the constraints. Three different methodologies were tried and compared for the deterministic case: 1) No-shrinking horizon implementation of scheduling level, 2) Shrinking horizon implementation of the scheduling level, and 3) Shrinking horizon implementation of scheduling level with closed-loop update. The results improved significantly from method 1 to method 3, by 3.92% and 18.93% subsequently.

Chapter 5

Conclusion

In the thesis, different stochastic, robust, and decision rule based optimization was implemented for steam allocation and oil production optimization in the SAGD process. In the third chapter of the thesis, we presented a first principles model of the SAGD process used in the NMPC formulation. Parametric uncertainty was introduced to the model via SOR, thus solving a multistage stochastic optimization problem. The use of an evolving scenario tree to model uncertainty helped make an intractable problem tractable in real-time optimization. The scenario tree method with a robust horizon performed well when compared to worst-case static robust method. When the affine policy method was implemented with a rolling-horizon method after the end of each prediction horizon, it provides the highest operating profits compared to the other methods. The affine policy method successfully gave higher operating profits while reducing the computational time compared to other stochastic methods.

With the formulation of a NMPC, that successfully allocates steam while maximizing revenue from oil production under SOR uncertainty, the problem was integrated with solving a scheduling level problem. The integrated optimization problem studied the behavior of well pad development scheduling with NMPC in SAGD. The fourth chapter of the thesis describes the formulation of the integrated optimization problem, with scheduling problem being modeled as a MILP and the NMPC modeled as a deterministic NLP. The deterministic problem was solved while considering fixed parameters based on the geographical location of well pads. The commissioning inputs, as well as steam targets for the commissioned wells were passed onto the control level optimizer. The lower level NMPC utilized the targets obtained from the scheduling level to inject steam into the process optimally thus maintaining subcool. Three different methodologies were tried and compared for the deterministic case: 1) No-shrinking horizon implementation of scheduling level, 2) Shrinking hori-

zon implementation of the scheduling level, and 3) Shrinking horizon implementation of scheduling level with closed-loop update. The results improved significantly from method 1 to method 3.

Future work

Based on the work done in the thesis, potential paths are presented below for future work.

Multiple sources of uncertainty

In the third chapter of this thesis, we discuss parametric uncertainty affecting the model with a single source of uncertainty being the SOR. The work provides optimal control action by assuming that all measurements available to the controller are deterministic, and that uncertainty in the model is sourced from only SOR parameter. Future work may include uncertainty from measured variables such as flow rate, temperature, and other geological parameters.

Integrated optimization

In the fourth chapter of the thesis, only the deterministic problem was solved in the current work and hence the NMPC or the scheduler are not hedged against uncertainty in parameters considered or market price fluctuations for the crude. The future work can be extended to incorporate uncertainty and utilizing affine based formulation for both the scheduling and control level problems. The hierarchical methodology of solving the integrated optimization problem can be modified and solved as a single large MINLP. Decomposition algorithms can modified and developed to solve such a large optimization problem in real time.

Bibliography

[1] R.M. Butler. *Thermal Recovery of Oil and Bitumen*. 01 1991.

[2] Yashas Mohankumar, Zukui Li, and Biao Huang. Steam allocation and production optimization in sagd reservoir under steam-to-oil ratio uncertainty. *Journal of Petroleum Science and Engineering*, page 106456, 2019.

[3] Hossein Shahandeh, Shahed Rahim, and Zukui Li. Strategic optimization of the oil sands development with sagd: Drainage area arrangement and development planning. *Journal of Petroleum Science and Engineering*, 137:172–184, 2016.

[4] Dharmesh Rameshchandra Gotawala, Ian Donald Gates, et al. Sagd subcool control with smart injection wells. In *EUROPEC/EAGE Conference and Exhibition*. Society of Petroleum Engineers, 2009.

[5] Zelimir Schmidt, James P Brill, H Dale Beggs, et al. Experimental study of severe slugging in a two-phase-flow pipeline-riser pipe system. *Society of Petroleum Engineers Journal*, 20(05):407–414, 1980.

[6] Michael Golan and Curtis H Whitson. Well test performance. 1991.

[7] Gisle O Eikrem, Ole M Aamo, Bjarne A Foss, et al. On instability in gas lift wells and schemes for stabilization by automatic control. *SPE Production & Operations*, 23(02):268–279, 2008.

[8] Esmaeil Jahanshahi, Sigurd Skogestad, et al. Simplified dynamic models for control of riser slugging in offshore oil production. *Oil and Gas Facilities*, 3(06):80–88, 2014.

[9] Andres Codas, Esmaeil Jahanshahi, and Bjarne Foss. A two-layer structure for stabilization and optimization of an oil gathering network. *IFAC-PapersOnLine*, 49(7):931–936, 2016.

[10] Dinesh Krishnamoorthy, Elvira M Bergheim, Alexey Pavlov, Morten Fredriksen, and Kjetil Fjalestad. Modelling and robustness analysis of model predictive control for electrical submersible pump lifted heavy oil wells. *IFAC-PapersOnLine*, 49(7):544–549, 2016.

[11] Najeh Alali, Mahmoud Reza Pishvaie, and Hadi Jabbari. A new semi-analytical modeling of steam-assisted gravity drainage in heavy oil reservoirs. *Journal of petroleum science and engineering*, 69(3-4):261–270, 2009.

[12] Zeinab Zargar, SM Ali, et al. Analytical treatment of sagd-old and new. In *SPE Canada Heavy Oil Technical Conference*. Society of Petroleum Engineers, 2016.

[13] Mohsen Keshavarz, Thomas G Harding, Zhangxin John Chen, et al. Modification of butler's unsteady-state sagd theory to include the vertical growth of steam chamber. In *SPE Canada Heavy Oil Technical Conference*. Society of Petroleum Engineers, 2016.

[14] Mohammad Rashedi, Ouguan Xu, Seraphina Kwak, Shabnam Sedghi, Jinfeng Liu, and Biao Huang. An integrated first principle modeling to steam assisted gravity drainage (sagd). *Journal of Petroleum Science and Engineering*, 163:501–510, 2018.

[15] Sagar N Purkayastha, Ian D Gates, and Milana Trifkovic. Real-time multivariable model predictive control for steam-assisted gravity drainage. *AIChE Journal*, 64(8):3034–3041, 2018.

[16] L Saputelli, M Nikolaou, and MJ Economides. Real-time reservoir management: A multiscale adaptive optimization and control approach. *Computational Geosciences*, 10(1):61–96, 2006.

[17] Dinesh Krishnamoorthy, Bjarne Foss, and Sigurd Skogestad. Gas lift optimization under uncertainty. *Computer Aided Chemical Engineering*, 40:1753–1758, 01 2017.

[18] J-D Jansen, DR Brouwer, G Naevdal, and CPJW Van Kruijsdijk. Closed-loop reservoir management. *First Break*, 23(1):43–48, 2005.

[19] Bjarne A Foss, John Petter Jensen, et al. Performance analysis for closed-loop reservoir management. *SPE Journal*, 16(01):183–190, 2011.

[20] Rajan G Patel, Japan J Trivedi, et al. Sagd real-time production optimization using adaptive and gain-scheduled model-predictive-control: A field case study. In *SPE Western Regional Meeting*. Society of Petroleum Engineers, 2017.

[21] Wenhan Shen, Zukui Li, Biao Huang, and Nabil Magbool Jan. Chance-constrained model predictive control for sagd process using robust optimization approximation. *Industrial & Engineering Chemistry Research*, 2018.

[22] Gijs van Essen, Maarten Zandvliet, Paul Van den Hof, Okko Bosgra, Jan-Dirk Jansen, et al. Robust waterflooding optimization of multiple geological scenarios. *Spe Journal*, 14(01):202–210, 2009.

[23] Kristian G Hanssen, Andrés Codas, Bjarne Foss, et al. Closed-loop predictions in reservoir management under uncertainty. *SPE Journal*, 22(05):1–585, 2017.

[24] Sebastian Engell. Feedback control for optimal process operation. *Journal of process control*, 17(3):203–219, 2007.

[25] Sergio Lucia, Joel AE Andersson, Heiko Brandt, Moritz Diehl, and Sebastian Engell. Handling uncertainty in economic nonlinear model predictive control: A comparative case study. *Journal of Process Control*, 24(8):1247–1259, 2014.

[26] Farough Motamed Nasab, Hossein Shahandeh, and Zukui Li. Strategic planning of steam assisted gravity drainage reservoir development under reservoir production and oil price uncertainty. *Industrial & Engineering Chemistry Research*, 57(29):9513–9526, 2018.

[27] A Ortız-Gómez, V Rico-Ramirez, and S Hernandez-Castro. Mixed-integer multiperiod model for the planning of oilfield production. *Computers & Chemical Engineering*, 26(4-5):703–714, 2002.

[28] Utsav Awasthi, Remy Marmier, and Ignacio E Grossmann. Multiperiod optimization model for oilfield production planning: Bicriterion optimization and two-stage stochastic programming model. *Optimization and Engineering*, pages 1–22, 2019.

[29] Ignacio Grossmann. Enterprise-wide optimization: A new frontier in process systems engineering. *AIChE Journal*, 51(7):1846–1857, 2005.

[30] L.T. Biegler and V.M. Zavala. Large-scale nonlinear programming using ipopt: An integrating framework for enterprise-wide dynamic optimization. *Computers & Chemical Engineering*, 33(3):575 – 582, 2009. Selected Papers from the

17th European Symposium on Computer Aided Process Engineering held in Bucharest, Romania, May 2007.

[31] Lorenz T. Biegler. Advanced optimization strategies for integrated dynamic process operations. *Computers and Chemical Engineering*, 114:3 – 13, 2018. FOCAPO/CPC 2017.

[32] Rasmus H. Nyström, Rüdiger Franke, Iiro Harjunkoski, and Andreas Kroll. Production campaign planning including grade transition sequencing and dynamic optimization. *Computers & Chemical Engineering*, 29(10):2163 – 2179, 2005.

[33] Yisu Nie, Lorenz T. Biegler, Carlos M. Villa, and John M. Wassick. Discrete time formulation for the integration of scheduling and dynamic optimization. *Industrial & Engineering Chemistry Research*, 54(16):4303–4315, 2015.

[34] Sebastian Engell and Iiro Harjunkoski. Optimal operation: Scheduling, advanced control and their integration. *Computers & Chemical Engineering*, 47:121 – 133, 2012. FOCAPO 2012.

[35] Cara R. Touretzky and Michael Baldea. Integrating scheduling and control for economic mpc of buildings with energy storage. *Journal of Process Control*, 24(8):1292 – 1300, 2014. Economic nonlinear model predictive control.

[36] Iiro Harjunkoski, Rasmus Nyström, and Alexander Horch. Integration of scheduling and control—theory or practice? *Computers & Chemical Engineering*, 33(12):1909 – 1918, 2009. FOCAPO 2008 – Selected Papers from the Fifth International Conference on Foundations of Computer-Aided Process Operations.

[37] Optimal grade transition campaign scheduling in a gas-phase polyolefin fbr using mixed integer dynamic optimization. In Andrzej Kraslawski and Ilkka Turunen, editors, *European Symposium on Computer Aided Process Engineering-13*, volume 14 of *Computer Aided Chemical Engineering*, pages 71 – 76. Elsevier, 2003.

[38] Moritz Paulus and Frieder Borggrefe. The potential of demand-side management in energy-intensive industries for electricity markets in germany. *Applied Energy*, 88(2):432–441, 2011.

[39] Masoud Soroush and Donald J Chmielewski. Process systems opportunities in power generation, storage and distribution. *Computers & chemical engineering*, 51:86–95, 2013.

[40] Dajun Yue and Fengqi You. Sustainable scheduling of batch processes under economic and environmental criteria with minlp models and algorithms. *Computers & Chemical Engineering*, 54:44–59, 2013.

[41] E. Gallestey, A. Stothert, D. Castagnoli, G. Ferrari-Trecate, and M. Morari. Using model predictive control and hybrid systems for optimal scheduling of industrial processes. *Automatisierungstechnik*, 51(6):285–293, 2003.

[42] Gijs van Essen, Paul Van den Hof, Jan-Dirk Jansen, et al. A two-level strategy to realize life-cycle production optimization in an operational setting. *SPE Journal*, 18(06):1–057, 2013.

[43] Gijs M Van Essen, Paul MJ Van den Hof, and Jan Dirk Jansen. Hierarchical economic optimization of oil production from petroleum reservoirs. *IFAC Proceedings Volumes*, 42(11):738–743, 2009.

[44] JC Li, B Gong, and HG Wang. Mixed integer simulation optimization for optimal hydraulic fracturing and production of shale gas fields. *Engineering Optimization*, 48(8):1378–1400, 2016.

[45] Alhaji Shehu Grema and Yi Cao. Receding horizon control for oil reservoir waterflooding process. *Systems Science & Control Engineering*, 5(1):449–461, 2017.

[46] Steen Hørsholt, Hamid Nick, and John Bagterp Jørgensen. A hierarchical multigrid method for oil production optimization. *IFAC-PapersOnLine*, 52(1):492–497, 2019.

[47] Baris Burnak, Justin Katz, Nikolaos A Diangelakis, and Efstratios N Pistikopoulos. Simultaneous process scheduling and control: a multiparametric programming-based approach. *Industrial & Engineering Chemistry Research*, 57(11):3963–3976, 2018.

[48] Jinjun Zhuge and Marianthi G Ierapetritou. An integrated framework for scheduling and control using fast model predictive control. *AIChE Journal*, 61(10):3304–3319, 2015.

[49] Yunfei Chu and Fengqi You. Moving horizon approach of integrating scheduling and control for sequential batch processes. *AIChE Journal*, 60(5):1654–1671, 2014.

[50] Antonio Flores-Tlacuahuac and Ignacio E Grossmann. Simultaneous scheduling and control of multiproduct continuous parallel lines. *Industrial & Engineering Chemistry Research*, 49(17):7909–7921, 2010.

[51] Michael Baldea, Juan Du, Jungup Park, and Iiro Harjunkoski. Integrated production scheduling and model predictive control of continuous processes. *AIChE Journal*, 61(12):4179–4190, 2015.

[52] Juan Du, Jungup Park, Iiro Harjunkoski, and Michael Baldea. A time scale-bridging approach for integrating production scheduling and process control. *Computers & Chemical Engineering*, 79:59 – 69, 2015.

[53] András Prékopa. *Stochastic programming*, volume 324. Springer Science & Business Media, 2013.

[54] Allen L Soyster. Convex programming with set-inclusive constraints and applications to inexact linear programming. *Operations research*, 21(5):1154–1157, 1973.

[55] Aharon Ben-Tal and Arkadi Nemirovski. Robust solutions of linear programming problems contaminated with uncertain data. *Mathematical programming*, 88(3):411–424, 2000.

[56] Aharon Ben-Tal and Arkadi Nemirovski. Robust solutions of uncertain linear programs. *Operations research letters*, 25(1):1–13, 1999.

[57] Aharon Ben-Tal and Arkadi Nemirovski. Selected topics in robust convex optimization. *Mathematical Programming*, 112(1):125–158, 2008.

[58] George B Dantzig. *Notes on Linear Programming, Part XVII: Linear Programming Under Uncertainty*. Rand Corporation, 1955.

[59] John R Birge and Francois Louveaux. *Introduction to stochastic programming*. Springer Science & Business Media, 2011.

[60] Alexander Shapiro and Andy Philpott. A tutorial on stochastic programming. *Manuscript. Available at www2. isye. gatech. edu/ashapiro/publications. html*, 17, 2007.

[61] Aharon Ben-Tal, Alexander Goryashko, Elana Guslitzer, and Arkadi Nemirovski. Adjustable robust solutions of uncertain linear programs. *Mathematical Programming*, 99(2):351–376, 2004.

[62] Giuseppe C Calafiore and Laurent El Ghaoui. *Optimization models*. Cambridge university press, 2014.

[63] Lorenz T Biegler. *Nonlinear programming: concepts, algorithms, and applications to chemical processes*, volume 10. Siam, 2010.

[64] Aharon Ben-Tal and Arkadi Nemirovski. Robust optimization–methodology and applications. *Mathematical Programming*, 92(3):453–480, 2002.

[65] Dimitris Bertsimas, David B Brown, and Constantine Caramanis. Theory and applications of robust optimization. *SIAM review*, 53(3):464–501, 2011.

[66] Sergio Lucia and Sebastian Engell. Potential and limitations of multi-stage nonlinear model predictive control. *IFAC-PapersOnLine*, 48(8):1015 – 1020, 2015. 9th IFAC Symposium on Advanced Control of Chemical Processes ADCHEM 2015.

[67] Dharmeshkumar R Gotawala, Ian D Gates, et al. A basis for automated control of steam trap subcool in sagd. *SPE Journal*, 17(03):680–686, 2012.

[68] Kohei Miura, Jin Wang, et al. An analytical model to predict cumulative steam/oil ratio (csor) in thermal-recovery sagd process. *Journal of Canadian Petroleum Technology*, 51(04):268–275, 2012.

[69] Neil Edmunds, Jeff Peterson, et al. A unified model for prediction of csor in steam-based bitumen recovery. In *Canadian International Petroleum Conference*. Petroleum Society of Canada, 2007.

[70] Guangyue Liang, Shangqi Liu, Pingping Shen, Yang Liu, and Yanyan Luo. A new optimization method for steam-liquid level intelligent control model in oil sands steam-assisted gravity drainage (sagd) process. *Petroleum Exploration and Development*, 43(2):301–307, 2016.